The role of Cep295 in centrosome biogenesis of human cells

Tsuchiya, Yuki

Doctor of Philosophy

Department of Genetics
School of Life Science
SOKENDAI (The Graduate University for Advanced Studies)

The role of Cep295 in centrosome biogenesis of human cells

Tsuchiya,Yuki

Student ID: 20141803
Department of Genetics, (SOKENDAI)

Abstract

To control proper cell division, the centrosome duplicates once per cell cycle and functions as the major microtubule organizing center (MTOC) in most animal cells. Centrioles covered with pericentriolar material (PCM) serve as the core structure of the centrosome. Like some animal mothers including humans, only a mature mother centriole can generate a new daughter centriole, which is crucial for centrosome duplication and strict control of centrosome number in a cell. However, the molecular mechanisms underlying the daughter-to-mother centriole conversion and how a daughter centriole acquires the ability to duplicate in the next cell cycle are poorly understood. Indeed, disorder of centrosome biogenesis and mitotic process are involved in human diseases such as cancer, genetic disease and ciliopathies. Therefore, principle of centriole biogenesis not only represents an important open question in biology, but also offers important therapeutic and diagnostic opportunities in medical science.

In this thesis, I mainly focused on the role of centrosomal protein 295kDa (Cep295) in centrosome biogenesis of human cells. I showed that a conserved protein, Cep295, is required for generation of a mature mother centriole that organizes a functional centrosome. Using the latest super-resolution-microscopy technique such as 3-dimensional structured illumination microscopy (3D-SIM) or stimulated emission depletion (STED) microscopy, I found that Cep295 is initially recruited to the proximal centriole wall in the early stages of centriole assembly. Cep295 then functions as a scaffold for proper assembly of a daughter centriole. Considering that Cep192 accumulation is recently shown to act as a meshwork to anchor other PCM components and organize functional PCM structure, the initial recruitment of Cep192 onto the

centriole wall should be a “seed” for PCM assembly. Moreover, Cep192 is also known as a component which acts upstream of the evolutionarily conserved centriole pathway. Importantly, using combination of biochemical and cytological analyses, I found that Cep295 binds physically to and recruits Cep192 onto the daughter centriole wall, which presumably provides the function of the new mother centriole for PCM assembly, MTOC activity and the ability for centriole formation. These findings lead me to propose that Cep295 is the most upstream factor in the conserved centriole pathway and promotes the daughter-to-mother centriole conversion.

Additionally, I provided the cytological evidence for a link between the patient with intellectual disability (ID) and mitotic defects. ID patients normally showed significant defects in both intelligence and adaptive behavior. Although mutations of several genes associated with proper progression of mitosis have been reported to underlie ID, the cytological evidence for actual patients with ID is rarely reported. Here, I discuss a new patient with a novel mutation of *CHAMP,* encoding a protein regulating kinetochore-microtubule attachment and chromosome segregation. Using whole exome sequencing (WES) analysis, my collaborators identified a de novo frameshift mutation in *CHAMP1*. We isolate lymphoblast cells from the *CHAMP1* patient and detect errors in chromosome segregation. Furthermore, I found that these cells exhibit an increase in centrosome number and resulting multipolar spindle formation. The phenotypes observed in the patient’s lymphoblastoid cells presumably stemmed from cytokinesis failure. I also confirmed the identical phenotypes in human culture cells depleted of *CHAMP1*. Overall, these data strongly support that *CHAMP1* mutations cause ID, and suggest that *CHAMP1* is critical for progression of cytokinesis and maintenance of centrosome number.

Table of Contents

Chapter 1:

General introduction

1.1 Main goal of the study

The purpose of my study is to understand some of the principal mechanisms of cell division, especially focusing on centrosome biology in human cells. In order to produce two identical daughter cells, a mother cell divides during mitosis inside our body, which is essential for cell growth, tissue repair and reproduction. Therefore, cell division is widely known as a crucial process in living cells, which is vital for life.

The centrosome is structure that is seen inside of cells, and it is only found in eukaryotic cells. The centrosome consists of two barrel-shaped structures called centrioles surrounded by pericentriolar material (PCM) and functions as the microtubule-organizing centers (MTOC), which is important for cell division, cell shape, and internal organization in a cell. Tight control and regulation of the centrosome number in a cell is essential for proper cell division, including proper chromosome segregation and robust formation of bipolar spindles during mitosis. In fact, aberration in centrosome biogenesis can lead to severe problems, such as multipolar spindle formation, chromosome misalignment and genomic instability, which are generally known as the hallmarks of cancer. Moreover, abnormal centrosome and spindle morphology are also found in a patient with autosomal recessive primary microcephaly (MCPH), which typically causes substantial defects in both intelligence and adaptive behavior. Therefore, understanding fundamental aspects of centrosome function and

biogenesis not only represents an important open question in biology, but also offers important therapeutic and diagnostic opportunities in medical science.

In chapter 2, I focused on the function of centrosomal protein of 295 kDa (Cep295) in human centrosome biology. Although it has recently been reported that a lot of proteins localizing to the centrosome or centriole regulate centrosome and centriole biogenesis, and also that some core components generate and organize functional centrosome, the underlying mechanisms how the cylindrical centrioles acquire MTOC activities as a functional centrosome in a cell are completely mysterious. Moreover, it is possible that other factors that are critical for centrosome and centriole biogenesis have not yet been identified. In this chapter, I suggest that Cep295 is required for centriole-to-centrosome conversion. In other words, understanding the Cep295 function in centrosome biology may help to answer the question: “how the cylindrical centrioles acquire MTOC activities as a functional centrosome in a cell”.

In chapter 3, I provide the biological evidence for linkage between the patient with intellectual disability (ID) and mitotic defects. ID is one of the neurodevelopmental disorder characterized by significant defects in both intelligence and adaptive behavior in the 5th edition of the Diagnostic and Statistical Manual [DSM-5; American Psychiatric Association (APA) 2013]. Although it has been suggested that mitotic defects cause ID, the cytological evidence for actual patients with ID was rarely reported. In this chapter, I discuss a novel mutation of *CHAMP1* that encodes a protein regulating kinetochore-microtubule attachment and chromosome segregation.

Overall, I just hope that my findings will help therapeutic and diagnostic opportunities in medical science.

1.2 Introduction

1.2.1 History and discovery of the centrosome

Walther Flemming, a pioneer of mitosis research, firstly described the cell division in animals in 1874-1876. From 1883 to 1887, notable developmental and cell biologists Edouard Van Beneden and Theodor Boveri, independently discovered that the centrosphere, which has become the later centrosome, was a small cellular organ in a cell and daughter cell receives this component from the parent cell for the first time (Paweletz, 2001). Edouard Van Beneden believed that the centrosome was at least as important as the nucleus when he observed its significant role during cell division. Theodor Boveri called it the centrosome and considered the centrosome as "the dynamic center of the cell" (Bloodgood, 2009)(Figure 1). It is notable that Boveri initially described a link between cancer cells and centrosome aberrations by microscopic observation (Gönczy, 2015). Although researchers in the field of the centrosome biology noticed the significance and dynamic behavior of the centrosome, the core components of the centrosome and its underlying mechanisms have been unclear for over one hundred years.

Nowadays the centrosome is known as self-replicating organelle acting as MTOC during mitosis, which is crucial for proper cell division in most animal cells. Moreover, *in vitro* and *in vivo* findings have been recently shown that centrosome amplification is actually involved in induction of cellular invasion or tumor development (Marthiens et al., 2016; Pellman, 2014). A noteworthy fact is that core concepts for centrosome biology, such as centrosome duplication, or MTOC function, are established by careful observation of the cell about a century ago.

1.2.2 Centrosome structure and composition

The centrosome is a non-membrane-bound organelle, consisting of a pair of microtubule-based structures termed centrioles, encircled by amorphous pericentriolar material (PCM) (Figure 2). Over one hundred proteins were recently identified by mass spectrometry analyses of purified human centrosomes (Andersen et al., 2003; Jakobsen et al., 2011). Considering that the centrosome is not surrounded by a membrane, it is likely that protein-protein interactions (PPIs) regulate its assembly and provide its beautiful symmetric architecture (Galletta et al., 2016).

Centrioles are small barrel-shaped structures characterized by nine-fold of radially symmetric microtubules, which serves the core structure of the centrosome. A mature centriole is ~250 nm in diameter and ~450 nm in long in human cells (Gönczy, 2012). The proximal end of centrioles is formed by triplet microtubule, whereas doublet microtubules are found at the distal part of centrioles in most animal cells. In recent years, outstanding studies independently demonstrated that SAS-6 (spindle assembly abnormal-6) as the core element of the cartwheel and this protein organized nine fold symmetry of the centriole by self-assembly of nine dimers (van Breugel et al., 2011; Kitagawa et al., 2011).

The PCM surrounds a pair of centrioles throughout cell cycle, which contributes to microtubule nucleation activity. It is estimated that PCM has layered structure and a lot of PCM components expand from inner circumstance side to outer circumstance side. Notably, proteins associated with microtubule nucleating activity are seen in the outer layers, whereas PCM components are found in the wall of the mother centriole (Lüders, 2012). Importantly, the mother centriole acquires additional PCM along with the mitotic progression (PCM expansion).

1.2.3 Roles of the centrosome

The centrosome plays important roles in regulation of multiple cellular functions, including cilia formation, cell signaling, polarity control, and cell division (Bolgioni and Ganem, 2015). The most popular function is that the centrosome functions as the main microtubule-organizing centers (MTOCs) in most of animal cells (Figure 3), and this is needed for chromosome segregation and proper spindle formation during mitosis. In addition, previous studies also reported that the centrosome functions as "actin-filament-organizing center" (Farina et al., 2015). Like a microtubule network contributing to cytoplasmic transport and maintenance of cell structure, actin filament is also known as cytoskeleton networks. Hence, the centrosome has significant impacts on intracellular architecture and cell polarity.

Centrioles are also known as the components of basal bodies, which are needed to generate cilia (short length) or flagella (long length): the main source of movement in eukaryotic cells. An extension of the centriole/basal body called "cilia" presents in G1/ G0 cells of the human body (Figure 3). Two different types of cilia have been recently identified: one is motile cilia generating the fluid flow during embryogenesis, and the other is immotile cilia that is considered as a flow sensor regulating cell signaling or contributing to cell polarity (Yoshiba and Hamada, 2014). Interestingly, previous studies also reported that some epithelial tissues contained many hundreds of cilia in each cell and immature centriole amplification termed "deuterosome formation" was required for generation of these cilia (Al Jord et al., 2014).

Although recent studies have focused on the molecular mechanisms for centriole biogenesis, cell-specific roles of the centrosome in different tissues or organs remain poorly understood.

1.2.4 Centrosome cycle

Centrosome duplication must be strictly regulated along with cell cycle progression, ensuring proper chromosome segregation and robust formation of bipolar spindles during mitosis in most animal cells. Formation of a daughter centriole next to each mother centriole occurs once per cell cycle, which is important for strict control of centrosome number (Avidor-Reiss and Gopalakrishnan, 2013; Brito et al., 2012; Gönczy, 2015). The centrosome cycle is achieved with several steps along with the cell cycle (Wang et al., 2014). During mitosis, one centrosome is seen at the pole of mitotic spindle, which contains a pair of daughter and mother centrioles. Like DNA materials, cohesin ring is known as a connector between daughter and mother centrioles (Wang et al., 2008). The physical separation of the mother-daughter centriole pair, termed "disengagement" occurs form late-mitosis to early G1 phase, which is required for centriole formation in the next cell cycle. Disengagement seems to be regulated by polo-like kinase 1 (Plk1), cyclin- dependent kinase 1 (CDK1), PCM, and separase (Wang et al., 2014). During G1 phase, cells have two mother centrioles (one is old mother centriole having appendage structure that is required for generation of cilia, and the other is new mother centriole coming from daughter centriole). During S phase, a new daughter centriole forms on each preexisting mother centrioles and elongates. During G2 phase, centrosomes gather additional PCM components. This is called centrosome maturation. Then, two mature centrosomes move in opposite directions termed centrosome separation, which is important for proper cell division in next mitosis (Figure 4).

1.2.5 Centrosome and human diseases

The number of centrosomes in a cell must be tightly controlled along with cell cycle progression to ensure the proper bipolar spindle formation during mitosis. Indeed, the increased number of centrosomes can often be seen in tumor cells,, which is generally known as the hallmarks of cancer. (Gönczy, 2015; Nigg and Raff, 2009). Importantly, a previous study of actual patients with breast cancer suggested that centrosome amplification was strongly correlated with malignant progression and involved in deleterious clinical outcomes in breast cancer (Denu et al., 2016). Furthermore, using the cBioPortal for Cancer Genomics providing large-scale cancer genomics data set (http://www.cbioportal.org/index.do)(Cerami et al., 2012; Lin and Scott, 2012), I also confirmed that centrosome-related genes encoding significant factors for centriole formation caused gene amplification in breast cancer cells (Figure 5).

Abnormal centrosome and spindle morphology are also found in a patient with autosomal recessive primary microcephaly (MCPH). Patients with MCPH typically shows birth defects as microcephaly and non-progressive mental retardation (Faheem et al., 2015). Several centrosome genes associated with MCPH have been identified: WD repeat-containing protein 62 (WDR62) (Bilgüvar et al., 2010), cyclin dependent kinase-5 regulatory subunit associated protein (CDK5RAP2) (Issa et al., 2013), abnormal spindle like primary microcephaly (ASPM) (Bond et al., 2002), centrosomal P4.1-associated protein (CPAP) (Issa et al., 2013), SCL/TAL1 interrupting locus (STIL) (Papari et al., 2013), centrosomal protein of 135 kDa (Cep135) (Hussain et al., 2012), centrosomal protein of 152 kDa (Cep152) (Guernsey et al., 2010), suggesting that strict regulation on the centriole and centrosome copy number plays a vital role in brain development.

1.2.6 Evolutionarily conserved pathway for centriole formation

Regarding the evolutionarily conserved pathway for centriole formation, humans and *Caenorhabditis elegans* share only five functional homologues, which are considered to be crucial factors for centriole formation: centrosomal protein of 192 kDa (Cep192) (Gomez-Ferreria et al., 2007; Zhu et al., 2008), polo-like kinase 4 (Plk4) (Bettencourt-Dias et al., 2005; Habedanck et al., 2005), human spindle assembly abnormal-6 (HsSAS-6) (Dammermann et al., 2004; Leidel et al., 2005), STIL (Arquint et al., 2012; Kitagawa et al., 2011; Tang et al., 2011; Vulprecht et al., 2012), CPAP (Kohlmaier et al., 2009; Schmidt et al., 2009; Tang et al., 2009) in humans. In the process of centriole formation in human cells, the presence of Cep192 and Cep152 (Cizmecioglu et al., 2010; Dzhindzhev et al., 2010; Hatch et al., 2010) at centrioles is required for the centriolar recruitment of Plk4. At the onset of centriole formation, Plk4 phosphorylates STIL, which leads to the formation of a complex between the phosphorylated STIL and HsSAS-6 (Kratz et al., 2015; Ohta et al., 2014). This phosphorylation event promotes recruitment of the HsSAS-6-STIL complex to centrioles, which is followed by centriolar loading of CPAP for attachment of the centriolar microtubules and centriole elongation (Kohlmaier et al., 2009; Schmidt et al., 2009; Tang et al., 2009). However, it is possible that other evolutionarily conserved factors critical for centriole formation have not yet been identified (Figure 6).

1.2.7 Figures

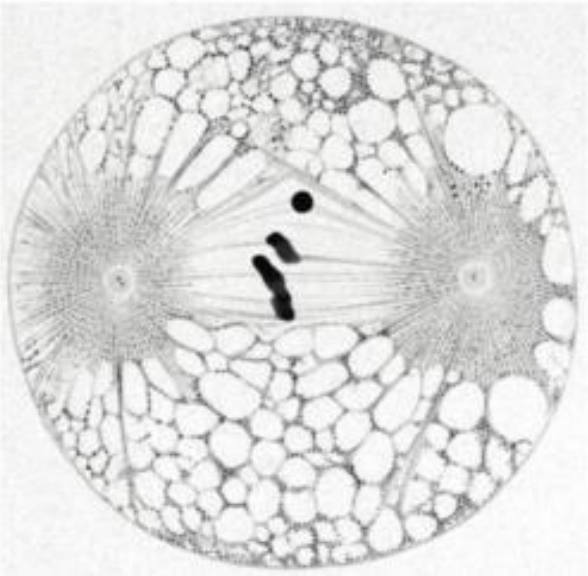

Figure 1: The initial discovery of the centrosome
The image is the first discovery of the centrosome in the *Ascaris megalocephala bivalen* embryo, form boveri's 1900 manuscript. This image is produced by (Gönczy, 2015)

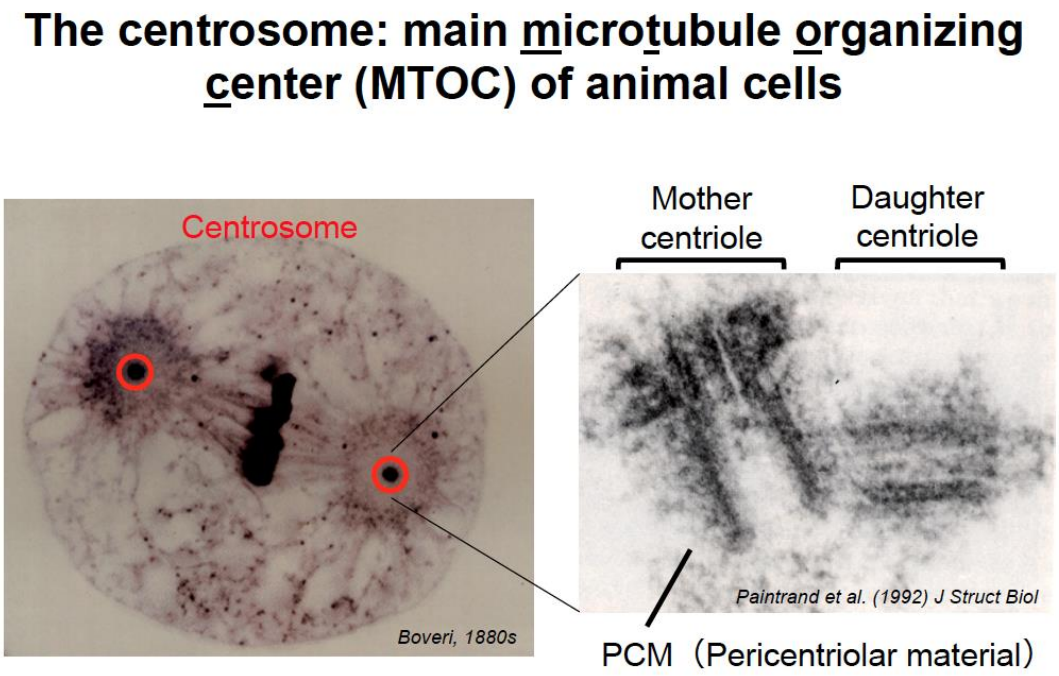

Figure 2: The centrosome structure

The centrosome consists of two orthogonally arranged microtubule-based structures called daughter and mother centrioles, surrounded by amorphous pericentriolar material (PCM). Only a mature mother centriole can form a new daughter centriole, which is important for centrosome duplication. This image is reproduced by (Delattre and Gonczy, 2004)

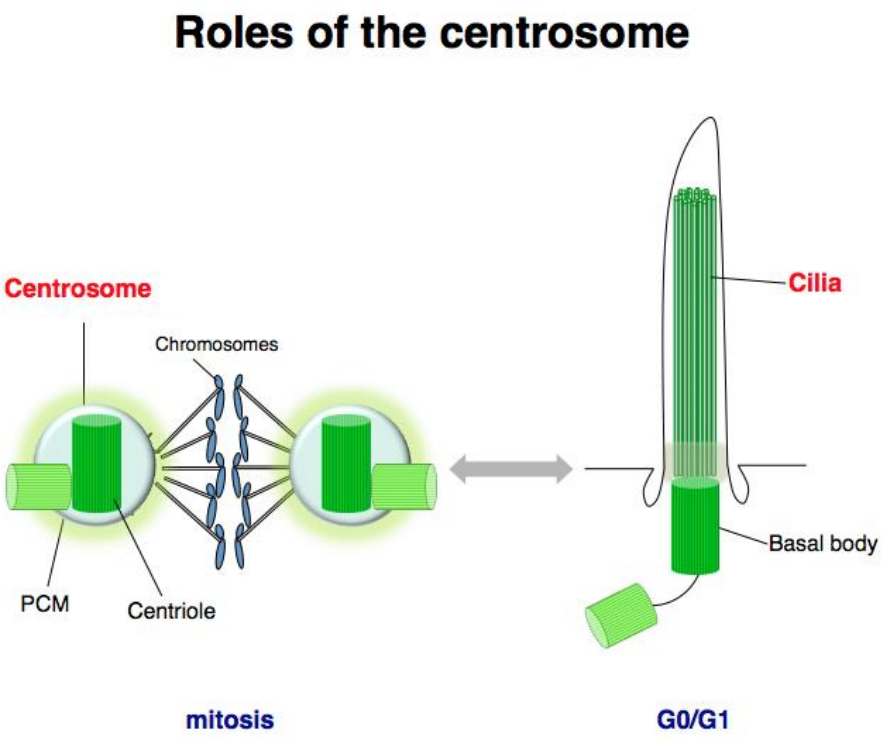

Figure 3: Functions of the centrosome

The most popular function is that the centrosome acts as the microtubule-organizing centers (MTOCs) in animal cells (left panel), which is important for proper spindle formation and chromosome segregation during mitosis. An extension of the centriole/basal body called “cilia” presents in G1/ G0 cells of the human body (right panel).

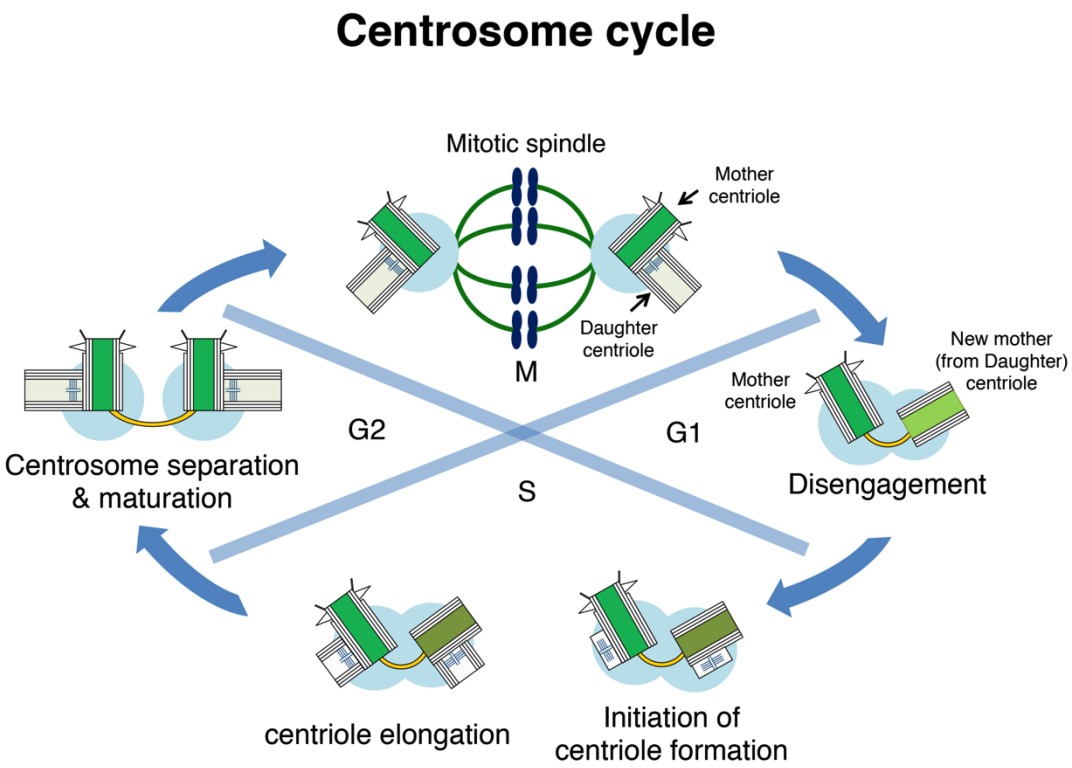

Figure 4: Centrosome cycle

During mitosis, one centrosome is seen at the poles of mitotic spindle, which contains a pair of daughter and mother centrioles. The physical separation of the mother-daughter centriole pair, termed "disengagement" occurs during late-mitosis. During G1 phase, cells have two mother centrioles (one is old mother centriole, and the other is new mother centriole coming from daughter centriole). During S phase, a new daughter centriole forms on each preexisting mother centrioles and elongates. During G2 phase, centrosome separation occurs, which is important for proper cell division.

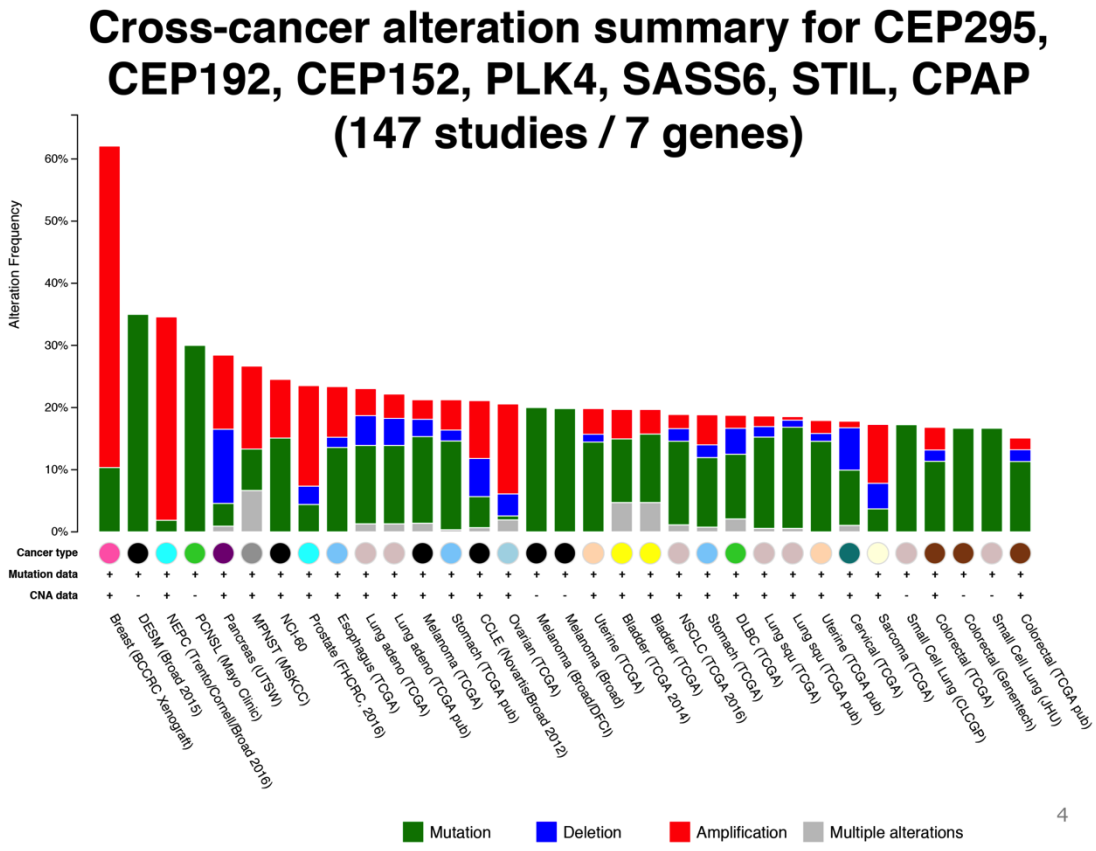

Figure 5: Cross-cancer alteration summary

The cBioPortal for Cancer Genomics providing large-scale cancer genomics data set (http://www.cbioportal.org/index.do)(Cerami et al., 2012; Lin and Scott, 2012). Interestingly, amplification of centrosome-related genes encoding significant factors for centriole formation such as Cep295, Cep192, Cep152, Plk4, HsSAS-6, STIL, and CPAP are found in breast cancer cells. With regard to this, it has recently been shown that centrosome amplification is strongly correlated with malignant progression and involved in deleterious clinical outcomes in breast cancer (Denu et al., 2016). Further studies will be needed to reveal linkages between clinical outcome and biological meaning of cancer specific centrosome amplification.

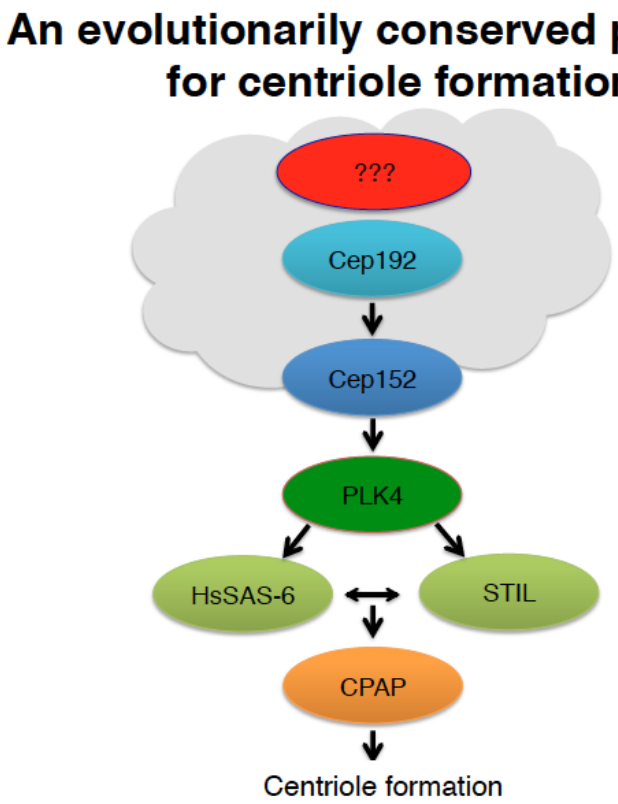

Figure 6: The conserved pathway for centriole formation

The evolutionarily conserved pathway for centriole formation, humans and *Caenorhabditis elegans* share five functional homologues, which are considered to be crucial factors for centriole formation: Cep192, Plk4, HsSAS-6, STIL, and CPAP in humans. In the process of centriole formation in human cells, the presence of Cep192 and Cep152 at centrioles is required for the centriolar recruitment of Plk4. Plk4 then recruits the HsSAS-6-STIL complex to centrioles, which is followed by centriolar loading of CPAP for attachment of the centriolar microtubules and centriole elongation. This image is reproduced by (Gönczy, 2012).

Chapter 2:

Analysis of Cep295 in human centrosome biology

2.1 Summary

The centrosome is the major microtubule-organizing center (MTOC) of most animal cells. Microtubule-based structures called “centrioles” surrounded by pericentriolar material (PCM) serve as the core structure of the centrosome. A daughter centriole forms on each preexisting mother centriole once per cell cycle, which is essential for centrosome duplication. Therefore, the newly-born daughter centriole in turn grows into a functional mother centriole in the next cell cycle. However, the underlying mechanisms remain unclear. In this thesis, I show that Cep295, a conserved protein from *Drosophila melanogaster* to human, is needed to generate a mature mother centriole that organizes a functional centrosome. I find that Cep295 localizes to the proximal part of the centriole wall in the very early stages of centriole formation. Cep295 then functions as a scaffold protein to assemble critical centriole proteins for proper daughter centriole formation. I also show that the physical association between Cep295 and Cep192 on the centriole wall is crucial for the ability of a mother centriole to recruit PCM components and MTOC related proteins and start duplicating a new daughter centriole. These findings lead me to propose that Cep295 acts upstream of the conserved pathway for centriole formation and facilitates the daughter-to-mother centriole conversion.

2.2 Introduction

2.2.1 Daughter to mother centriole conversion

The daughter-to-mother centriole conversion is an essential event for generating a functional centrosome because, in this process, a daughter centriole recruits the PCM components that are important for the microtubule nucleating activity of centrosomes. Moreover, only the mature mother centriole can generate a new daughter centriole (Wang et al., 2011) (Figure 7). It has recently been shown that the physical separation of the mother-daughter centriole pair, termed “disengagement”, licenses centrioles to duplicate once per cell cycle (Tsou and Stearns, 2006). In addition, polo-like kinase 1 (Plk1) is known as a critical regulator of centrosome maturation, which is required for recruitment of γ-tubulin ring complexes in human (Lane and Nigg, 1996; Petronczki et al., 2008). However, the molecular mechanisms underlying daughter-to-mother centriole conversion and how a mother centriole acquires the ability to form a new centriole in the next cell cycle are incompletely understood.

2.2.2 Centrosomal protein 295kDa (Cep295)

Andersen and his colleagues firstly suggested that KIAA1731 is a novel candidate centrosomal protein in human lymphoblastic cells by using a mass spectrometry-based proteomic analysis (Andersen et al., 2003). In addition, previous studies using genome-wide RNAi screens in Drosophila cells sequentially reported that Ana1 (anastral spindle phenotype 1) is required for efficient centriole formation (Dobbelaere et al., 2008; Goshima et al., 2007). As for evolutionary conservation, previous studies indicated that KIAA1731 should be the homologue of Drosophila Ana1 in human. However, the role of this protein in centriole formation was poorly understood.

Tsou's group initially described KIAA1731 as Cep295 in human and suggested that this protein coordinates only the centriole-to-centrosome conversion but does not affect centriole formation per se in human cells (Izquierdo et al., 2014). In addition, it has recently been shown that the Cep135–Cep295/Ana1–Cep152/Asl interactions enable the centriole-to-centrosome conversion in both *Drosophila melanogaster* and humans (Fu et al., 2016).

In this study, I identify Cep295 as a novel conserved factor acting upstream of Cep192 in centriole biogenesis. Cep295 appears to be recruited to the procentriole assembly site at the early stages of centriole duplication. Furthermore, I show that the interaction between Cep295 and Cep192 is crucial for the integrity of centriole structure and for daughter-to-mother centriole conversion**.**

2.2.3 Figure

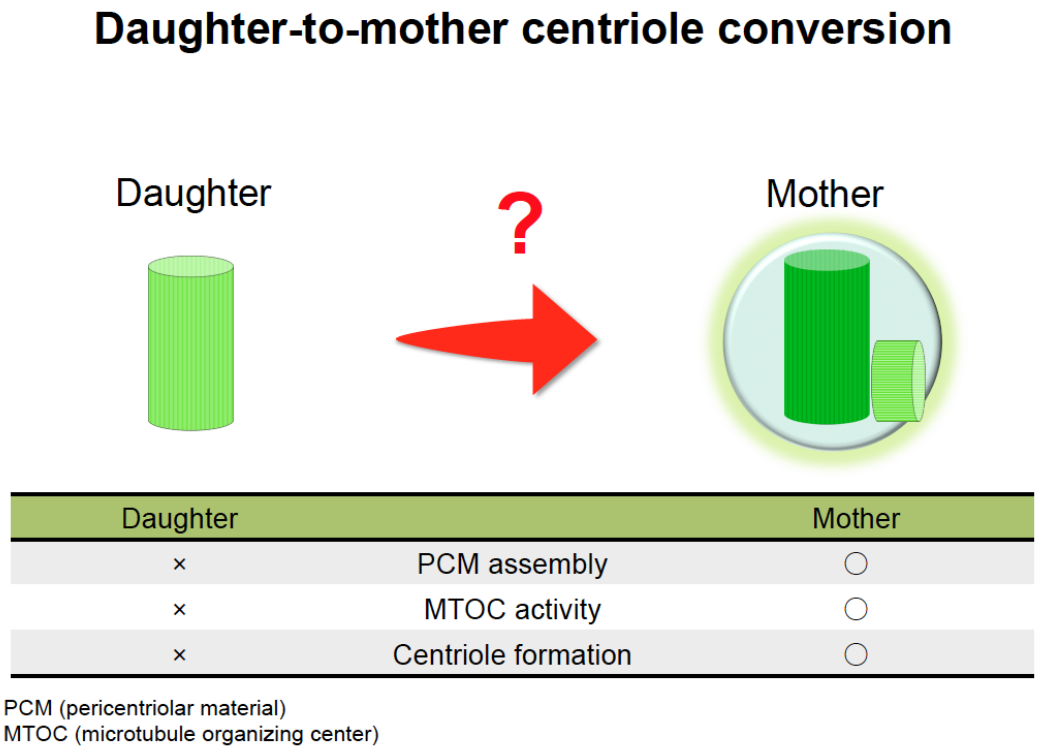

Figure 7: The differences between daughter and mother centrioles

Only the mother centriole can assemble the PCM components that are important for the MTOC activity as functional centrosomes. The most important difference between daughter and mother centrioles is that only the mature mother centriole can generate a new daughter centriole (centriole formation).

2.3 Results

2.3.1 Cep295 is an evolutionarily conserved protein

Although it has been recently suggested that Cep295/KIAA1731 somehow mediates the centriole-to-centrosome conversion but it is dispensable for centriole assembly in human cells (Izquierdo et al., 2014), and also that sequential loading of Cep135, Ana-1/Cep295, and Asterless/Cep152 onto daughter centrioles is needed for their maturation to become mother centrioles in *Drosophila* cells (Fu et al., 2016), the exact role of Cep295 in centriole and centrosome biogenesis and molecular mechanisms of the centriole-to-centrosome conversion regulated by Cep295 remain incompletely understood. Moreover, it is not clear whether its functional homologues in other species also play similar roles in these events.

Centrioles are evolutionarily conserved organelles. Therefore, I could speculate that the core components and the underlying molecular mechanisms are also conserved. In fact, previous forward genetic approaches and functional genomic studies have identified the core pathway for centriole formation in *C. elegans* (Dammermann et al., 2004; Delattre et al., 2004; Kirkham et al., 2003; Leidel and Gönczy, 2003; Leidel et al., 2005; O'Connell et al., 2001). Importantly, all proteins in this pathway were evolutionarily conserved up to human. In order to determine whether Cep295 is a conserved factor involved in centriole formation across species, I firstly conducted a BLAST analysis in eukaryotes. Previous studies suggested that *Drosophila* Ana-1 (anastral spindle phenotype), which is implicated in centriole formation (Blachon et al., 2009; Dobbelaere et al., 2008; Goshima et al., 2007) and human Cep295 appear to share a short homologous sequence (Knorz et al., 2010). Using an iterative BLAST search for

the short stretch, I succeeded in identifying a 43-amino acid (aa) region of homology in other species (Figure 8,9). Accordingly, I termed the conserved short sequence as the "PICA (present in C-terminal of Ana-1)" motif. I also noticed that Cep295 family proteins share another conserved region within the DDC8-like (differential display clone 8) domain at their N-terminus (Figure 8-10). These data suggest that Cep295 is a protein conserved across species.

2.3.2 Cep295 is crucial for bipolar spindle formation and centriole assembly

In order to determine and confirm whether Cep295 has significant impacts on centriole biogenesis during the cell cycle and mitosis. Next, I performed phenotypic analysis in human cells. I found that RNAi-mediated depletion of Cep295 dramatically decreased the number of centrioles and caused abnormal spindle formation during mitosis in HeLa cells, compared to control mitotic cells that had four centrioles and assembled a normal bipolar spindle (21 ± 1% of cells treated with siRNA targeting against endogenous Cep295, compared with 94 ± 1% of control cells with ≥4 centrioles; (Figure 11,12). This result is consistent with the previous report that Cep295 is crucial for the maintenance of proper centriole numbers in human cells (Izquierdo et al., 2014).

The similar defects in mitotic spindle formation and centriole number were also found when using RNAi targeting against different sequences of Cep295 ORF (Open Reading Frame) or in different human cell lines such as HeLa cells, U2OS cells (Figure 13) or RPE1 cells (data not shown). Note that the specificity of Cep295 siRNA was confirmed by using immunofluorescence and western blot analyses, and also that depletion of Cep295 had no significant impact on cell cycle progression (Figure 14,15).

2.3.3 Domain analysis of Cep295

I next aimed to identify which domains of Cep295 are required for its centriolar localization and for the assembly of centrosomes. I depleted endogenous Cep295 proteins using siRNA and expressed RNAi-resistant full-length or deletion constructs at comparable levels (Figure 16-19). Whereas the number of centrosomes marked with γ-tubulin was reduced in most of the interphase cells upon depletion of endogenous Cep295, expression of full-length Cep295 functionally rescued this phenotype (17% ± 2% and 49% ± 4% of cells with ≥2 centrosomes, respectively; Figure 16-19). In contrast, a Cep295 mutant lacking the conserved DDC8-like domain did not localize to the centriole and failed to rescue the phenotype provoked by depletion of endogenous Cep295 (21% ± 4% of cells with ≥2 centrosomes; Figure 16-19). I found that another mutant lacking the PICA domain, but not the ALMS (Alstrom syndrome) motif, lost the ability to form centrosomes despite localizing to centrioles (17% ± 7% of cells with ≥2 centrosomes; Figure 16,18,19). I also noticed that overly expressed Cep295 frequently co-localized with the microtubule networks through the C-terminal region including the ALMS domain (Figure 20). These data suggest that the two conserved domains, DDC8-like and PICA, are required for the function of Cep295 in the assembly of centrosomes and also that the conserved DDC8-like domain mediates the centriolar localization of Cep295.

2.3.4 localization of Cep295 during the cell cycle

In order to investigate the precise centriolar distribution of Cep295 across the cell cycle, I performed immunofluorescence analyses using specific antibodies against

endogenous Cep295 (Figure 17). Consistent with the recent study (Izquierdo et al., 2014), Cep295 gradually became enriched at daughter centrioles as the cell cycle progressed (Figure 21,22). However, I also observed an intense signal of Cep295 on mother centrioles in G1 phase, suggesting that Cep295 is not a daughter-specific centriolar protein (Figure 22).

2.3.5 Cep295 forms ring-like structures and localizes at the proximal end of centrioles

Owing to the development of the latest super-resolution-microscopy technique, I can easily detect very fine structure of the centrosome in human cells (Figure 23). To examine the detailed distribution of Cep295 on daughter or mother centrioles, I used 3-dimensional structured illumination microscopy (3D-SIM). 3D-SIM analyses revealed that Cep295 was recruited to the proximal part of both mother and daughter centrioles and formed ring-like structures around the centriole wall (Figure 24). I also noticed that Cep295 was recruited to daughter centrioles before the appearance of a GT335 signal, which marks polyglutamylated centriolar microtubules (also known as GT335). This observation suggests that the recruitment of Cep295 to daughter centrioles occurs in the early stages of centriole formation.

2.3.6 Cep295 is a centriole wall protein

To measure the diameter of centriolar rings of Cep295 and GT335, I quantified the fluorescence intensity and determined the distance between the two peaks at opposite sides of the rings (240 ± 10 nm; n = 9 cells; Figure 25). Interestingly, the diameter of the

Cep295 ring on mother centrioles was very close to that of GT335 (Sonnen et al., 2012) (221 ± 40 nm; n = 6 cells; Figure 25), suggesting that Cep295 is a component of the proximal end of the centriole wall. Furthermore, I found that the diameter of an N-terminal fragment of Cep295 fused with GFP at the C-terminus in mother centrioles is shorter than the diameter of endogenous Cep295 detected by a C-terminal specific antibody (Figure 26). This orientation of Cep295 at mother centrioles is in line with the *Drosophila* Ana-1 orientation as previously described (Fu et al., 2016), supporting the notion that the function of Cep295 for centriole formation is evolutionarily conserved.

2.3.7 Cep295 is essential for maturation of new mother centrioles

The previous studies suggested that depletion of Cep295/Ana-1 had no significant impact on assembly of daughter centrioles per se, but perturbed their maturation to become functional mother centrioles in the next cell cycle (Izquierdo et al., 2014; Fu et al., 2016). Although they showed that Cep295/Ana-1 is required for the centriole-to-centrosome conversion in *Drosophila* and human cells, the mechanism by which Cep295 regulates this process still remains unclear. I therefore attempted to clarify the exact function of Cep295 in centriole/centrosome biogenesis (Figure 27). By using triple staining analysis, I firstly confirmed that new mother centrioles were unable to recruit centrosomal proteins such as γ-tubulin in Cep295-depleted interphase cells. In contrast, older mother centrioles which were marked with Odf2 (Ishikawa et al., 2005), an appendage marker of mature mother centrioles that is important for primary cilia formation, could assemble functional centrosomes (Figure 28).

I also confirmed that new mother centrioles failed to recruit centrosomal protein of

110KDa (CP110), a distal end marker of the centrioles, suggesting that centriole formation at the new mother centriole was defective upon Cep295 depletion (Figure 28). I therefore sought to identify which step of the conserved centriole pathway is impaired at the new mother centriole in Cep295-depleted cells. Depletion of Cep295 affected centriolar targeting of the critical factors, including Plk4, STIL, HsSAS-6, and CPAP, to new mother centrioles during interphase, whereas that to older mother centrioles did not appear to be affected as much (Figure 29,30). Conversely, depletion of Plk4, HsSAS-6 and STIL, did not affect Cep295 localization to mother centrioles, even though centriole formation was perturbed under these conditions, suggesting that Cep295 is recruited upstream of these factors (Figure 31). To investigate further the different phenotypes at new and older mother centrioles upon Cep295 depletion, I tested the effects of Cep295 depletion on centriole overduplication induced by Plk4 overexpression in human cells. Consistently, I found that depletion of Cep295 largely suppressed centriole overduplication at new mother centrioles but not at older mother centrioles (Figure 32). Taken together, these data indicate that Cep295 is required for the earlier stages of centriole formation at new mother centrioles.

It is well known that Cep192 assembles the PCM components, which is essential for the organization of a functional centrosome with MTOC activity during mitosis. Cep192 is also known as a recruiter of Plk4 and Cep152, and is believed to be the most upstream factor of the evolutionarily conserved centriole pathway (Kim et al., 2013; Sonnen et al., 2013). Interestingly, I found that Cep295 depletion induced complete loss of Cep192 and Cep152 at only one of the two mother centrioles during interphase. This result suggests that, in the absence of Cep295, the new mother centriole lost the ability to hold essential proteins, Cep192 and Cep152, for PCM assembly and centriole

formation (Figure 33).

Next, to identify when in the cell cycle a new mother centriole becomes defective in centrosome assembly, I decided to examine the phenotype induced by Cep295 depletion at an earlier time point (~24 hours after the RNAi treatment) and observe the redistribution of Cep192 to daughter centrioles just after mother–daughter centriole disengagement (Tsou and Stearns, 2006) during the previous mitosis. By using multiple staining analysis, I found that in control cells, Cep192 localized to both mother and daughter centrioles just after disengagement. Intriguingly, however, in the complete absence of Cep295 at both mother and daughter centrioles, I found that only mother centrioles marked with Odf2 hold PCM components such as γ-tubulin, NEDD1, CDK5RAP2 and Cep192 whereas daughter centrioles did not recruit PCM components after centriole disengagement in late mitosis (Figure 34,35). In line with this result, recruitment of other PCM proteins to daughter centrioles was already affected just after centriole disengagement in the absence of Cep295 (Figure 34,35). While observing centriole disengagement in Cep295-depleted cells, I found that depletion of Cep295 caused precocious mother–daughter centriole disengagement during anaphase in mitosis, which may have occurred due to PCM loss at separated daughter centrioles (Figure 36). Overall, these findings show that Cep295 is crucial for the conversion of daughter centrioles to become functional mother centrioles from the earliest stages after centriole disengagement.

2.3.8 Cep295 is crucial for the integrity of a daughter centriole

Why was the daughter centriole already unable to recruit PCM proteins after

centriole disengagement in Cep295-depleted cells? A previous study claimed that Cep295 is required for the centriole-to-centrosome transition (Izquierdo et al., 2014), but not for centriole formation itself. However, this conclusion seemed to be drawn from experiments that used a limited number of centriole markers against newly formed centrioles in Cep295-depleted cells. Given that upon Cep295 depletion, Cep192 was not present at the daughter centrioles that had just disengaged from mother centrioles (Figure 34), I assumed that formation of the daughter centrioles might be already defective. These considerations prompted me to reexamine whether depletion of Cep295 causes defects in daughter centriole formation. In control cells, 3D-SIM analyses revealed that Cep192 was recruited to the wall of newly formed daughter centrioles that were linked with mother centrioles. In stark contrast, I found that the recruitment of Cep192 to the daughter centriole wall did not occur in Cep295-depleted cells (Figure 37). I also found that the arrangement of Cep192 at the mother centriole was affected in the same condition even though some Cep192 still remained at the mother centriole. Although the upstream factors regulating centriolar loading of Cep192 remain unknown, these data indicate that Cep295 is crucial for the initial recruitment of Cep192 at a newly born daughter centriole.

Next, to precisely monitor the order in which Cep295 and Cep192 are recruited to the assembly site of procentrioles, I used the gated STED microscopy. This technique enabled me to distinguish the precise distribution of these two proteins at procentrioles from that at the mother centrioles (Figure 38). I analyzed centriolar localization of the two proteins in human G1 cells, and found that Cep295 was recruited to the procentriole assembly site even while Cep192 localization was limited at the mother centrioles. This observation implies that Cep295 could provide a scaffold for assembly of the proximal

end of a procentriole. To tackle this idea, I next examined whether this centriolar recruitment of Cep295 occurs in the absence of the cartwheel structure, which serves as the base structure of the procentriole. Upon depletion of HsSAS-6, an essential component of the cartwheel structure (van Breugel et al., 2011; Kilburn et al., 2007; Kitagawa et al., 2011; Nakazawa et al., 2007), a portion of Cep295 appeared to be recruited onto the mother centriole wall and formed a cap-like structure, presumably at the potential assembly site of a procentriole (Figure 39). This result suggests that centriolar localization of Cep295 occurs independently of the formation of the cartwheel structure. Taken together, these data support the notion that Cep295 provides a platform for the proximal end of procentrioles in the early stages of centriole formation, and functions upstream of the evolutionarily conserved pathway for centriole formation.

Given the above results, I postulated that Cep295 is involved in the assembly of the proximal end of the centriole structure. The gated STED microscopy analyses demonstrated that newly formed daughter centrioles exhibited a significant reduction in the number of polyglutamylated centriolar microtubules, as marked by GT335, especially at the proximal end (Figure 40). I then tested the integrity of the cartwheel structure upon Cep295 depletion. To monitor this, I quantified the fluorescence signal intensity of HsSAS-6 at centrioles. Although centriolar recruitment of HsSAS-6 was detectable in Cep295-depleted interphase cells, the signal intensity of HsSAS-6 was considerably weaker in these Cep295-depleted interphase cells than in control cells (Figure 41). I next looked at Cep135, a proximal centriolar component (Kleylein-Sohn et al., 2007) and intriguingly found that depletion of Cep295 caused complete loss of Cep135 from the daughter centrioles just after centriole disengagement (Figure 42). This is in line with the previous finding that depletion of Ana-1 also affected Cep135

recruitment to daughter centrioles in *Drosophila* cells (Fu et al., 2016). On the other hand, I could detect only 34% reduction of Cep295 at centrioles by Cep135 depletion in human cells (Figure 43,44). Overall, I conclude that Cep295 is critical for proper formation of daughter centrioles. Given the previous study (Izquierdo et al., 2014) and my observation (Figure 45) that Cep295 regulates the stability of a new mother centriole, I speculate that incomplete daughter centriole formation by Cep295 depletion could lead to instability and defective function of the resulting new mother centriole in the next cell cycle.

2.3.9 The Cep295-Cep192 interaction promotes centrosome biogenesis

To understand how Cep295 recruits Cep192 to a newly formed daughter centriole, I tested whether Cep295 associates with Cep192. Remarkably, the interaction between the two proteins was detected by immunoprecipitation (IP) assays in human cells and yeast two-hybrid analyses (Figure 46). I noted that the expression of Cep295 increased the protein levels of Cep192 in a concentration-dependent manner *in vivo*, suggesting that Cep295 may also stabilize Cep192 (Figure 47). By using a co-IP assay and yeast two-hybrid analyses with deletion constructs of Cep295, I narrowed down the Cep295 region required for Cep192-binding to the short stretch spanning aa 1942–2144 (Figure 48-51).

I also found that Cep295 fragments including the interaction region are sufficient for binding to the C-terminal region of Cep192 in human cells (Figure 50,51). I therefore reasoned that the association between Cep295 and Cep192 might be needed for recruitment of Cep192 onto the daughter centriole wall. I depleted endogenous Cep295

using siRNAs and expressed full-length Cep295 or deletion constructs lacking the Cep192-binding region at comparable levels in HeLa cell. As expected, I found that expression of the Cep295 mutant that failed to bind Cep192 could not recruit Cep192 onto the wall of a newly formed daughter centriole (Figure 52). To address whether these defective daughter centrioles could become functional mother centrioles in the next cell cycle, I focused on the recruitment of γ-tubulin to the resulting new mother centriole. While depletion of endogenous Cep295 resulted in a significant reduction of γ-tubulin foci in most interphase cells, the expression of full-length Cep295 could functionally rescue this phenotype (15% ± 4% and 52% ± 3% of cells with ≥2 centrosomes, respectively; Figure 52). In contrast, a Cep295 mutant lacking the Cep192-binding region is unable to rescue the phenotype provoked by depletion of endogenous Cep295 (22% ± 4% of cells with ≥2 centrosomes; Figure 52). Taken together, these data strongly suggest that the association between Cep295 and Cep192 is crucial for daughter-to-mother centriole transition.

I next sought to identify the region of Cep192 for binding to Cep295 and for its centriolar loading. Firstly, by using immunofluorescence analyses with Cep192 deletion mutants, I found that a short fragment of Cep192 (aa 1501–1860) was sufficient for its tergeting to the centriole in human cells. In contrast, the Cep192 mutants that lack regions containing aa 1501-1860 did not localize to the centriole (Figure 53). Secondly, consistent with these observations, co-IP analyses revealed that the Cep192 mutants lacking the region of aa 1501–1860 failed to associate with endogenous Cep295 (Figure 53,54). In contrast, the C-terminal fragments of Cep192 containing the region of aa 1501–1860 were capable of binding to endogenous Cep295 (Figure 53,54). Thirdly, to confirm the Cep295-Cep192 interaction *in vitro* with the bacterially-purified

recombinant proteins, I purified Cep295 and Cep192 fragments (aa 1727-2204 of Cep295 and aa 1501-2040 of Cep192) containing the interacting regions that were identified by co-immunoprecipitation experiments. I showed that the two proteins interact with each other by GST pull-down assays (Figure 54), which suggests the physical interaction between Cep295 and Cep192. Next, to address whether the centriolar loading of Cep192 is needed for centriole-to-centrosome transition, I depleted endogenous Cep192 and expressed a Cep192 deletion mutant that fails to interact with Cep295. I found that the Cep192 mutant did not recruit γ-tubulin at centrosomes and form mitotic bipolar spindles in Cep192 depleted cells (Figure 55) whereas the full-length of Cep192 rescued the phenotypes. This result supports the notion that the Cep295-Cep192 association is needed for centriolar recruitment of Cep192 and centriole-to-centrosome conversion. Furthermore, I conducted an additional experiment using the short fragment of Cep192 that interacts with Cep295. Interestingly, expression of the Cep192 fragment localizing to centrioles inhibited centrosomal recruitment of PCM proteins such as γ-tubulin and endogenous Cep192 (Figure 56,57). This result implies the dominant negative effect of the Cep192 fragment that masked the Cep192-interaction site of centriolar Cep295, on centriolar recruitment of endogenous Cep192 and on PCM assembly. Overall, these findings strongly suggest that Cep192 localized to the newly formed daughter centriole via Cep295-Cep192 interaction, and that this interaction is necessary for centriole-to-centrosome conversion.

2.3.10 Figures

Figure 8: Schematic diagrams for Human Cep295 (HsCep295) and Drosophila Ana-1 (DmAna-1)

The DDC8-like (differential display clone 8) domain is shown in gray box, the ALMS (Alstrom syndrome) domain in black box. These domains are identified in previous study (Knorz et al., 2010). The positions of two evolutionarily conserved domains are indicated in orange and blue lines, respectively. The conserved short sequence indicated in blue line was termed as the "PICA (present in C-terminal of Ana-1)" motif.

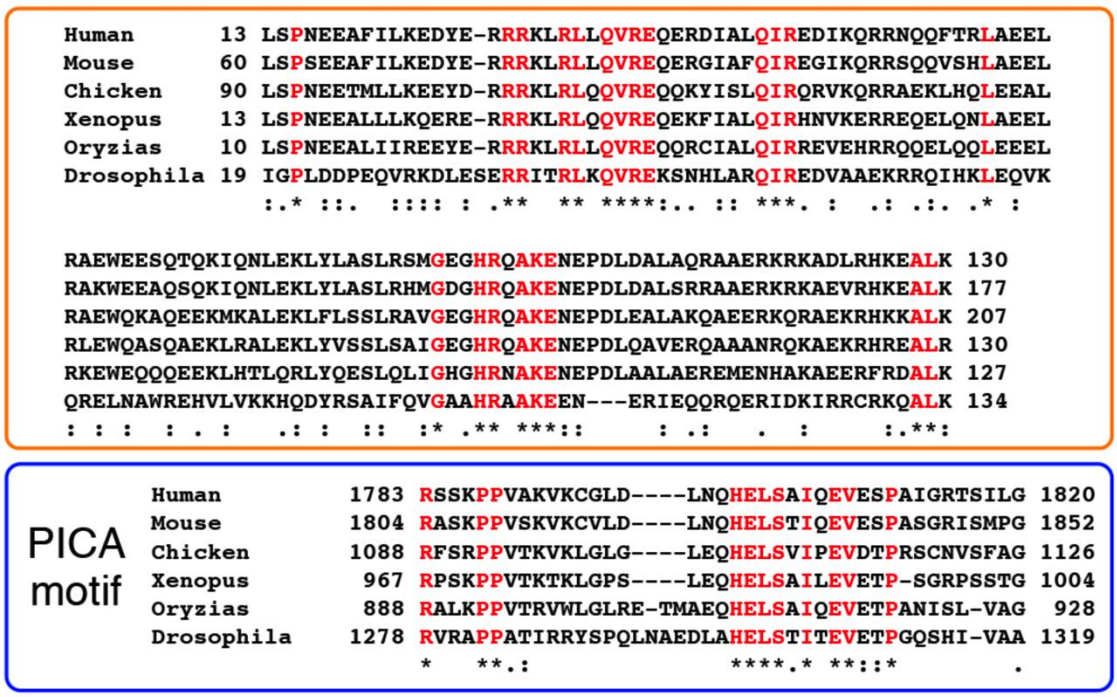

Figure 9: Alignments of the evolutionarily conserved domains within human, mouse, chicken, Xenopus and Orizias Cep295 and Drosophila Ana1

The orange and blue boxes indicate the conserved region within the DDC8-like domain and PICA (Present in C-terminal of Ana-1) motif, respectively. Asterisks indicate the residues identical in all aligned sequences; colons: conserved substitutions; periods: semi-conserved substitutions. Identical residues determined by Cluster W2 are shown in red.

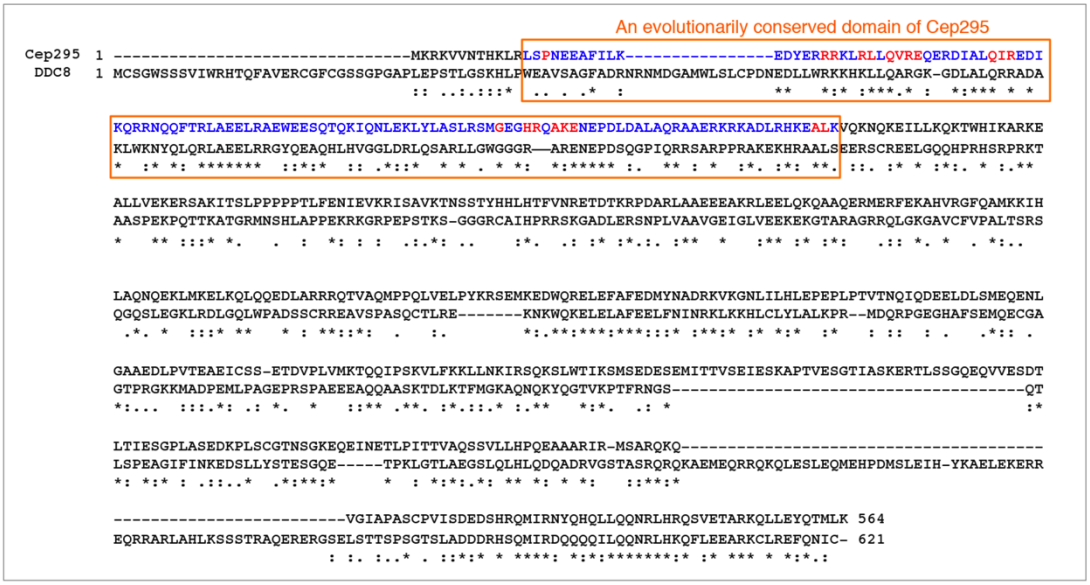

Figure 10: Alignments of DDC8 and the N-terminal domain of Cep295

The orange box indicates the PINA (Present in N-terminal of Ana-1) motif. Evolutionarily conserved residues are colored in red and others in blue. Asterisks indicate the residues identical in the aligned sequences; colons: conserved substitutions; periods: semi-conserved substitutions. This analysis was performed with ClustalW2.

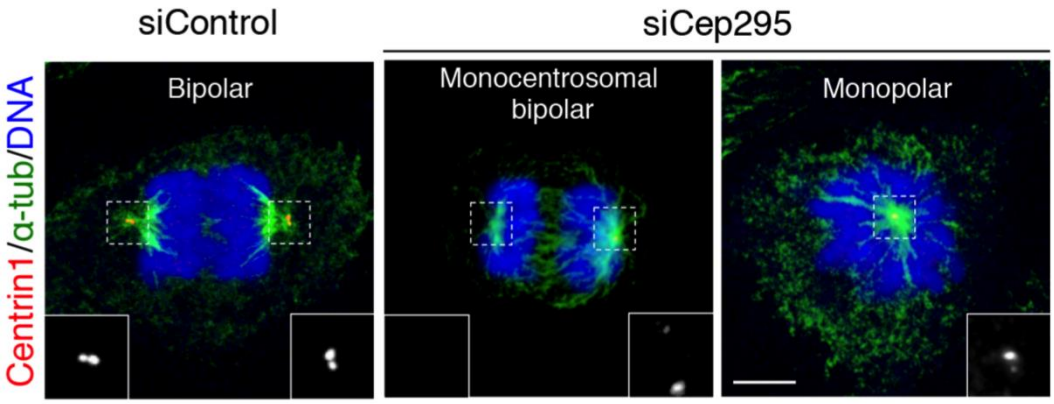

Figure 11: Cep295 ensures proper mitotic spindle and centriole formation
Cep295-depleted HeLa cells were stained with antibodies against centrin1 (red) and α-tubulin (green). Nuclei are shown in blue. Insets show approximately two-fold magnified views around the centrosome. Scale bar, 5 μm.

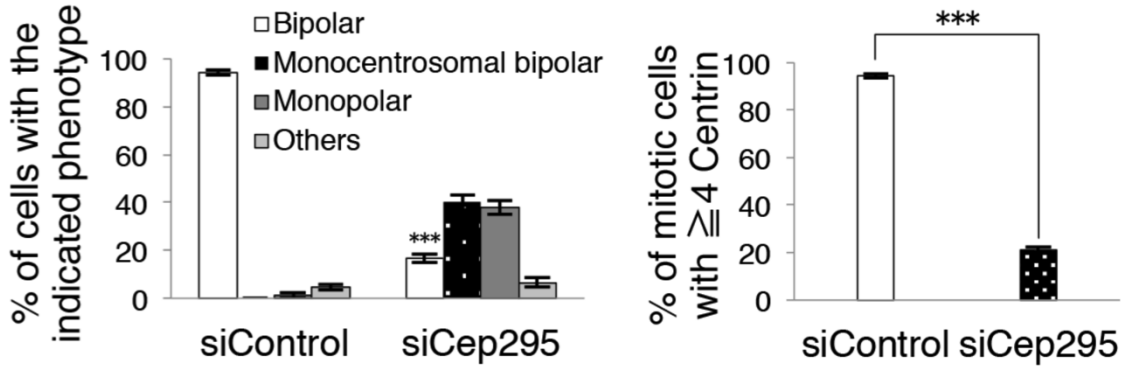

Figure 12: Cep295 is required for proper mitotic spindle and centriole formation
Histograms represent frequency of mitotic cells with the indicated phenotype (the left side) or with ≥4 centrin foci (the right side). Values are mean percentages ± standard error of the mean (s.e.m) from three independent experiments (N = 30 for each condition). ***, $P < 0.001$, (two-tailed t-test).

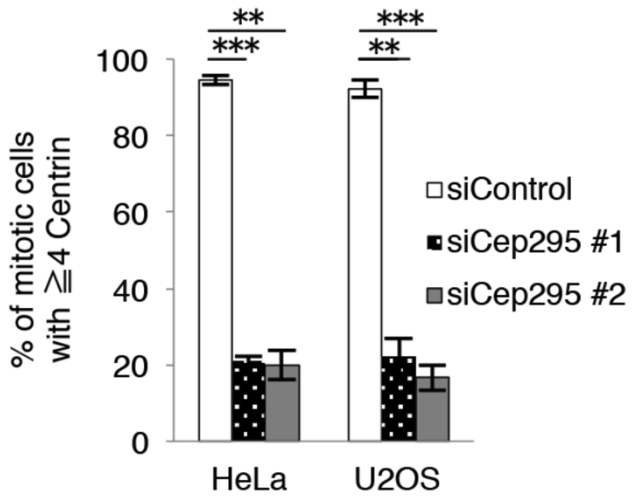

Figure 13: Cep295 is required for maintenance of the proper centriole number

HeLa and U2OS cells were treated with control siRNA or siRNA targeting against different sequences of Cep295 for 72 hours. Histograms represent frequency of mitotic cells with ≥4 centrin foci. Values are mean percentages ± s.e.m from three independent experiments ($N = 30$ for each condition). ***, $P < 0.001$; **, $P < 0.01$ (two-tailed *t*-test).

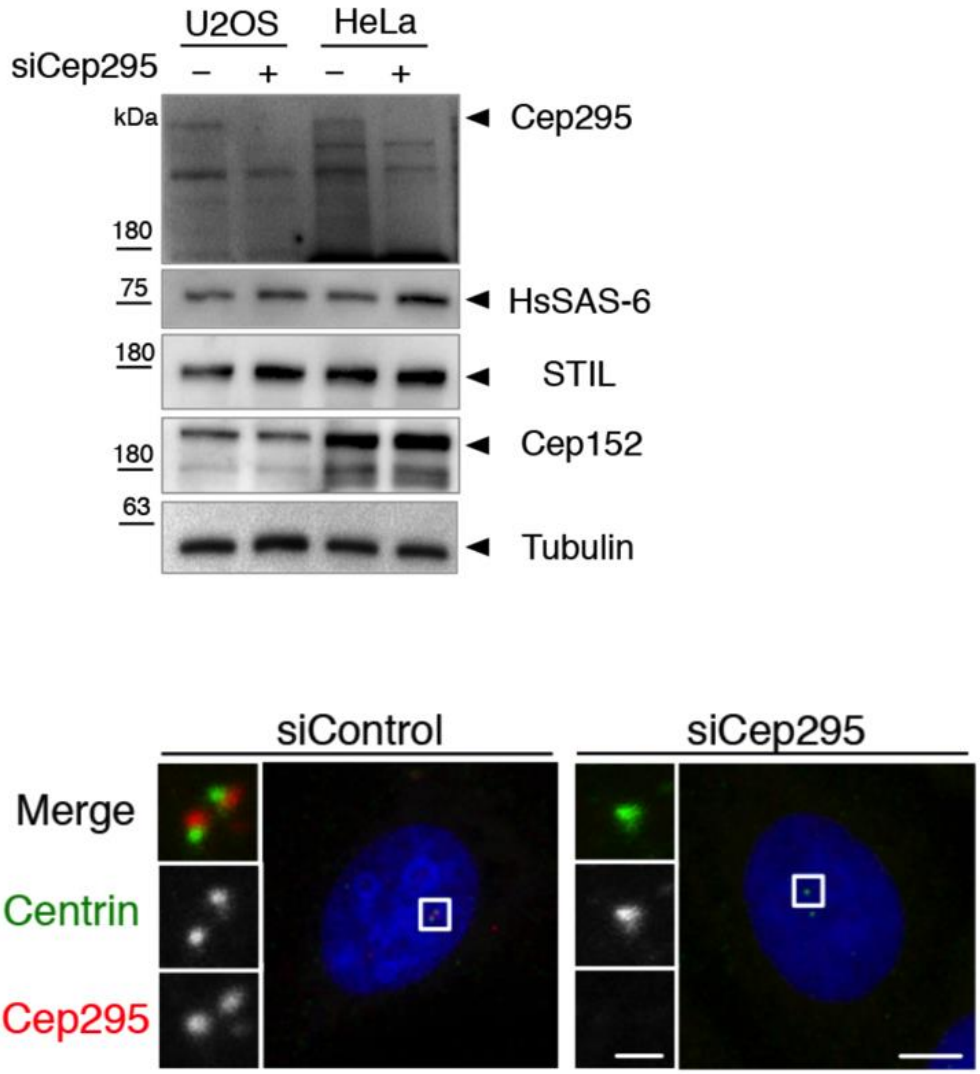

Figure 14: The efficiency of siRNA targeting Cep295 and the specificity of Cep295 antibody were confirmed by WB and immunofluorescence analyses

(WB analysis) HeLa and U2OS cells were treated with control siRNA or siRNA targeting Cep295 for 48 hours. Total cell lysates were analyzed by western blotting using Cep295, HsSAS-6, STIL, Cep152, or α-Tubulin antibodies, as indicated. The same result was obtained in 293T cells.

(Immunofluorescence analysis) Cep295-depleted HeLa cells were stained with antibodies against Cep295 (red) and centrin (green). Nuclei are shown in blue. Insets show approximately three-fold magnified views around the centrosome. Scale bars, 5 μm in the low-magnified view, 1 μm in the inset.

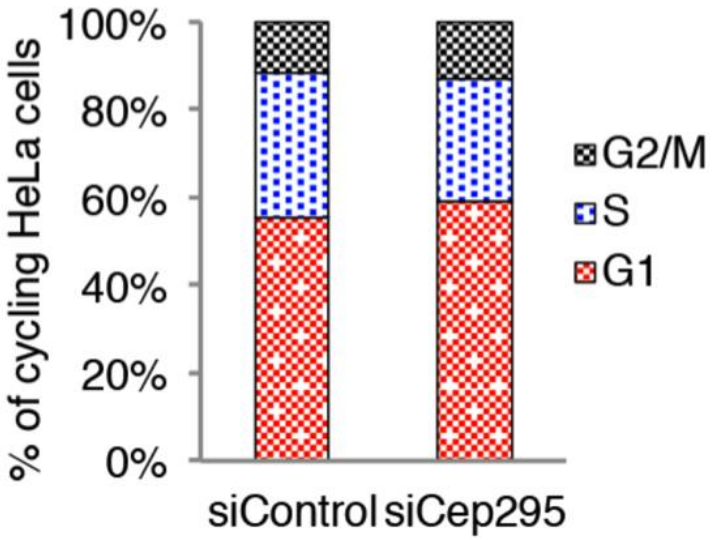

Figure 15: No significant difference in cell cycle between control and Cep295-depleted HeLa cells

The cell cycle phase of each control or Cep295-depleted cell was judged by the pattern of PCNA, centrin and DAPI staining. G1: interphase cells without PCNA; S: interphase cells with PCNA; G2: interphase cells with separate pairs of centrin foci; mitosis: mitotic cells with separate pairs of centrin foci and condensed nuclei.

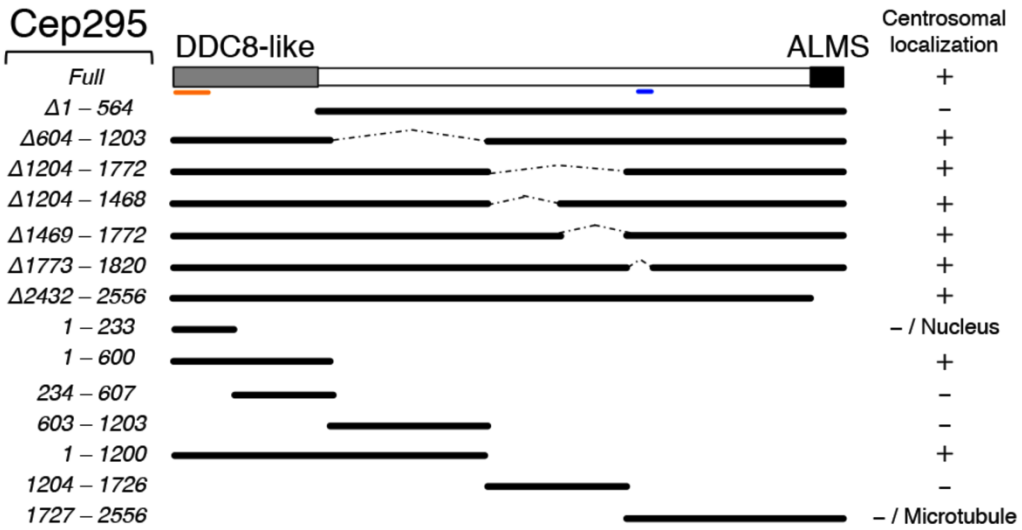

Figure 16: Schematic of full-length Cep295 and the deletion constructs used for immunofluorescence assay in HeLa cells

All constructs encode siRNA-resistant forms of Cep295. The table shows presence (+) or absence (-) of centriolar localization of the deletion mutant proteins examined in the cells depleted of endogenous Cep295.

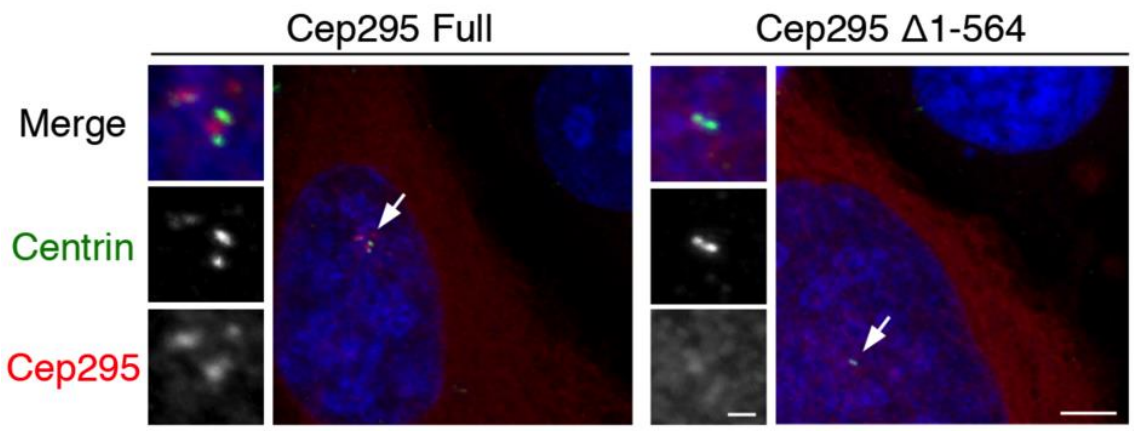

Figure 17: DDC8-like domain (aa 1-564) is required for centriolar localization of Cep295

The cells were stained with antibodies against Cep295 (red) and centrin (green). Nuclei are shown in blue. Arrows point to the centrioles. Scale bars, 5 μm in the low-magnified view, 1 μm in the inset.

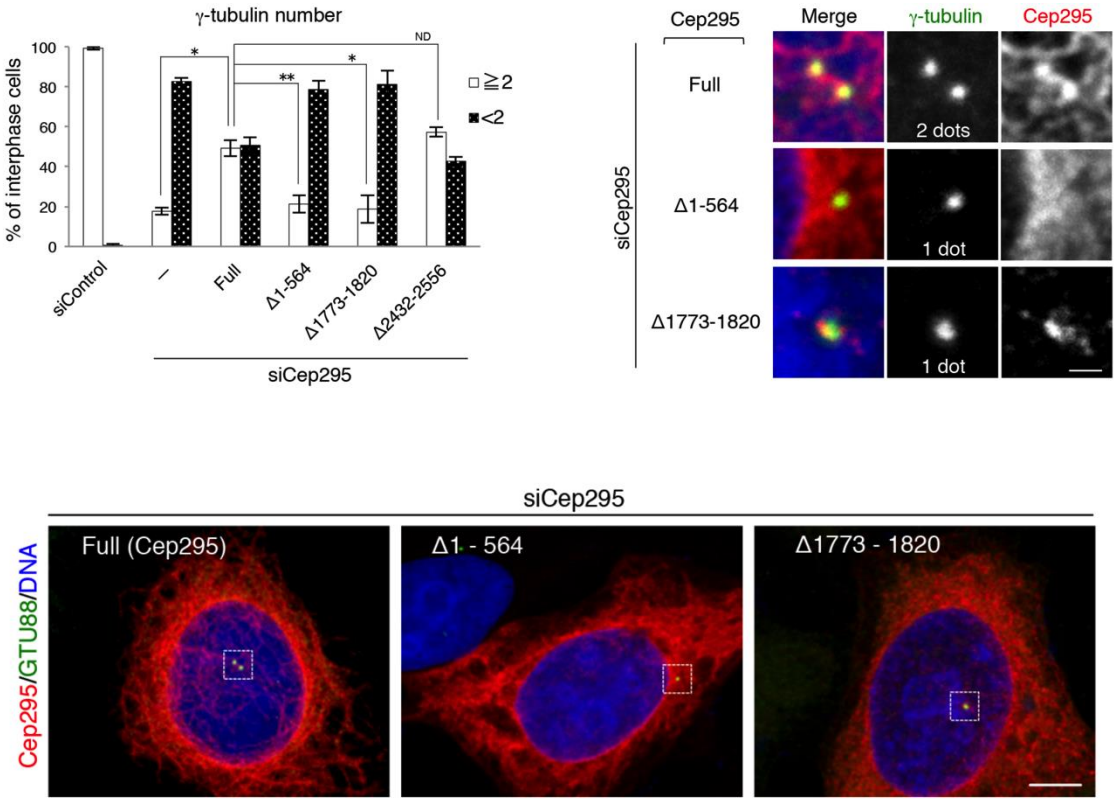

Figure 18: Rescue experiments of full-length Cep295 and the indicated mutants

For rescue experiments, Cep295-depleted HeLa cells were transfected with full-length Cep295 and the indicated mutants.

Histograms represent frequency of interphase cells with the indicated number of γ-Tubulin foci in each condition. Values are mean percentages ± s.e.m from three independent experiments (N > 50 for each condition). **, $P < 0.01$; *, $P < 0.05$; NS, not significant (two-tailed *t*-test).

(upper right panel) The cells were stained with antibodies against Cep295 (red) and γ-tubulin (green). Nuclei are shown in blue. Scale bar, 1 μm.

(lower panel) The low-magnified images shown in upper panel. Scale bar, 5 μm.

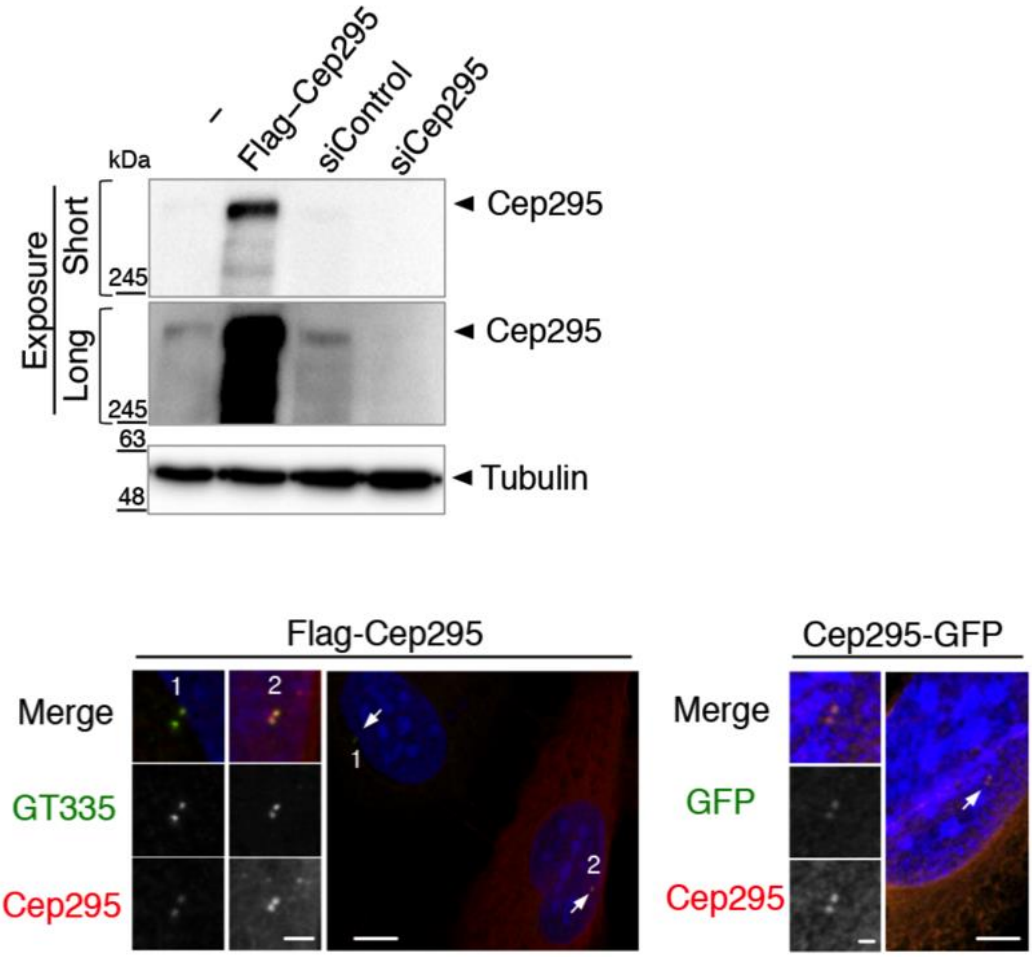

Figure 19: Quality control check for the exogenous expression of full-length Cep295 in human cells

(WB analysis) U2OS cells were transfected with an empty vector (–) or pCMV5 vector encoding Flag-tagged Cep295 full-length, and treated with control siRNA or siRNA targeting endogenous Cep295 for 48 hours. Total cell lysates were analyzed by western blotting using Cep295 or α-Tubulin antibodies.

(Immunofluorescence analysis) Immunofluorescence analysis revealed that Cep295 full-length proteins tagged with Flag at N-terminus (left side) or with GFP at C-terminus (right side) localized to the centriole. U2OS cells expressing the tagged Cep295 proteins were stained with the indicated antibodies. Nuclei are shown in blue. Insets show the magnified views of centrioles (arrows). Scale bars, 10 μm in the low-magnified view, 2 μm in the inset. 1: weakly expressed Cep295, 2: highly expressed Cep295 (exogenous). (left side). Scale bars, 5 μm in the low-magnified view, 1 μm in the inset (right side).

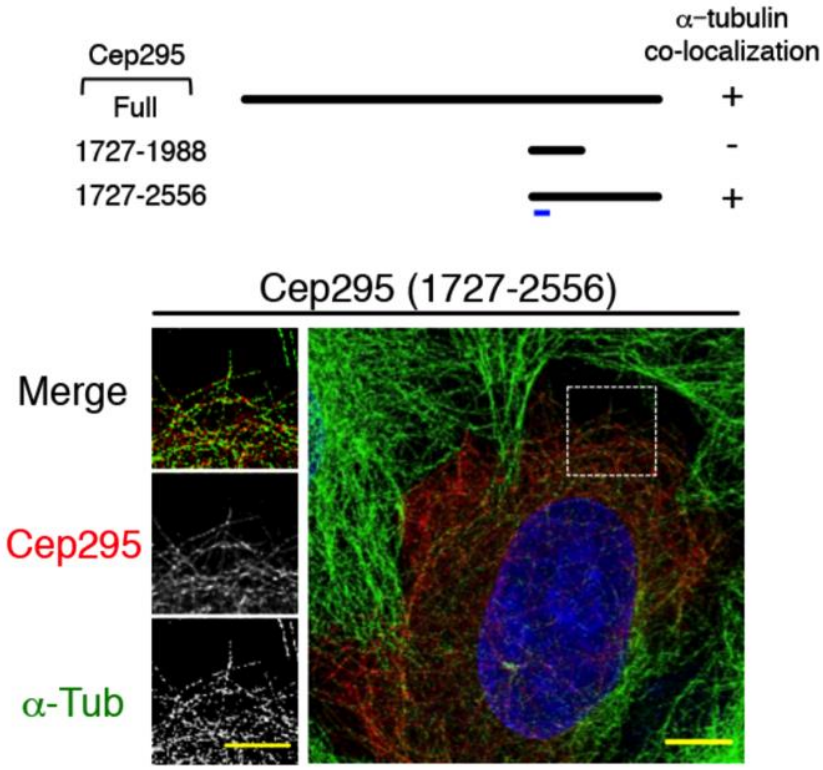

Figure 20: Expression of C-terminal region of Cep295 in human cells leads to formation of filamentous structures

U2OS cells were transfected with pCMV5 vector encoding Cep295 full-length, aa 1727-1988 or aa 1727-2556 for 24 hours. The cells were fixed and stained with antibodies against Cep295 (red) and α-tubulin (green). Note that Cep295 fragment (aa 1727-2556) co-localized with α-Tubulin. Insets show approximately two-fold magnified views. Scale bars, 5 μm in the low-magnified view, 2 μm in the inset.

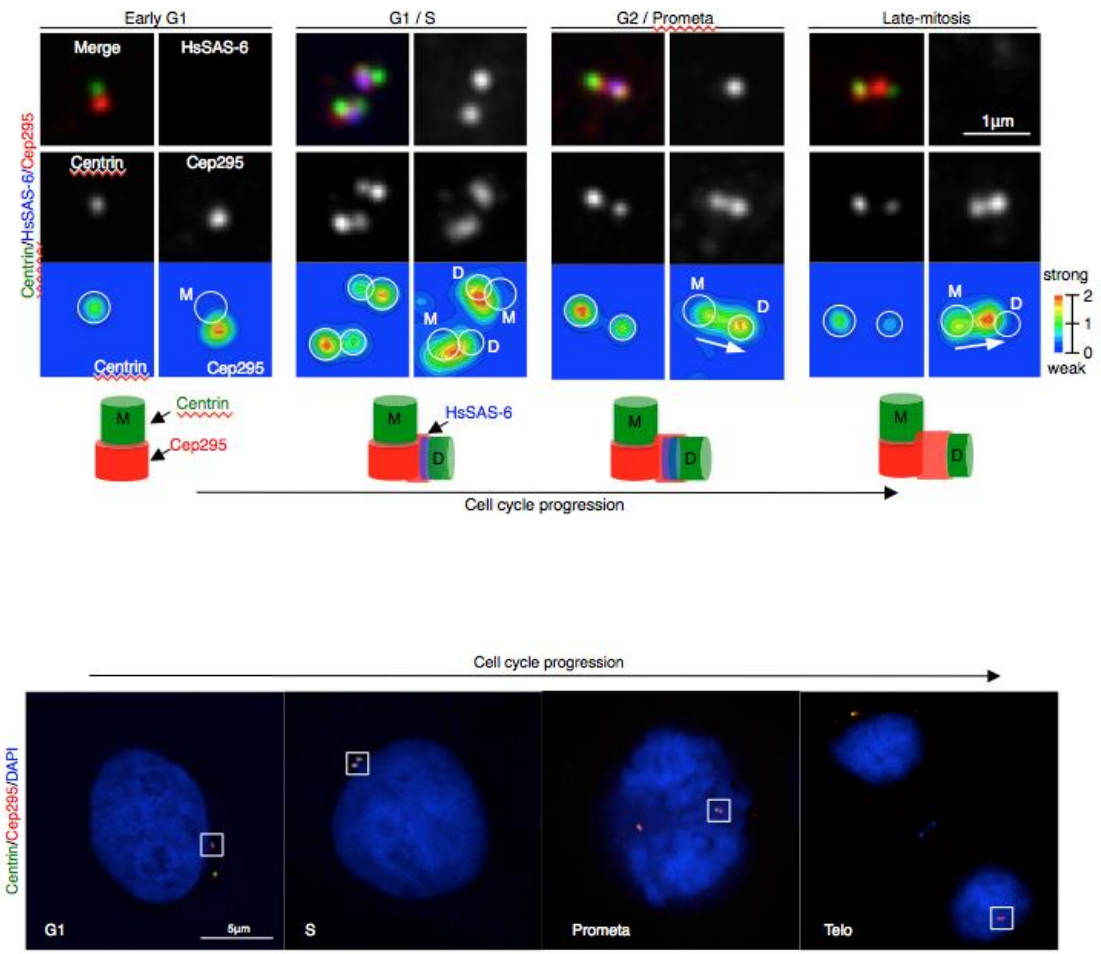

Figure 21: Centriolar distribution of Cep295 at different cell cycle stages

(upper right panel) HeLa cells were stained with the indicated antibodies. The bottom panels represent quantification of the local signal intensity of centrin (left) and Cep295 (right). The local signal intensity was visualized in the indicated colors (M: mother centriole; D: daughter centriole). The schematic models represent the localization of Cep295, HsSAS-6 and centrin during the cell cycle. Note that HsSAS-6 disappears in early G1 phase and late mitosis. In G1/S phase, the centrosomal linker connects the proximal end of two mother centrioles. Scale bar, 1 µm.

(lower panel) HeLa cells at different stages of the cell cycle were stained with the indicated antibodies. Nuclei are shown in blue. Magnification of the insets is shown in upper panel. Scale bar, 5 µm.

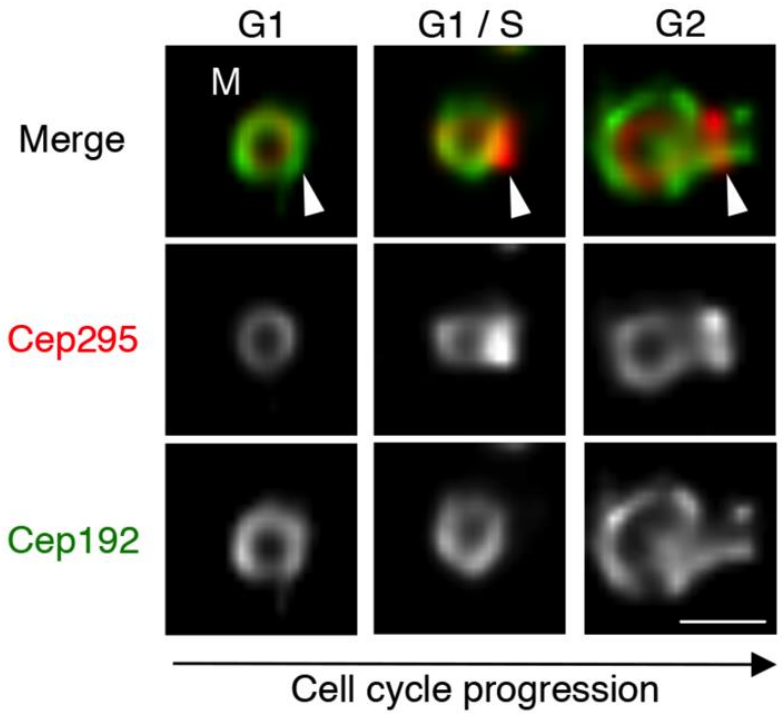

Figure 22: Cep295 localizes to the assembly site of a new daughter centriole in the earliest stage (arrowheads) and forms a ring-like structure

The images were obtained by TCS SP8 HSR system using antibodies against Cep192 (green) and Cep295 (red). Scale bar, 500 nm.

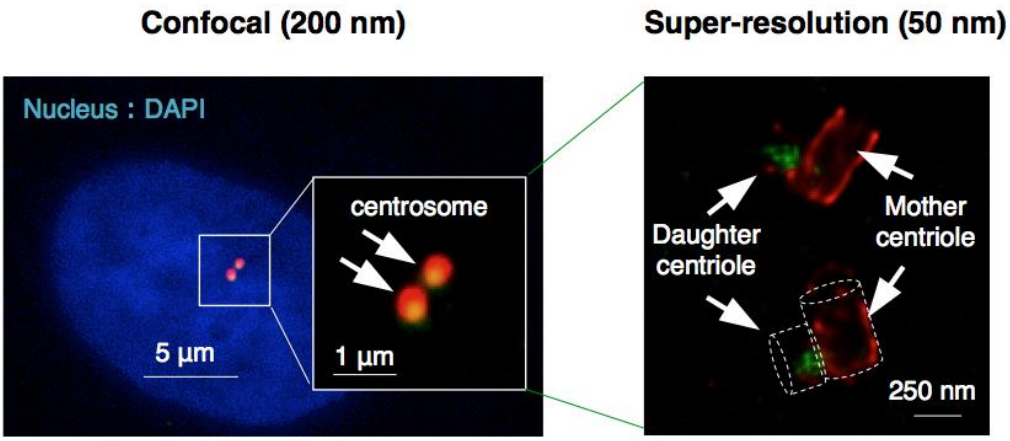

Figure 23: Confocal and super-resolution images

The images were obtained by confocal microscopy or stimulated emission depletion microscopy (STED) system using antibodies against HsSAS-6 (green) and Cep192 (red).

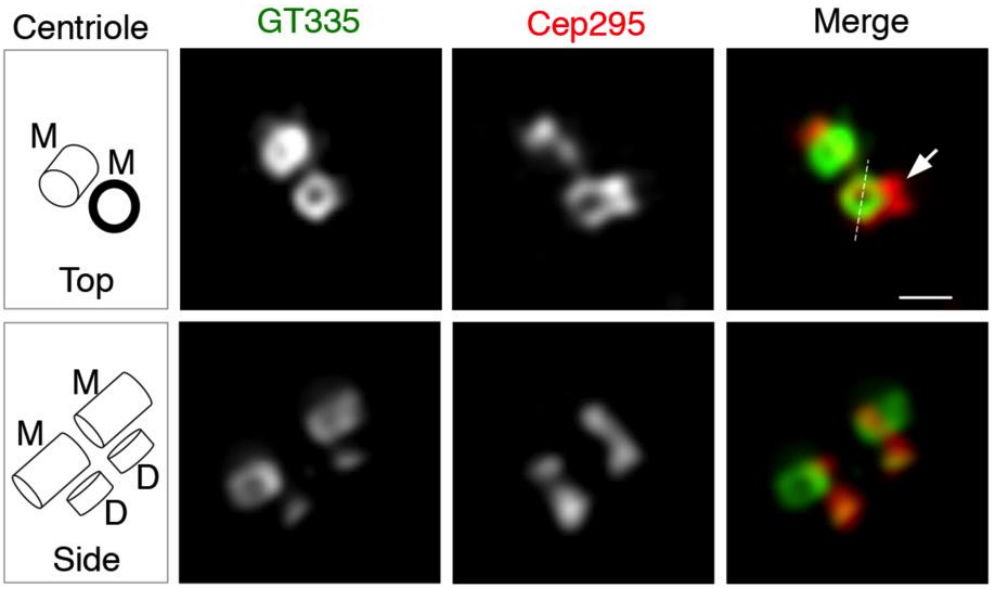

Figure 24: 3D-SIM images representing top and side views of Cep295 at mother centrioles

GT335 was used as a centriole wall marker. An arrow points to recruitment of Cep295 onto the daughter centriole wall before the glutamylation of centriolar mitrotubules. Scale bar, 400 nm.

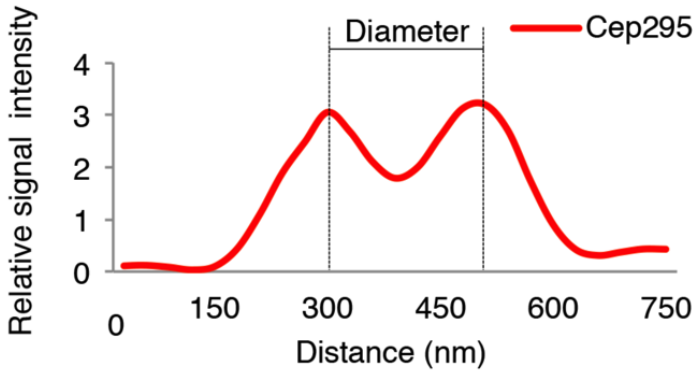

Protein	*Diameter (nm)*	*N*
Cep295 (Mother)	240 ± 10	9
GT335 (Mother)	221 ± 40	6

Figure 25: Quantification of the Cep295 diameter at mother centrioles

The graph shows the signal intensity of Cep295 at the mother centriole along the dotted line in Figure 24. For quantification of the diameter, the distances between intensity maxima were measured (mean ± s.d.).

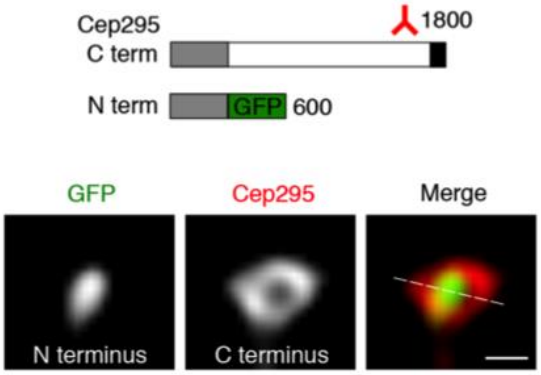

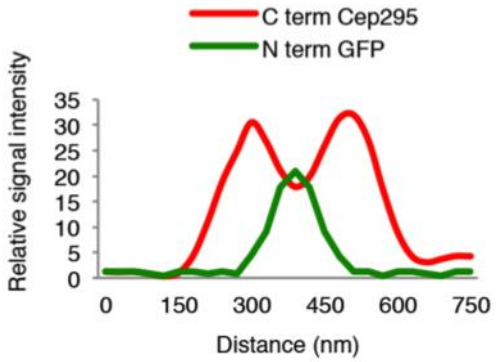

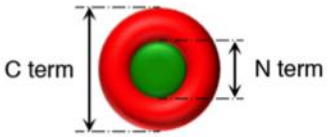

Cep295	*Diameter (nm)*	*N*
N terminus	219 ± 28	9
C terminus	446 ± 17	9

Figure 26: The orientation of Cep295 at centrioles

(upper right panel) Schematic diagrams for Cep295. The DDC8-like domain is shown in gray box, the ALMS domain in black box. To investigate the orientation of Cep295 within the centriole structure, we marked the N-terminal region of Cep295 with GFP-tag and the C-terminal region with a specific antibody raised against aa 1831-1932 of Cep295. Since tagging at the N-terminus of Cep295 somehow affects its localization and expression, the indicated Cep295 short fragment tagged with GFP at its C-terminus was used for marking the Cep295 N domain.

The images representing top view of Cep295 at mother centrioles were obtained by TCS SP8 HSR system using antibodies against GFP (green) and Cep295 (red). Scale bar, 200 nm.

(lower panel) The graph shows the signal intensity of Cep295 at the mother centriole along the dotted line in the images representing top view of Cep295. For quantification of the diameter, the distances between intensity maxima were measured.

Schematic representation of a top view of Cep295 at the mother centriole. The external diameter was measured for quantification (mean ± s.d.).

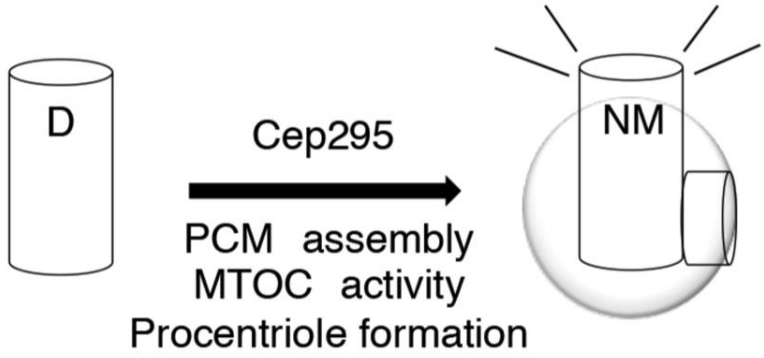

Figure 27: Clarification of the exact function of Cep295 in centrosome biogenesis
Schematic of Cep295 function described in 2.3.7

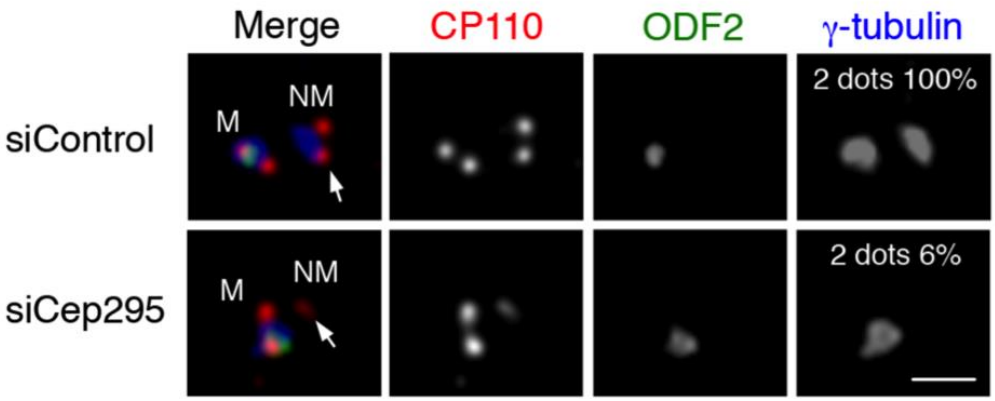

Figure 28: Three color staining of centrioles in control and Cep295-depleted cells
The cells were stained with antibodies against CP110 (red), γ-tubulin (blue) and ODF2 (green). ODF2 was used as an older mother centriole marker. Arrows point to a new mother centriole (M: older mother centriole; NM: new mother centriole). Scale bar, 1 μm

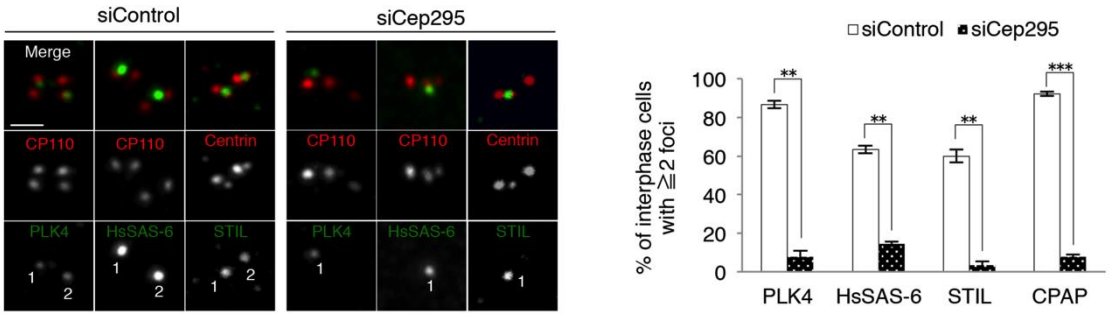

Figure 29: Cep295 is crucial for a new mother centriole to generate a procentriole
HeLa cells transfected with control siRNA or Cep295 siRNA for 72 hours were stained with indicated antibodies. CP110 and centrin were used as centriole markers. Scale bar, 1 μm. The number represents the number of Plk4/HsSAS-6/STIL foci.

Histograms represent frequency of interphase cells with ≧2 Plk4/HsSAS-6/STIL/CPAP foci in each condition. Values are mean percentages ± s.e.m from three independent experiments (N = 30 for each condition). ***, $P < 0.001$; **, $P < 0.01$, (two-tailed t-test).

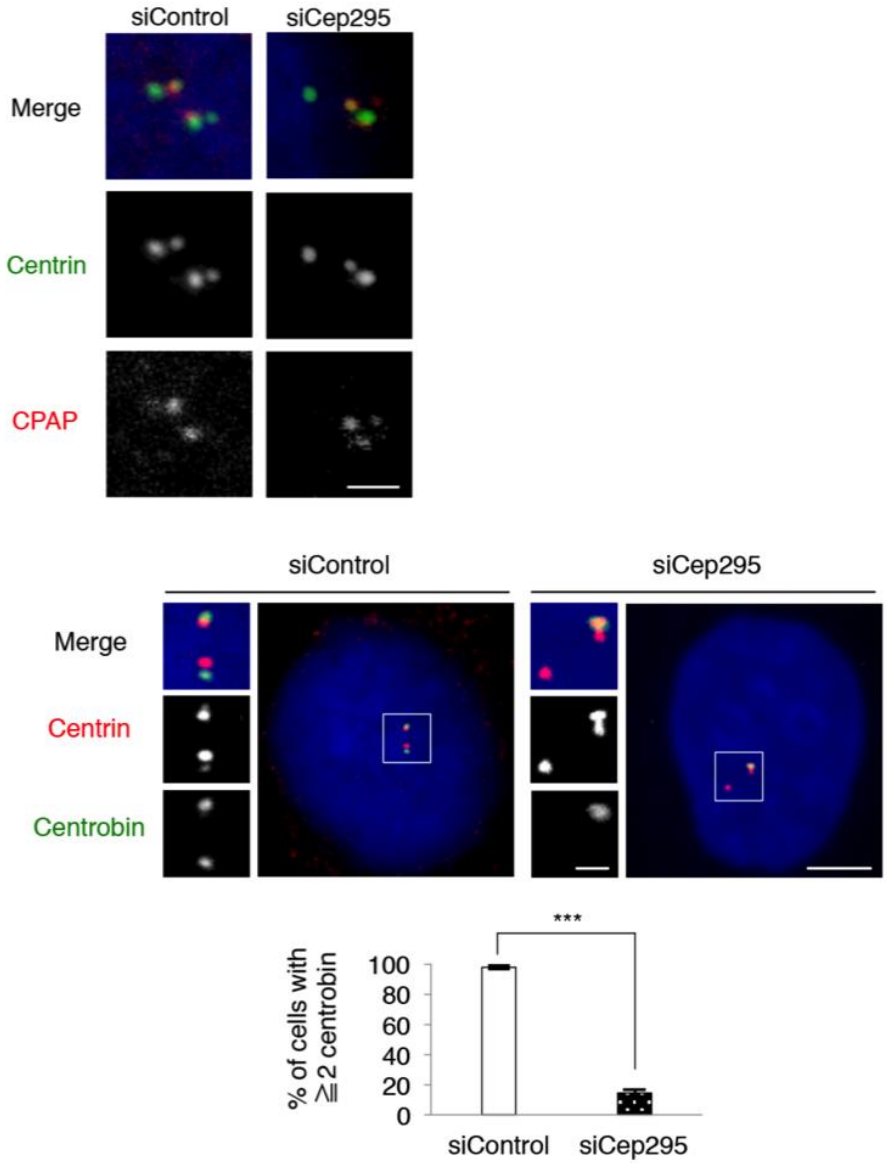

Figure 30: CPAP and centrobin were reduced at the new mother centriole in Cep295-depleted cells

HeLa cells transfected with control siRNA or Cep295 siRNA for 72 hours were stained with the indicated antibodies. Nuclei are shown in blue. Histograms represent frequency of interphase cells with ≥2 centrobin foci. Values are mean percentages ± s.e.m from three independent experiments ($N = 30$ for each condition). ***, $P < 0.001$, (two-tailed *t*-test). Scale bar, 1 μm (upper panel). Scale bars, 5 μm in the low-magnified view, 1 μm in the inset (lower panel).

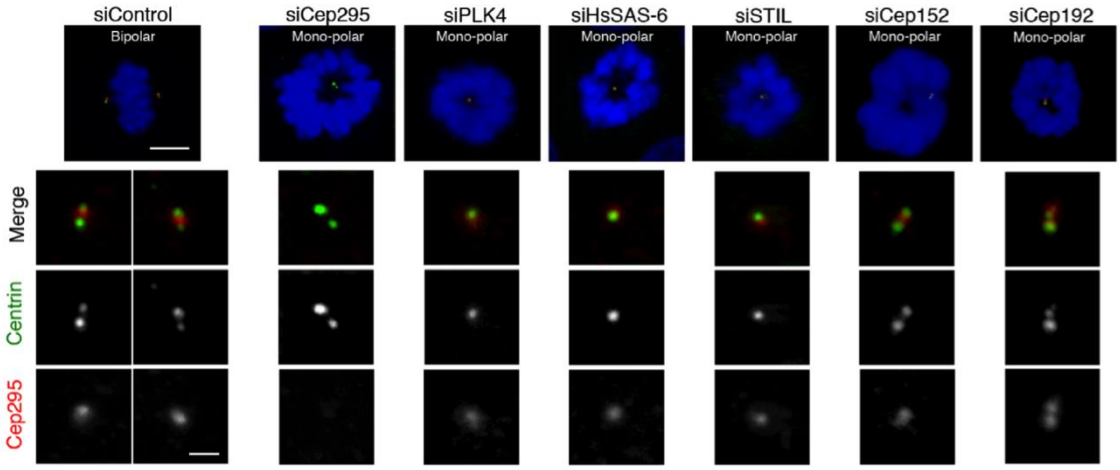

Figure 31: Depletion of critical factors for centriole formation did not affect Cep295 localization at the mother centriole

HeLa cells transfected with control siRNA or the indicated siRNAs for 48 hours were stained with antibodies against centrin1 (green) or Cep295 (red). Nuclei were shown in blue. To make sure the efficiency of each RNAi treatment, I chose the mitotic cells having only one or two centrin foci and thus being indicative of defects in centriole formation. Scale bars, 5 μm in the low-magnified view, 1 μm in the inset.

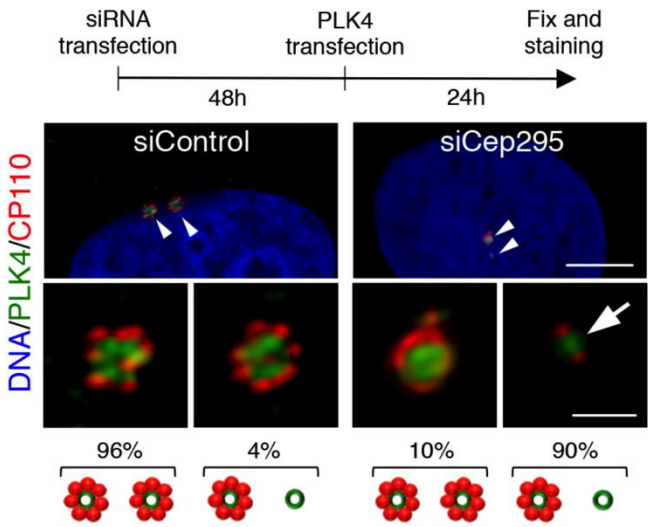

Figure 32: The effects of Cep295 depletion on centriole overduplication induced by Plk4 overexpression in human cells

HeLa cells were treated with control siRNA or Cep295 siRNA, followed by transfection with an empty vector (–) or, pCMV5-Plk4ΔPEST-FLAG wild-type. The cells were stained with antibodies against Flag (green) or CP110 (red). An arrow points to the defect in multiple centriole formation induced by PLK4 over-expression, upon Cep295 depletion. Scale bars, 5 μm in the low-magnified view, 1 μm in the inset. Schematic illustrations show frequency of interphase cells with 2 or 1 over-duplicated centriole foci.

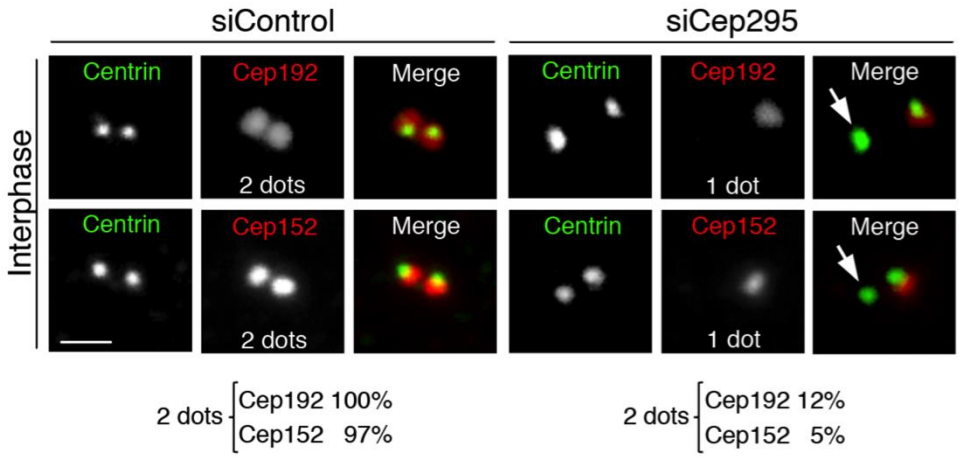

Figure 33: Cep295 is crucial for a new mother centriole to organize a functional PCM

Cep295-depleted HeLa cells were stained with the indicated antibodies. Almost all control cells harbor ≥2 Cep192 and ≥2 Cep152 foci per cell, whereas only 12% and 5% of Cep295-depleted cells have ≥2 Cep192 and ≥2 Cep152 foci per cell, respectively. Scale bar, 1 μm

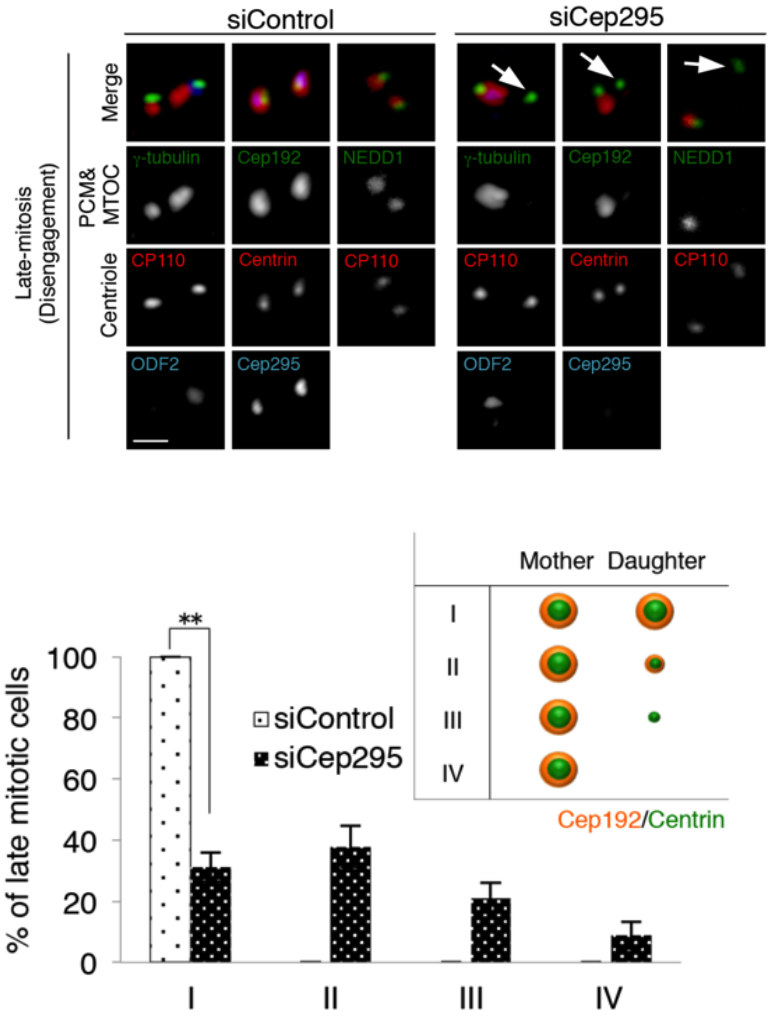

Figure 34: Cep295 is crucial for a new mother centriole to organize a functional PCM

To monitor the expression levels of Cep295 at the mother and daughter centrioles, the triple staining analysis was performed with the indicated antibodies as shown in the representative panels. HeLa cells were transfected with control or Cep295 siRNA for 24 hours. Arrows point to the defective recruitment of PCM components in the Cep295-depleted cells just after disengagement. Scale bar, 1 μm.

Histograms represent frequency of late mitotic cells with the indicated category in each condition. Values are mean percentages ± s.e.m from three independent experiments (N = 30 for each condition). **, $P < 0.01$, (two-tailed t-test).

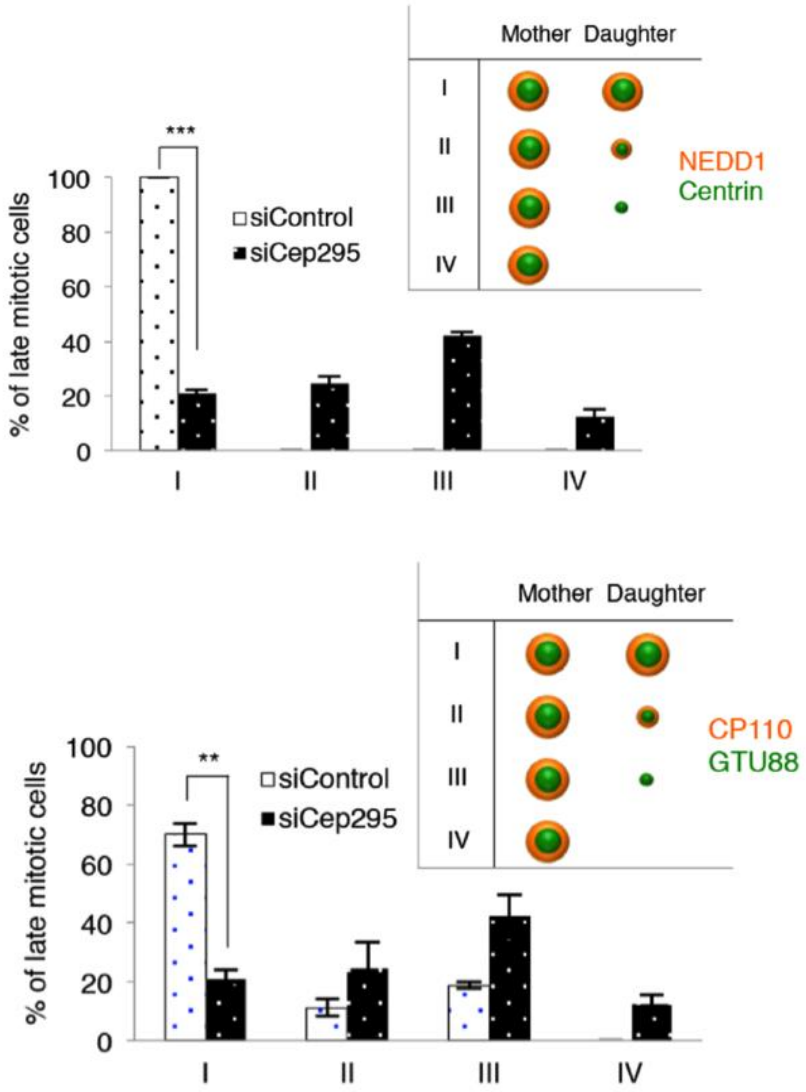

Figure 35: Quantification of the experiments shown in Figure 34

Histograms represent frequency of late mitotic cells with the indicated category. Values are mean percentages ± s.e.m from three independent experiments (N = 30 for each condition). ***, $P < 0.001$; **, $P < 0.01$, (two-tailed t-test).

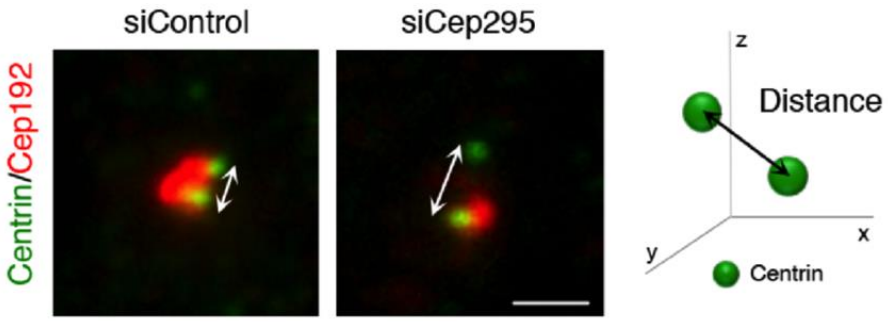

Late-anaphase	*Distance (3D)*	*N*
siControl	0.98 ± 0.028 µm	24
siCep295	1.55 ± 0.061 µm	18

Figure 36: Depletion of Cep295 causes early disengagement during late mitosis HeLa cells treated with control or Cep295 siRNA for 24 hours were stained with antibodies against centrin1 (green) and Cep192 (red). The 3D distances between the two centrin foci were measured for late-anaphase centrioles (mean ± s.d.). Scale bar, 1 µm.

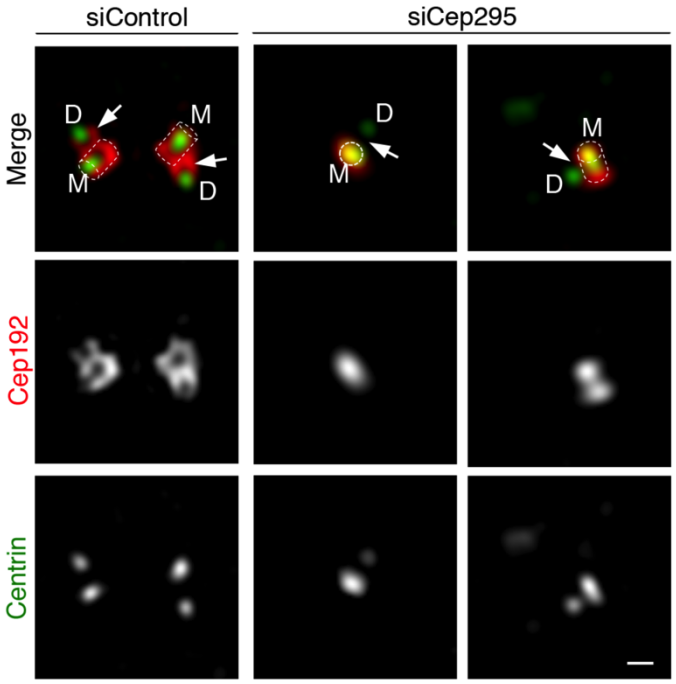

Figure 37: Depletion of Cep295 causes the defective distribution of Cep192

3D-SIM images represent centriolar distribution of Cep192 in control and Cep295-depleted HeLa cells (M: mother centriole; D: daughter centriole). Arrows point to the daughter centriole wall ($N = 5$). Dotted lines indicate the shape of centriole cylinders in this figure. Scale bar, 400 nm.

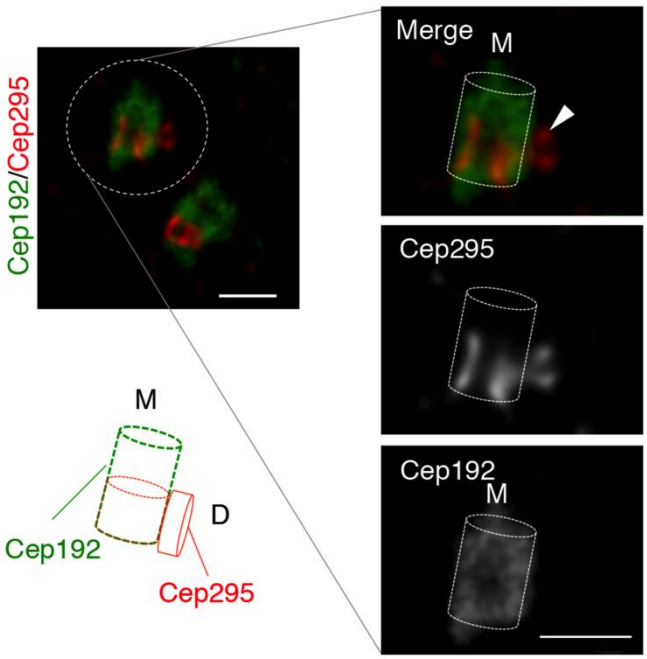

Figure 38: The centriolar localization of Cep295 and Cep192

U2OS cells were transfected with Flag-tagged Cep192 plasmid for 24 hours. The cells were fixed and stained with antibodies against Flag (green) and Cep295 (red) for STED microscope. The right panels show magnified views. Arrowhead points to the cap-like structure of Cep295 at the procentriole assembly site before recruitment of Cep192 (N = 10). Scale bar, 500 nm. The schematic illustrates the centriolar localization of Cep295 and Cep192.

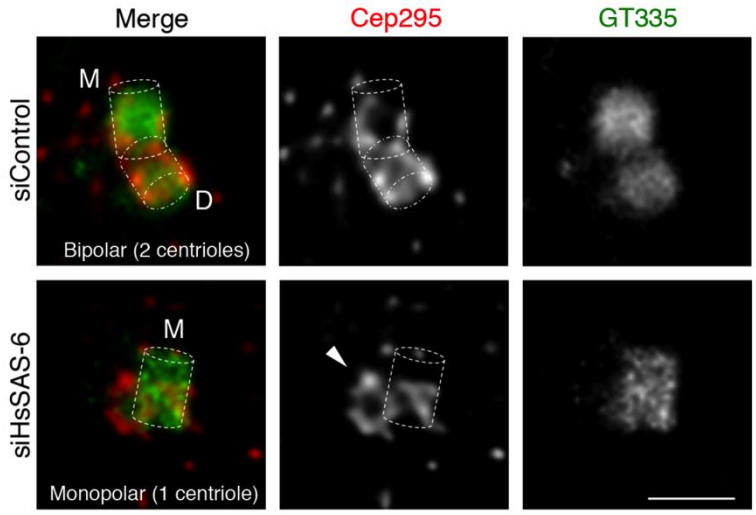

Figure 39: STED images showing centriolar distribution of Cep295 in the presence or absence of HsSAS-6

HeLa cells were treated with control siRNA or HsSAS-6 siRNA for 48-60 hours and stained with antibodies against GT335 (green) and Cep295 (red). To make sure the efficacy of HsSAS-6 depletion, we chose the Hs-SAS-6-depleted cells having only one mother centriole with a mono-polar spindle. Arrowhead shows centriolar distribution of Cep295 without the cartwheel structure ($N = 3$). Scale bar, 500 nm.

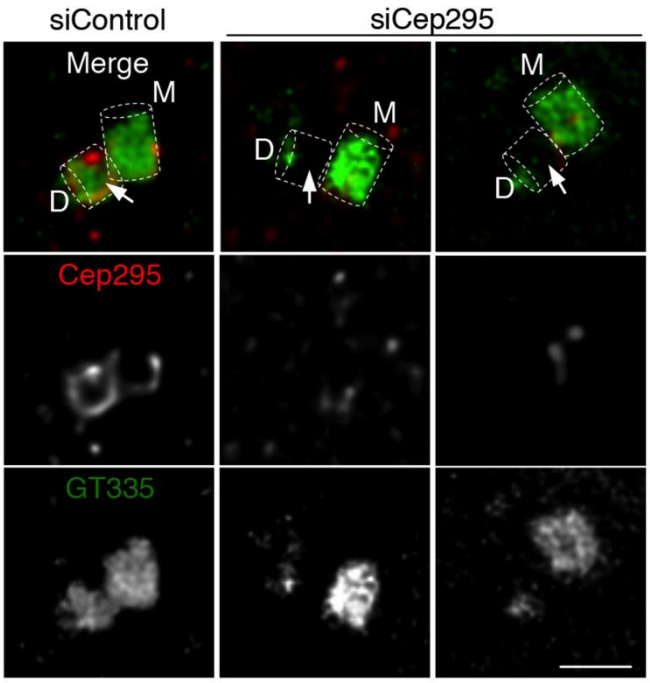

Figure 40: Depletion of Cep295 causes the defective procentriole formation
Control and Cep295-depleted HeLa cells were visualized by STED microscope using the indicated antibodies. Arrows point to poly-glutamylation of centriolar microtubules stained with GT335 antibody at the daughter centrioles ($N = 3$). Scale bar, 500 nm.

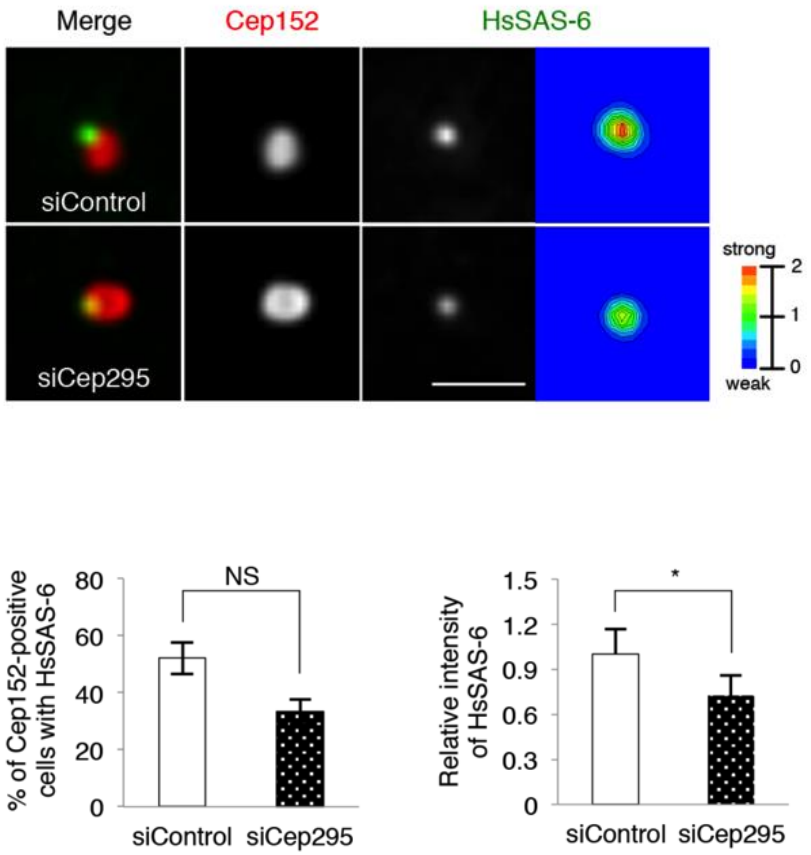

Figure 41: Depletion of Cep295 leads to the defective centriole formation

Cep295 depletion results in defective recruitment of HsSAS-6. HeLa cells were transfected with control siRNA or Cep295 siRNA, and stained with antibodies against HsSAS-6 (green) and Cep152 (red). Cep152 was used as a mother centriole marker. Scale bar, 1 μm.

(left side) The panels represent quantification of the local signal intensity of HsSAS-6. The local signal intensity was visualized in the indicated colors.

(middle side) Histograms represent frequency of Cep152-positive cells with HsSAS-6

(right side) Histograms represent relative signal intensity of HsSAS-6. Values are mean percentages ± s.e.m from three independent experiments (N > 15 for each condition). *, $P < 0.05$; NS, not significant (two-tailed *t*-test).

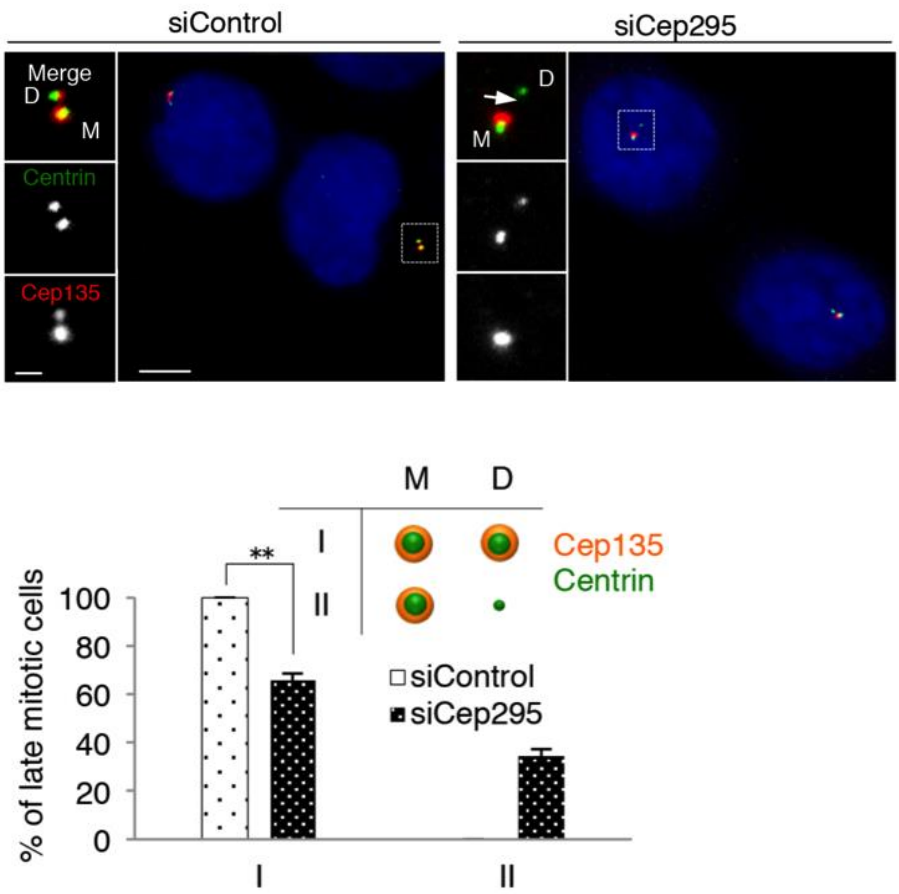

Figure 42: Cep295 is crucial for the integrity of a newly born daughter centriole at the older mother centriole

HeLa cells treated with control siRNA or siRNA targeting endogenous Cep295 for 24 hours were stained with antibodies against centrin1 (green) and Cep135 (red; a proximal component of centrioles). Nuclei are shown in blue. The arrow indicates defective recruitment of Cep135 to the disengaged daughter centriole. Scale bars, 5 μm in the low-magnified view, 1 μm in the inset.

Histograms represent frequency of late-mitotic cells with the indicated category in each condition. Values are mean percentages ± s.e.m from three independent experiments (N = 30 for each condition). **, $P < 0.01$, (two-tailed t-test).

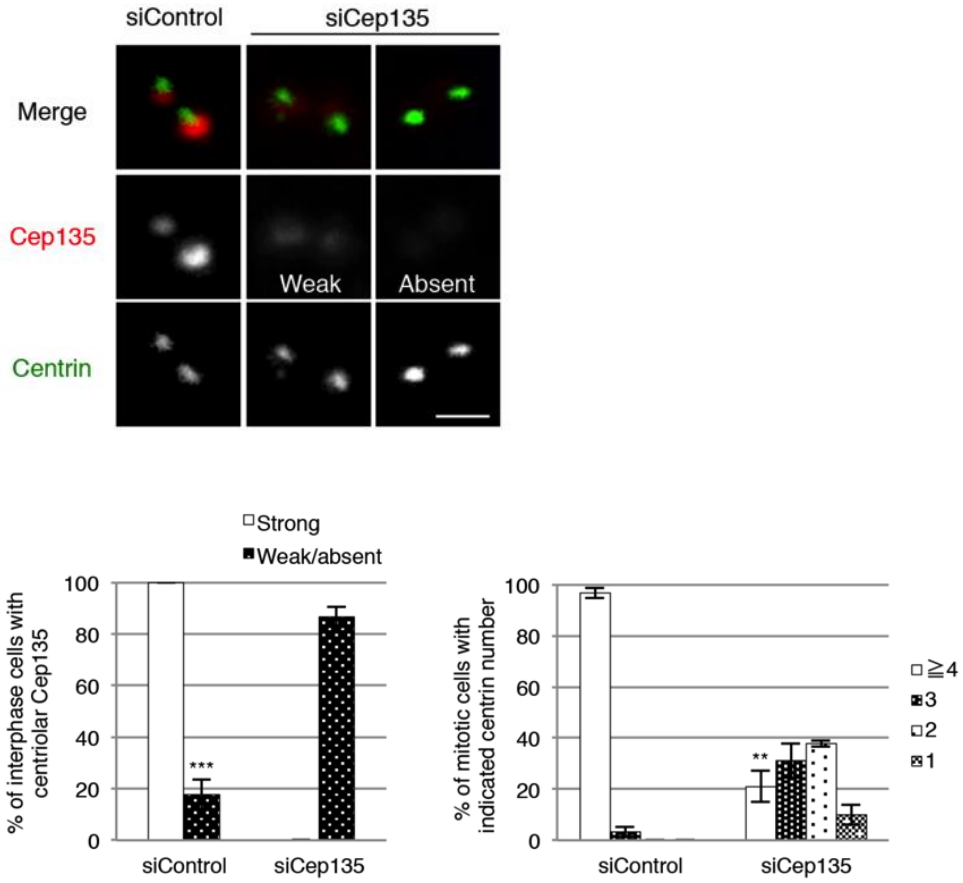

Figure 43: Cep135 depletion results in defective centriole formation

(left side) U2OS cells were transfected with control siRNA or Cep135 siRNA for 4 days. Scale bar, 1 μm.

(middle side) Histograms represent frequency of interphase cells with the indicated intensity of centriolar Cep135.

(right side) Histograms represent frequency of mitotic cells with the indicated number of centrin foci (h). Values are mean percentages ± s.e.m from three independent experiments (N = 30 for each condition). ***, $P < 0.001$; **, $P < 0.01$, (two-tailed t-test).

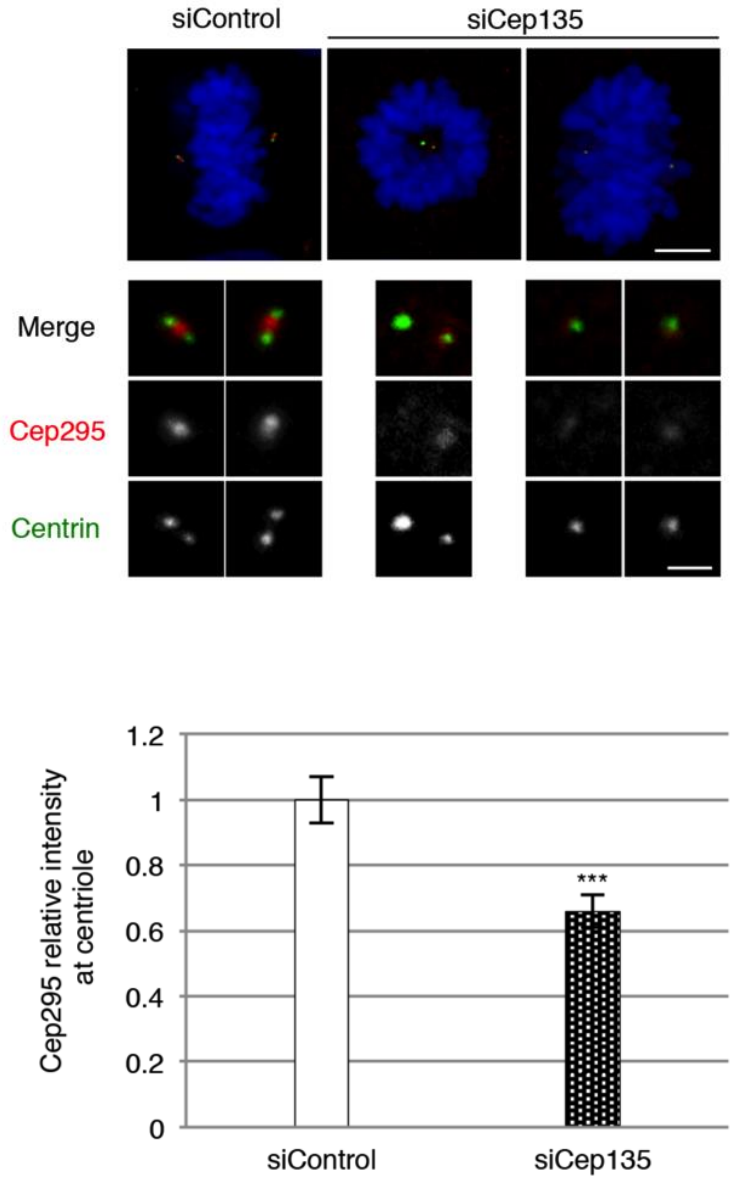

Figure 44: Cep135 depletion reduces Cep295 intensity at centrioles

U2OS cells were transfected with control siRNA or Cep135 siRNA for 4 days. Scale bar, 5 μm. Histograms represent the relative intensity of centriolar Cep295. Values are mean percentages ± s.e.m from three independent experiments (N = 20 for each condition). ***, $P < 0.001$, (two-tailed t-test).

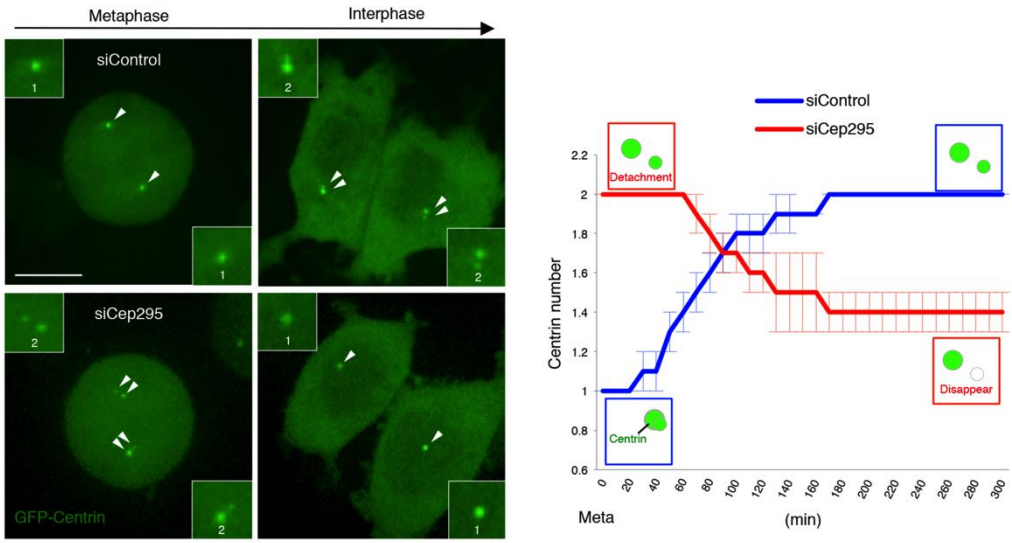

Figure 45: Depletion of Cep295 causes centriole disassembly

Live imaging of cycling HeLa cells expressing GFP-centrin1 (green) and treated with control siRNA or Cep295 siRNA. Representative images are shown in (d). Scale bar, 10 μm. Arrowheads point to GFP-centrin foci. Insets show magnified images of the fluorescent foci. The numbers in the insets indicate the number of GFP-centrin foci. (e) Quantification of the number of centrin foci in HeLa cells treated with control siRNA or Cep295 siRNA over time. Means ± s.e.m are shown (n =10). Time zero corresponds to the start of metaphase.

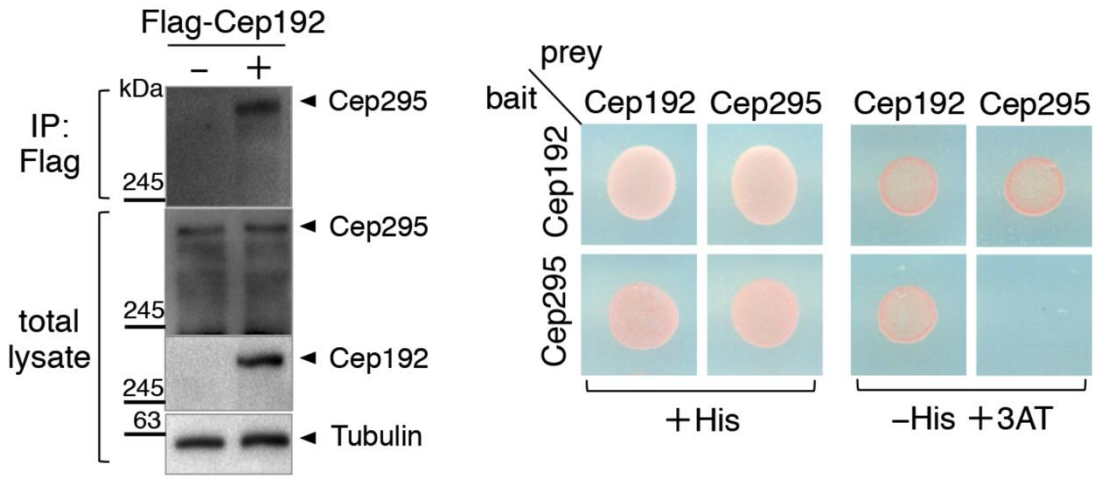

Figure 46: Physical interaction between endogenous Cep295 and Cep192

U2OS cells were transfected with Flag-tagged Cep192 full-length for 24 hours. The proteins were then immunoprecipitated from cell lysates with Flag beads. Total cell lysate and immunoprecipitates (IPs) were analyzed by western blotting using Flag, Cep295 or α-tubulin (loading control) antibodies. The same result was obtained in 293T cells.

Yeast two-hybrid assay showing the interaction between full-length Cep192 and full-length Cep295. The indicated clones were grown on the plates lacking histidine and containing 50 mM 3-AT at 30℃.

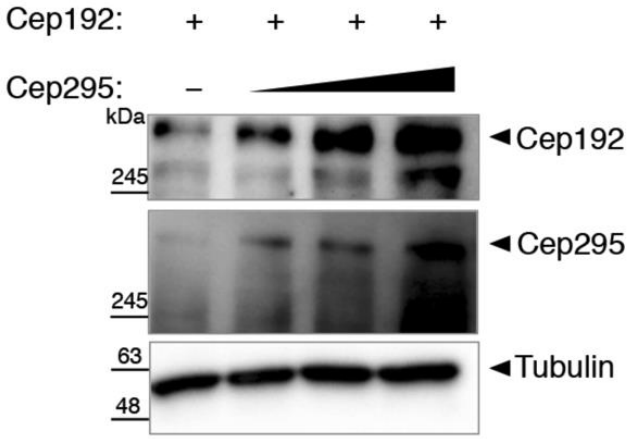

Figure 47: Cep295 promotes Cep192 stabilization in a concentration-dependent manner

U2OS cells were transfected with the constant amount of Flag-Cep192 vector and also with various amounts of Flag-Cep295 vector. Total protein levels in each condition were analyzed by western blotting with antibodies against Cep192, Cep295 and tubulin (loading control).

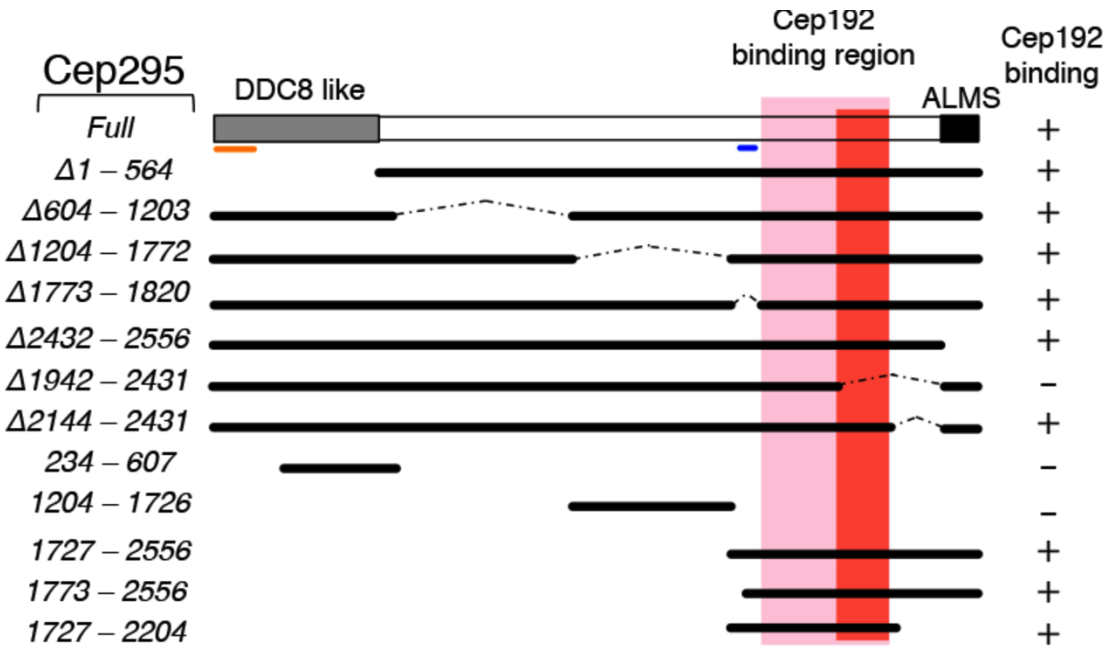

Figure 48: Schematic of full-length Cep295 and the deletion mutants used for co-IP assays with Flag-tagged full-length Cep192 in U2OS cells

The sufficient and necessary regions for Cep192-binging in Cep295 are represented in pink and red, respectively. The DDC8-like domain, ALMS domain, and two evolutionarily conserved domains are indicated.

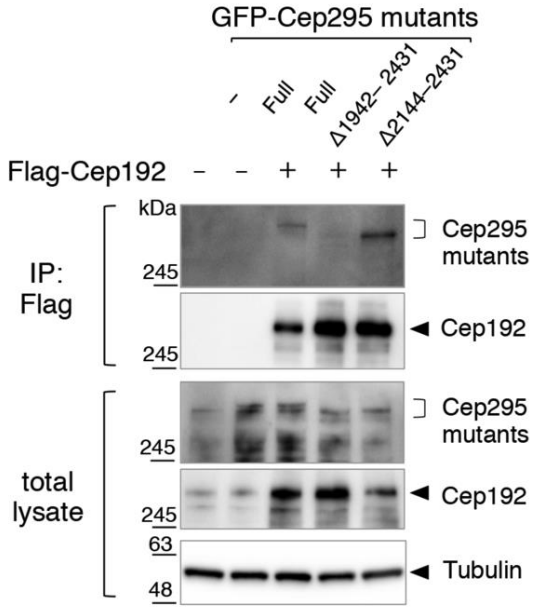

Figure 49: Co-immunoprecipitation assay in U2OS cells testing interaction between Flag-Cep192 and the indicated Cep295-GFP deletion mutants

The Flag-tagged proteins were immunoprecipitated using Flag beads from the cell lysate. Total cell lysates and IPs were analyzed by western blotting using the indicated antibodies.

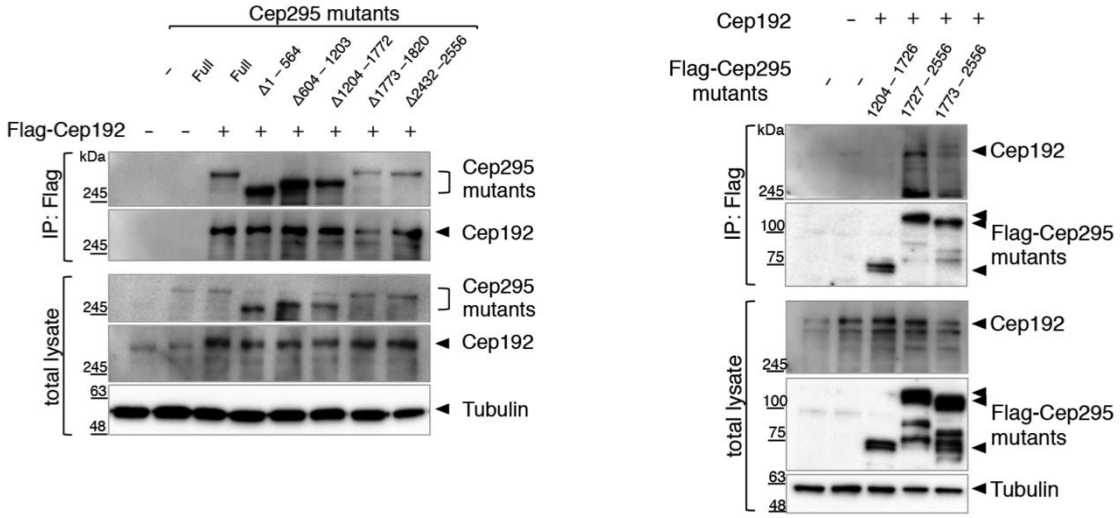

Figure 50: Co-immunoprecipitation assay

Co-immunoprecipitation assay in U2OS cells testing interaction between Flag-Cep192 and the indicated Cep295 deletion mutants in (left side), between non-tagged Cep192 and Flag-Cep295 deletion mutants in (right side). The Flag-tagged proteins were immunoprecipitated using Flag beads from the cell lysate. Total cell lysates and IPs were analysed by western blotting using the indicated antibodies.

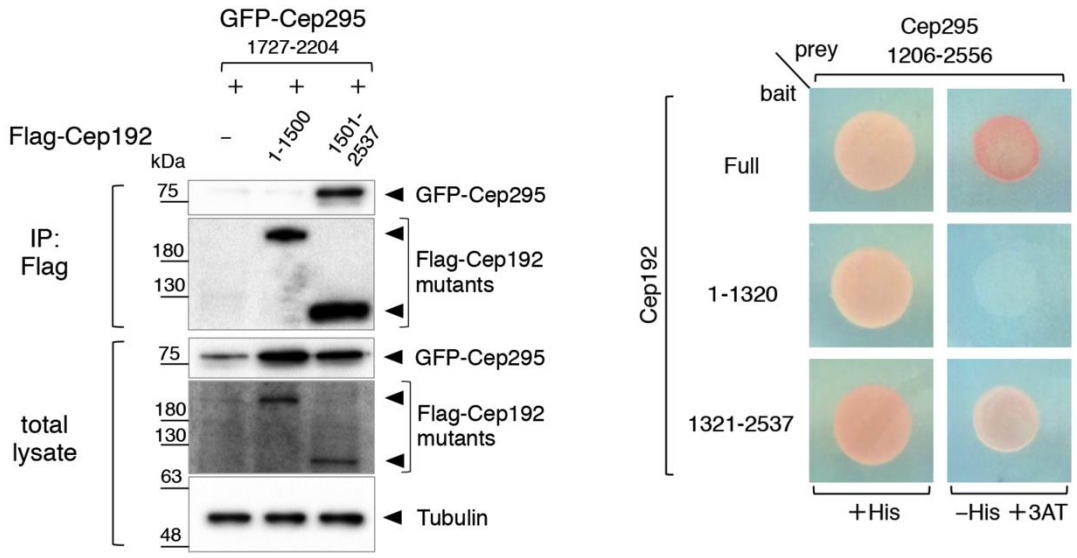

Figure 51: Interaction between Cep295 fragment containing the Cep192-interacting region and N-terminal or C-terminal fragment of Cep192

Co-immunoprecipitation assay in U2OS cells testing interaction between Cep295 fragment containing the Cep192-interacting region and N-terminal or C-terminal fragment of Cep192. The Flag-tagged proteins were immunoprecipitated using Flag beads from the cell lysate. Total cell lysates and IPs were analyzed by western blotting using the indicated antibodies.

Yeast two-hybrid assay for testing interaction between the full-length or fragments of Cep192 and the C-terminal fragment of Cep295. The indicated clones were grown on the plates lacking histidine and containing 50 mM 3-AT.

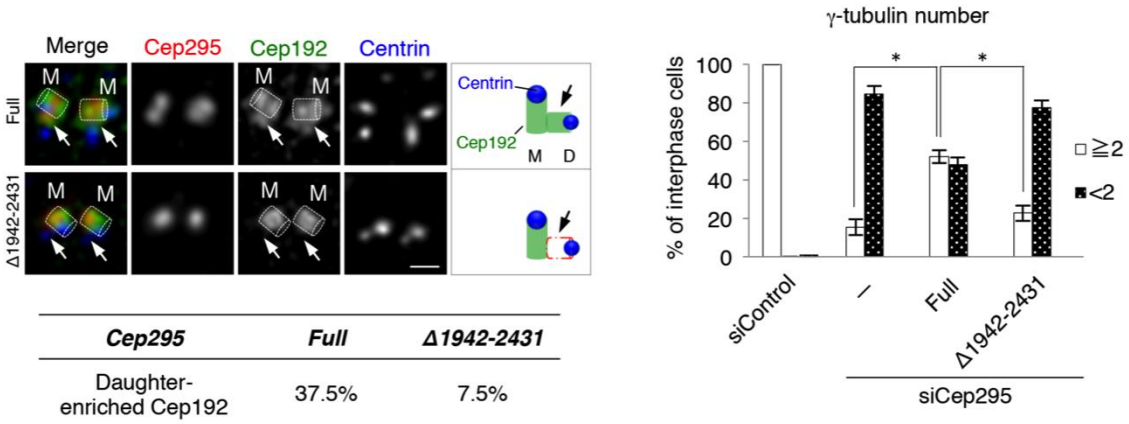

Cep295	*Full*	*Δ1942-2431*
Daughter-enriched Cep192	37.5%	7.5%

Figure 52: Interaction between Cep295 and Cep192 is required for the recruitment of Cep192 to a newly formed daughter centriole

Three color staining of Cep295-depleted HeLa cells expressing full-length Cep295 and the mutant protein lacking aa 1942-2431. The phenotype was analyzed mostly in the first round of cell cycle (~48 hours after the RNAi treatment). The cells were analyzed by TCS SP8 HSR system using antibodies against Cep192 (green), Cep295 (red) and CP110 (blue). Arrows point to the daughter centriole wall. M: mother centriole indicated as a cylinder. Scale bar, 1 μm.

For rescue experiments, Cep295-depleted HeLa cells were transfected with full-length Cep295 and the indicated mutant. Histograms represent frequency of interphase cells with the indicated number of γ-Tubulin foci in each condition. Values are mean percentages ± s.e.m from three independent experiments (N > 50 for each condition). *, $P < 0.05$ (two-tailed *t*-test).

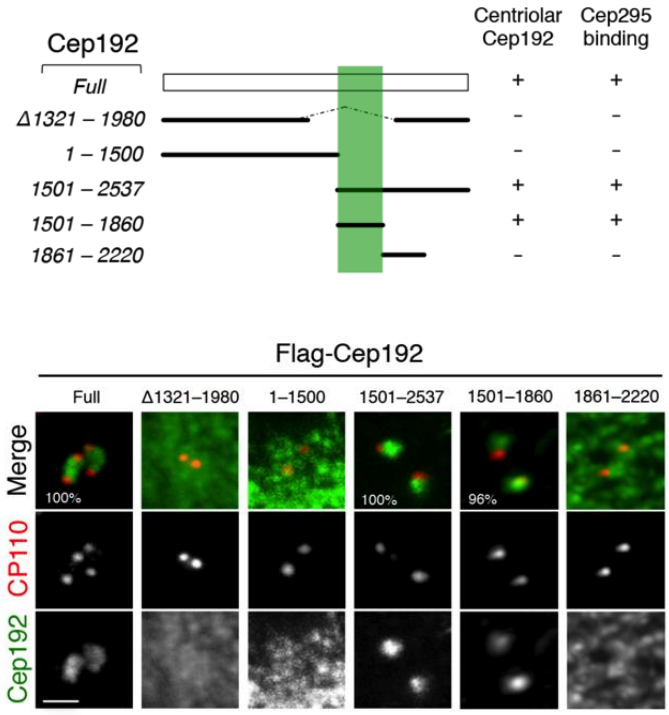

Figure 53: Interaction between Cep295 and Cep192 is required for centriolar localization of Cep192

(upper panel) Schematic of full-length Cep192 and the deletion mutants used for co-IP assays with endogenous Cep295 in U2OS cells. The minimal Cep295-binging region in Cep192 is represented in grey.

(lower panel) U2OS cells were transfected with Flag-Cep192 full-length and the indicated mutants. The cells were stained with antibodies against Cep192 (green) and CP110 (red). Scale bar, 1 μm.

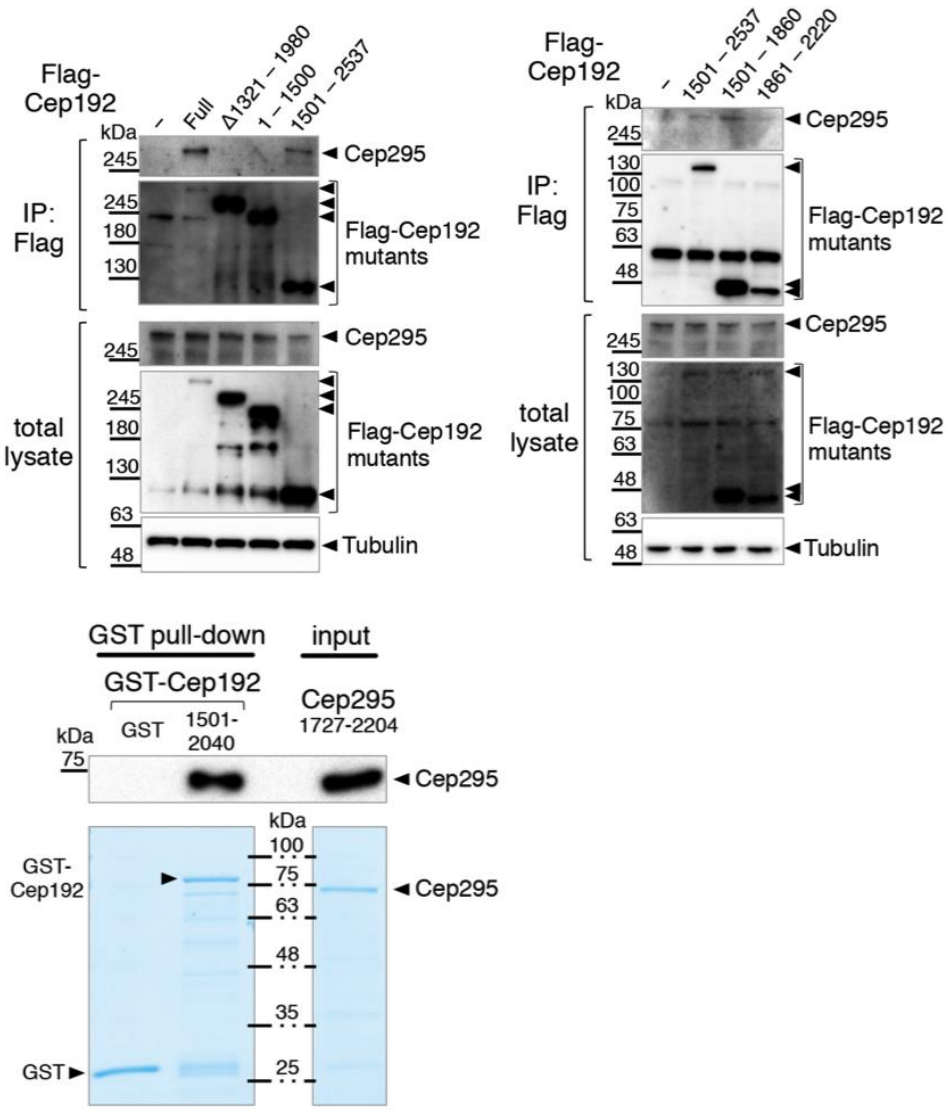

Figure 54: Interaction between Cep295 and Cep192

(upper panel) U2OS cells expressing Flag-Cep192 full length or the deletion mutant proteins were immunoprecipitated with FLAG beads. Total cell lysates and IPs were analyzed by western blotting using Cep295, Flag or tubulin antibodies.

(lower panel) GST pull-down assay showing the interaction between Cep295 and Cep192 fragments (aa 1727-2204 of Cep295 and aa 1501-2040 of Cep192) *in vitro*. These bacterially-purified recombinant proteins contain the interacting regions that were identified by co-immunoprecipitation experiments.

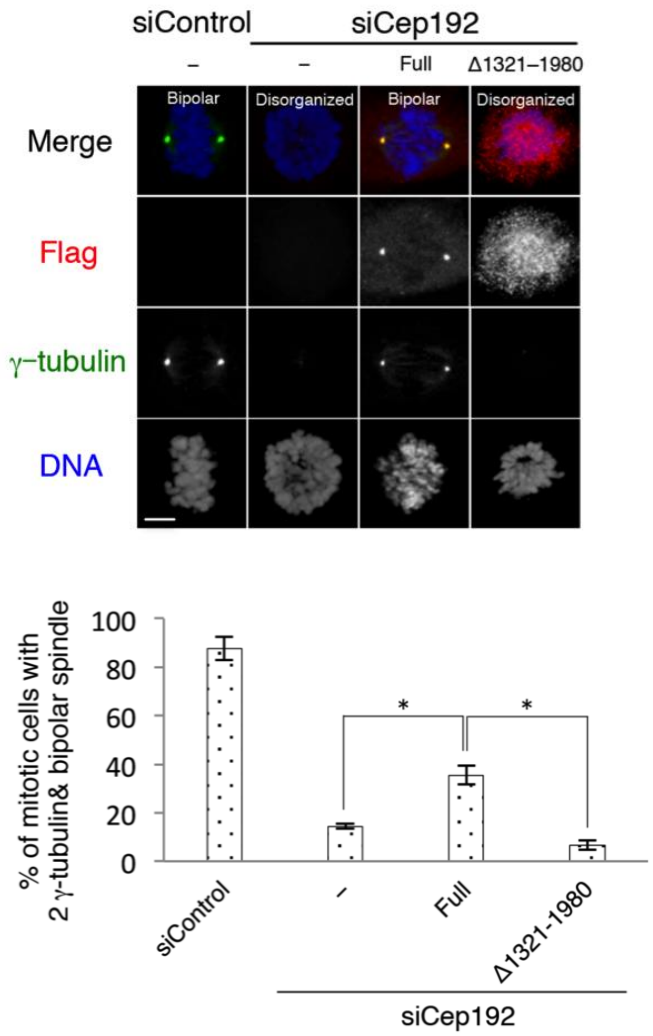

Figure 55: Binding of Cep192 to Cep295 recruits Cep192 onto the daughter centriole.

For rescue experiments, Cep192-depleted U2OS cells were transfected with RNAi-resistant full-length Cep295 and the indicated mutant. Scale bar, 5 μm.

Histograms represent frequency of bipolar mitotic spindles with the indicated number of γ-Tubulin foci. Values are mean percentages ± s.e.m from three independent experiments ($N = 30$ for each condition). *, $P < 0.05$ (two-tailed t-test).

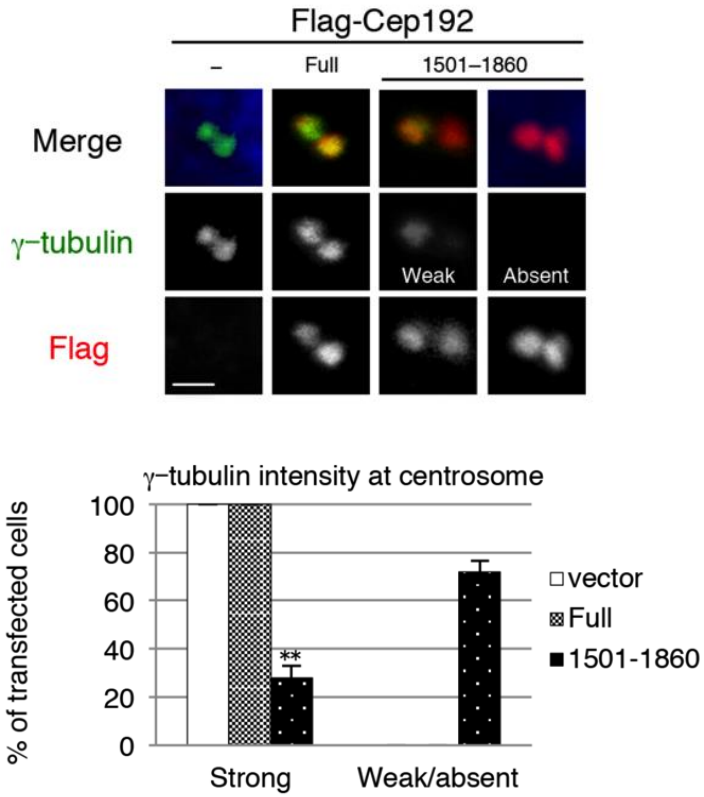

Figure 56: Dominant negative effects of the Cep192 fragment that binds to Cep295
U2OS cells were transfected with full-length Cep295 and the indicated mutant. Scale bar, 1 μm. Histograms represent frequency of transfected cells with the indicated intensity of γ-Tubulin foci. Values are mean percentages ± s.e.m from three independent experiments ($N = 30$ for each condition). **, $P < 0.01$ (two-tailed *t*-test).

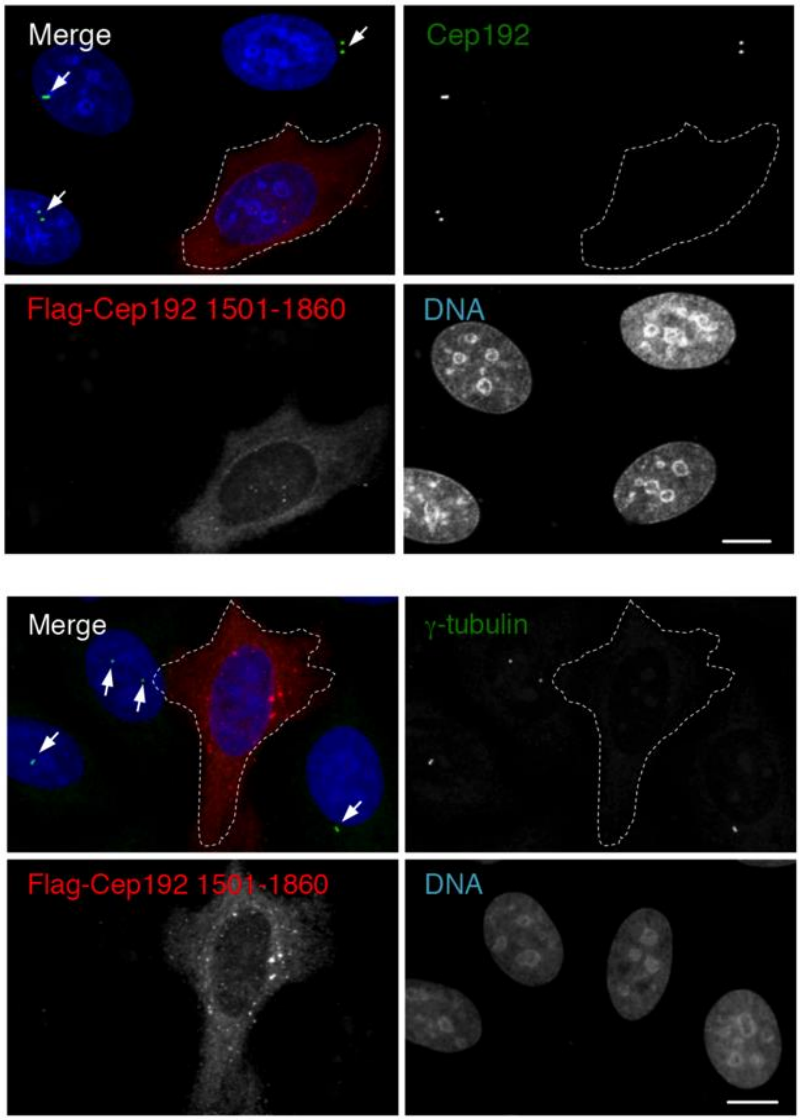

Figure 57: Expression of the Cep192 fragment that binds to Cep295 inhibited centrosomal recruitment of γ-tubulin and endogenous Cep192

HeLa cells expressing the indicated Flag-Cep192 mutant proteins were stained with antibodies against Flag (red) and Cep192 or γ-Tubulin (green). Nuclei are shown in blue. Arrows point to Cep192 or γ-Tubulin foci. Scale bar, 10 μm.

2.4 Discussion

In conclusion, my work indicates that Cep295 promotes the recruitment of Cep192 onto daughter centrioles, which is a critical step for daughter-to-mother centriole conversion (as shown in below). In addition, Cep295 depletion results in defects in the structure of the proximal parts of daughter centrioles. Consistent with the previous study, we also confirmed that such compromised daughter centrioles finally disassembled during interphase in the next cell cycle.

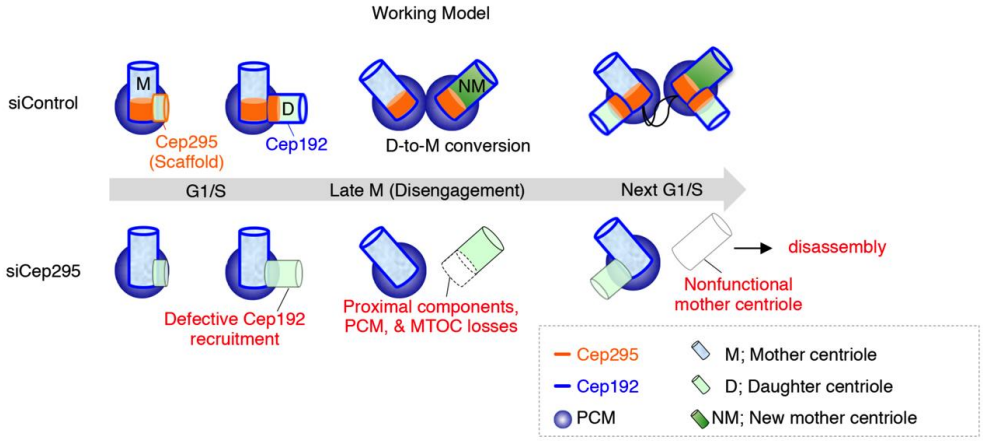

A speculative model of the role of Cep295 in centriole biogenesis

Cep295 promotes recruitment of Cep192 onto the wall of a newly formed daughter centriole. Cep295 is also critical for the integrity of the proximal part of the daughter centriole and for stability of the resulting centriole in the next cell cycle. The events coordinated by Cep295 are thus critical for the ability of a new mother centriole to duplicate, recruit PCM components and act as the MTOC.

2.4.1 How can Cep295 localize to daughter centrioles?

My study suggests that Cep295 is present at the potential assembly site of a procentriole even before cartwheel formation (Figure 39). Similarly in *Chlamydomonas*, the amorphous ring structure is generated before the appearance of the cartwheel

(Shiratsuchi et al., 2011; Toole et al., 2003). Even though I could not find a potential homolog of Cep295 in *Chlamydomonas,* it is tempting to speculate that Cep295 provides a similar function serving as a platform to promote the initiation of procentriole assembly. It will be interesting to investigate whether Cep295 molecules on the mother centriole are rearranged and moved to the assembly site of a procentriole to trigger centriole formation. It should also be noted that while this study was under review, another studies reported that Cep295 and Ana1 regulate centriole elongation in human (Chang et al., 2016) and *Drosophila* cells (Saurya et al., 2016), respectively.

2.4.2 A position of Cep295 in the pathway for centriole formation

Although it has recently been claimed that the interaction between Cep135-Ana1/Cep295-Asterless/Cep152 is required for centriole-to-centrosome conversion (Fu et al., 2016), this interaction could not sufficiently explain the function of Cep295 in recruiting PCM components at centrioles in humans. This molecular network seems to be critical for centriole formation in *Drosophila* cells. However, given that both Cep152 and Cep135 are not known to be essential for PCM assembly in human cells (Cizmecioglu et al., 2010; Dzhindzhev et al., 2010; Hatch et al., 2010; Lin et al., 2013), it is unlikely that the Cep135/Cep295/Cep152 complex is responsible for the conversion of daughter centrioles into the functional mother centrioles that organize PCM in human cells. Moreover, this interaction cannot explain the reduction of Cep192 at centrioles upon Cep295 depletion, since Cep192 is known to be upstream of centriolar loading of Cep152 (Kim et al., 2013; Sonnen et al., 2013) in human cells. In contrast, as shown in my study, the defects in centriolar loading of Cep192 following

Cep295 depletion can lead to the reduction of Cep152 at centrioles. These considerations lead us to propose that the Cep295-Cep192 interaction is fundamental for the functions of Cep295 in centriole-to-centrosome conversion and Cep295 acts upstream of Cep192 in the pathway for centriole formation, because this interaction could potentially enable the mother centrioles to duplicate, recruit PCM, and nucleate microtubules.

2.4.3 The role of interaction between Cep295 and Cep192

Although PCM components are known to be crucial for MTOC activity, the underlying mechanisms of PCM assembly are still mysterious. Recently, *in vitro* reconstitution experiments using purified SPD-5/CDK5RAP2, SPD-2/Cep192, and PLK1 revealed that these recombinant proteins promoted the formation of the porous network. Using EM and biochemical analysis, they also claimed that the porous network was likely to represent the structural framework of the PCM in *C. elegans*. It will be interesting to investigate whether recombinant Cep295 and Cep192 impact on the porous network formation in human. Actually, my date suggested that expression of Cep295 stabilized Cep192 in a concentration-dependent manner. Moreover, co-expression of Cep192 with Cep295 formed dot-like foci in the cytoplasm and γ-tubulin localized to these foci, suggesting that Cep295-Cep192 interaction should be critical steps for PCM assembly. Further studies will be needed to explain how the physical interaction between Cep295 and Cep192 helps to initiate the assembly of a functional centrosome.

2.4.4 How could older mother centrioles duplicate without Cep295?

I speculate that although Cep295 is essential for the initial recruitment of Cep192 to the daughter centriole through direct interaction between the two proteins, another mechanism including perhaps the self-assembly of Cep192 may contribute to the maintenance of Cep192 at centrioles. Indeed, some Cep192 proteins still remained at the older mother centriole even in the absence of Cep295 (Figure 34). It has recently been shown that Cep192 recruits Plk4 for centriole formation and assembles PCM around mother centrioles (Kim et al., 2013; Sonnen et al., 2013). I therefore speculate that, in the absence of Cep295, the remnant Cep192 is sufficient to recruit critical centriole components, such as Plk4, STIL and HsSAS-6, at the procentriole assembly site on the older mother centriole to promote centriole formation even though the integrity of the resulting daughter centriole may be affected. In addition, I also noticed that overexpression of Cep295 did not induce centriole overduplication, suggesting that Cep295 is important for ensuring the proper formation of a new daughter centriole, but not sufficient for generating extra daughter centrioles. Based on the findings in this study, I propose that Cep295 acts upstream of the conserved pathway for centriole formation and promotes the daughter-to-mother centriole conversion.

2.4.5 Is Cep295 a potential target for anti-cancer drugs?

In general, mitotic inhibitors, such as paclitaxel or vinblastine, are used in cancer treatment. Given that the centrosome acts as MTOC, the centriole-to-centrosome conversion regulated by Cep295 could be a potential target for anti-cancer drugs. However, I think that Cep295 is a NOT good target for anti-cancer drugs. Although the

centrosome is important for cell division in a cell, one big problem is that cancer cells can divide without centrosome. With regards to this problem, a previous study reported that PLK4 inhibitor which efficiently blocked centriole formation was not able to inhibit cell division in cancer (Wong et al., 2015). In addition, physical removal of centrosomes by a laser did not have a significant impact on bipolar spindle assembly (Hinchcliffe, 2001; Khodjakov and Rieder, 2001). Consistently, CRISPR-Cas9 knockout screening in human cancer cell lines revealed that some core centriolar proteins, such as SAS-6, STIL or Cep135, were not required for cell proliferation in cancer cells (Hart et al., 2015). I also confirmed that some cells showed monocentrosomal bipolar spindles normally without centrosomes in Cep295 depleted cells.

2.4.6 What is a potential target for anti-cancer drugs?

I think that Cep192 is a good candidate for anti-cancer drugs so far. There are several reasons for this view. Firstly, Cep192 is known as a key component of the centriole as well as pericentriolar material (PCM) organizing a functional centrosome. In fact, depletion of Cep192 effectively inhibits not only centriole formation but also PCM expansion (Sonnen et al., 2013). Secondly, in contrast to somatic cells, it is well known that mammalian oocytes lack canonical centrioles (Manandhar, 2005). Therefore, in mouse oocytes, multiple acentriolar microtubule-organizing center (MTOCs) replaces canonical centrosome function and generates spindle microtubules (Schuh and Ellenberg, 2007). Interestingly, Cep192 is seen at the spindle poles during meiotic spindle assembly in mouse oocytes (Clift and Schuh, 2015), suggesting that Cep192 is essential for bipolar spindle assembly in the absence of centrosomes and this mechanism might be conserved in higher vertebrates. Thirdly, Cep192 seems to be

involved in acentrosomal pathway in human cancer cells, which helps to form bipolar spindles in the absence of centrioles. Acentrosomal bipolar spindles are effectively induced by depletion of core factors for centriole formation. Indeed, I confirmed that Cep192 localized to spindle poles during mitosis in the absence of centrioles and Cep192 seemed to be associated with spindle pole forcing. Consistently, a previous study showed that depletion of Cep192 resulted in disorganized non-bipolar structures (Gomez-Ferreria et al., 2007). Furthermore, CRISPR-Cas9 knockout screening revealed that Cep192 was required for cell proliferation in human cancer cell lines (Hart et al., 2015; Post et al., 2015), suggesting Cep192 is crucial for bipolar spindle assembly in both presence and absence of centrosomes.

Centrosomal coiled-coil proteins tend to self-assemble to form dimer or oligomer. Usually, self-assembly of these proteins could be important for centrosome biogenesis such as SAS-6 or PLK4. Cep192 also binds to itself in human and *Drosophila* cells (Galletta et al., 2016; Kim et al., 2013). However, the significance of Cep192 self-interaction is unclear. Note that overexpression of Cep192 induced mitotic defects in humans (Zhu et al., 2008), suggesting proper protein levels of Cep192 are also important for mitotic spindles. These considerations lead me to propose that the Cep192 self-interaction is crucial for bipolar spindle assembly and inhibition of Cep192 self-assembly could block bipolar spindles during mitosis. Indeed, I found that overexpression of Cep192 fragment protein containing self-assembly site dramatically inhibits PCM assembly in human cancer cells. Moreover, overexpression of this region effectively induced cell death. I believe that small chemical components inhibiting Cep192 self-interaction could function as mitotic inhibitor and be a potential target for cancer treatment.

2.5 Material and methods

2.5.1 Cell culture and transfection

HeLa, U2OS and HEK293T cells were obtained from the ECACC (European collection of cell cultures). To generate HeLa cells stably expressing GFP-centrin1(Piel et al., 2000), centrin1 cDNA was subcloned into the pEGFP-N1 vector (Clontech). GFP-centrin1 fusion proteins were expressed and then isolated by using the limited dilution method with 500 μg/ml G418. The cell lines used in this study have been authenticated by STR profiling in ECACC. All cells were cultured in Dulbecco's modified Eagle's medium (DMEM) containing 10% fetal bovine serum (FBS) at 37 ºC in a 5% CO_2 atmosphere.

Transfection of siRNA or DNA constructs into HeLa, U2OS and HEK293T cells was conducted using Lipofectamine RNAiMAX (Life Technologies) or Lipofectamine 2000 (Life Technologies), respectively. Unless otherwise noted, the transfected cells were analyzed 48-72 hours after transfection with siRNA and 24 hours after transfection with DNA constructs.

2.5.2 RNA interference

The following siRNAs were used: Silencer Select siRNA (Life Technologies) against Cep295 #1 (s229742), Cep295 #2 (s229743), Cep192 #1 (s226819), Cep192 #2 (s30227), STIL (s12863), SAS-6 (s46487), CPAP (s31623), Cep135 (s18587), and negative control #1 (4390843); custom siRNA (Sigma Genosys) against 3'UTR of Plk4 (5'-CTCCTTTCAGACATATAAG-3'); custom siRNA (Nihon Bio Co., Ltd.) against

Cep152(Graser et al., 2007) and Cep135(Fu et al., 2016)，(Lin et al., 2013). Unless otherwise noted, Cep295 #1, Cep192 #1 and custom siRNA (Nihon Bio Co., Ltd.) against Cep135(Fu et al., 2016)，(Lin et al., 2013) were used in this study.

2.5.3 Plasmids

The full-length Cep295 was amplified from cDNA library of HeLa cells. Note that the Cep295 clone lacks the exon 11 of the full-length sequence registered in the NCBI. The Cep295 cDNA was subcloned into the pCMV5 vectors for expression of N-terminal Flag-tagged, C-terminal GFP-tagged or non-tagged proteins, respectively, in human cells. The pCMV5-Cep295 deletion mutant constructs, such as Δ1–564, Δ604–1203, Δ1204–1772, Δ1204–1468, Δ1469–1772, Δ1773–1820 and Δ2432–2556, were created using PrimeSTAR mutagenesis basal kit (TaKaRa) according to manufacturer's protocol. The pCMV5-Cep295-GFP deletion mutant constructs, such as Δ1942–2431 and Δ2144–2431 were created using PrimeSTAR mutagenesis basal kit (TaKaRa). The Cep295 fragments, such as 1–233, 1–600, 234–607, 603–1203, 1204–1726, 1727–2556, and 1773–2556 were subcloned into the pCMV5-Flag vector, and 1–233, 1–600, 1–1200, and 1727–2204 were subcloned into the pCMV5-GFP vector.

The pcDNA3-Flag construct encoding full-length Cep192 was kindly provided by Dr. Erich A Nigg. The constructs for expression of Flag-tagged Cep192 deletion mutant proteins were generated with PrimeSTAR mutagenesis basal kit (TaKaRa). The pcDNA3 construct encoding full-length PLK4-Flag was kindly gifted from Dr. Hiroyuki Mano.

2.5.4 Antibodies

The following primary antibodies were used in this study: Rabbit polyclonal antibodies against Cep295/KIAA1731 (Sigma, HPA038596, IF 1:1000, WB 1:1000), Cep192 (a gift from Laurence Pelletier, IF 1:1000), Cep192 (Bethyl laboratories, A302-324A, WB 1:1000), Cep152 (Bethyl laboratories, A302-480A, IF 1:1000), Cep152 (Bethyl laboratories, A302-479A, WB 1:1000), CP110 (a gift from Brian David Dynlacht, IF 1:500), CP110 (proteintech, 12780-1-AP, IF 1:500), CPAP (a gift from Pierre Gönczy, IF 1:500), CPAP/CENP-J (Proteintech,11517-1-AP, IF 1:500), STIL (Abcam, ab89314, IF 1:500, WB 1:1000), Cep135 (Abcam, ab196809, IF 1:1000); mouse monoclonal antibodies against centrin-2 (Millipore, 20H5, IF 1:1000), HsSAS-6 (Santa Cruz Bio-technology, Inc., sc-81431, IF 1:500, WB 1:1000), Plk4 (Merck Millipore, clone 6H5, MABC544, IF 1:500), γ-tubulin (GTU88) (Sigma-Aldrich, T5192, IF 1:1000), Polyglutamylation Modification (GT335, mAb) (AdipoGen, AG-20B-0020-C100, IF 1:5000), FLAG-tag (Sigma, F1804, IF 1:1000, WB 1:1000) and α-tubulin (Sigma-Aldrich, DM1A, IF1:1000); goat polyclonal antibody against GFP, FITC-conjugated (Abcam, ab6662, IF 1:300). Alexa 488- labeled Cep192 (Bethyl laboratories, A302-324A, IF 1:200) and ODF2 (Abcam, ab43840, IF 1:200) were generated with Alexa Fluor labeling kits (Life Technologies) and used for three color staining in Fig. 3b, and 5f. The following secondary antibodies were used: Alexa Fluor 488 goat anti-mouse IgG (H+L) (Molecular probes, A-11001, 1:500), Alexa Fluor 568 goat anti-rabbit IgG (H+L) (Molecular probes, A-11011, 1:500) for IF; Alexa Fluor 555 goat anti-rabbit IgG (H+L) (Molecular probes, A-21428, 1:500) for STED; Goat polyclonal antibodies-HRP against mouse IgG (Promega, W402B, 1:5 000), rabbit IgG (Promega, W401B, 1:5000) for WB. For detection of exogenous Cep295, because there

was a technical difficulty to detect the N-terminal tag of full-length Cep295, we used Cep295 antibody.

2.5.5 Microscopy

For immunofluorescence analysis, the cells cultured on coverslips (Matsunami: No 1 for confocal microscope, No 1s for SIM, STED microscope) were fixed using -20ºC methanol for 7 minutes and washed with PBS. The cells were permeabilized after fixation with PBS/0.05% TritonX-100 (PBSX) for 5 minutes three times, and incubated for blocking in 1% BSA in PBSX for 30 minutes at room temperature (RT). The cells were then incubated with primary antibodies for 24 hours at 4 °C, washed with PBSX three times, and incubated with secondary antibodies for 1 hour at RT. The cells were thereafter washed with PBSX twice, stained with 0.2 μg ml^{-1} Hoechst 33258 (DOJINDO) in PBS for 5 minutes at RT, washed again with PBSX and mounted onto glass slides.

Counting the number of immunofluorescence signals was done using an Axioplan2 fluorescence microscope (Carl Zeiss) with a 100x/1.4 NA plan-APOCHROMAT objective. Quantification of the signal intensity in Fig. 2a and supplementary Fig. 4a was performed using DeltaVision Personal DV-SoftWoRx system (Applied Precision) equipped with a CoolSNAP CH350 CCD camera. Serial section images along the z-axis were stacked with the “quick projection” algorithm in softWoRx. The signal intensities of centriolar Cep295, Centrin, and HsSAS-6 were quantified with the Data Inspector tool in softWoRx. I assessed cells from several fields for each experiment. The investigators were normally blinded to the sample ID during experiments and outcome

assessment. Once a field was determined, I counted all cells which match the criteria within the field. In the experiments using the cells expressing Flag-tagged full-length or mutants of Cep295, we counted cells adequately-expressing the Cep295 proteins at comparable levels and excluded cells expressing the Cep295 proteins at low levels or cells excessively-expressing the Cep295 proteins.

Confocal microscopy images were taken by the Leica TCS SP8 HSR system equipped with a Leica HCX PL APO ×63 / 1.4 oil CS2 objectives and excitation wavelength 405, 488, and 561 nm. To obtain high-resolution images, the pinhole was adjusted at 0.5 airy units. Scan speed was set to 200 Hz in combination with 5 fold line average in 856 x 100 format (pixel size 43 nm). The images were collected at 130 nm z steps. For deconvolution, Huygens essential software (SVI; Scientific Volume Imaging) was used.

Stimulated Emission Depletion (STED) images were taken by a Leica TCS SP8 STED 3X system with a Leica HC PL APO 100×/1.40 oil STED WHITE, and 660 nm gated STED. Scan speed was set to 100 Hz in combination with 5 fold line average in a 512 x 80 format (pixel size 15-20 nm). The images were collected at 180 nm z steps. The STED images were processed by deconvolution with Huygens professional software (SVI). The resolution of green signal (~80 nm, Alexa488) is generally lower than that of red signal (~50 nm, Alexa555) in this system. In this study, we mainly looked at our protein of interest at centrioles in red whereas the other protein was visualized in green.

3D-SIM images were taken by the Nikon N-SIM imaging system with Piezo stage, Apo TIRF 100× oil objective lens (NA1.49), excitation wavelength 488 and 561 nm, and iXon DU-897 EMCCD camera (Andor Technology Ltd.), The images were

collected at 100 nm z steps. Quantification of the signal intensity and reconstruction in Figure24, 25 and Figure 37 were performed using NIS-Elements AR software.

2.5.6 Immunoprecipitation and western blotting

For preparation of human cell lysates for western blotting, HEK293T and U2OS cells were collected 24 hours after transfection, washed in PBS and lysed on ice- for 20 minutes in lysis buffer (20 mM Tris/HCl pH7.5, 50 mM NaCl, 1% TritonX-100, 5 mM EGTA, 1 mM DTT, 2 mM $MgCl_2$ and 1/1000 protease inhibitor cocktail (nakarai tesque)). Insoluble material was removed after centrifugation for 15 minutes at 15,000 rpm. For immunoprecipitation of Flag-tagged Cep192 proteins, whole cell lysates were incubated with Flag antibody-conjugated M2 agarose (SIGMA) for 2 hours or overnight at 4 ºC. The beads were washed at least three times with lysis buffer and resuspended in SDS-sample buffer before loading onto 5–12% polyacrylamide gels, followed by transfer on Immobilon-P membrane (Millipore corporation). The membrane was probed with the primary antibodies, followed by incubation with their respective HRP-conjugated secondary antibodies (Promega). Washes were performed in PBS containing 0.02% Tween (PBST). The signal was detected with Chemi Doc XRS+ (BIO RAD).

2.5.7 Yeast two-hybrid analysis

Full-length or fragments of Cep192 or Cep295 were cloned into the modified version of the vectors pSM671 (bait) and pSM378 (prey) (gifts from Satoru Mimura). Yeast strain L40 was grown in complete medium (yeast extract peptone dextrose;

(YPD)) and transformed with the indicated vectors. Positive colonies were grown on plates lacking leucine and tryptophan in the presence of histidine at 30℃. After a few days, cells were streaked on plates containing 50 mM 3-amino-1,2,4-triazole (Sigma) without leucine, tryptophan, and histidine. The Plates were incubated at 30℃ for a few days.

2.5.8 *In vitro* binding assay

Cep295 or Cep192 fragments were cloned in pGEX system vectors (GE healthcare) encoding for GST-tags. This analysis was performed as described previously(Shiratsuchi et al., 2015) with slight modifications. The recombinant protein expression of the fragments was performed in *E. coli* strain BL21 gold (DE3) in LB medium. Protein expression was induced at 18 ºC by addition of 0.3 mM IPTG and allowed to proceed for 18 hours. Cell pellets expressing GST-Cep295 and Cep192 fragments (aa 1727-2204 of Cep295 and aa 1501-2040 of Cep295) were lysed by lysozyme treatment and sonication, resuspended in lysis buffer containing 50 mM Tris-HCl (pH 7.5), 500 mM NaCl, 5 mM EDTA, 1 mM DTT, 1:1000 protease inhibitor cocktail (Sigma) and 0.5% TritonX-100. The lysates were incubated with Glutathion sepharose beads (GE healthcare). The beads were then washed ten times with lysis buffer supplemented with additional 500 mM NaCl at high salt concentrations. Cep295 fragment proteins were then eluted from the beads by removal of the GST-tags by prescission protease (GE healthcare) in a buffer containing 20 mM Tris-HCl (pH 7.5), 150 mM NaCl, 0.5 mM EDTA, 1 mM DTT.

For GST pull-down assay, the Glutathion sepharose beads which retain bacterially

purified GST-Cep192 fragment were resuspended in ice-cold lysis buffer and incubated with ~5 μg bacterially purified Cep295 for 2 hours at 4 °C. The resin was washed seven times with ice-cold lysis buffer and resuspended in SDS sample buffer. Proteins were separated by SDS-PAGE and stained with SimplyBlue^{TM} Safe (Invitrogen).

2.5.9 Live cell imaging

A Confocal Scanner Box, Cell Voyager CV1000 (Yokogawa Electric Corp) equipped with a 63×oil immersion objective lens and the stage incubator for 35mm dish was used for live cell imaging. HeLa cells stably expressing GFP-centrin1 were treated with control siRNA or Cep295 siRNA for 24 hours and cultured on 35 mm glass-bottom dishes (MatTek Co.) at 37 ºC in a 5% CO_2 atmosphere. Images were taken by Back-illuminated EMCCD camera. After 24 hours from transfection, the cells were visualized every 10 min over 24–48 hours. To count the number of centrin foci, the images were collected at 1 μm z steps (from 25 to 30 Z-planes and generated using ImageJ (National Institutes of Health)).

Chapter 3:

Analysis of linkage between a novel mutation in an intellectual disability (ID) patient and mitotic defects

3.1 Summary

Patients with intellectual disability (ID) typically exhibit significant defects in both intelligence and adaptive behavior. Genetic aberration involved in proper progression of mitosis has been reported to underlie ID. Here, we report a new patient with a novel mutation of *CHAMP1*. *CHAMP1* encodes a protein regulating kinetochore-microtubule attachment and chromosome segregation. Using whole exome sequencing (WES) analysis, we identify a de novo frameshift mutation in *CHAMP1*. We isolate lymphoblast cells from the *CHAMP1* patient and detect errors in chromosome segregation. Furthermore, I find that these cells exhibit an increase in centrosome number and resulting multipolar spindle formation. The phenotypes observed in the patient's lymphoblastoid cells presumably stemmed from cytokinesis failure. I also confirm the identical phenotypes in human culture cells depleted of *CHAMP1*. Overall, these data strongly support that *CHAMP1* mutations cause ID, and suggest that *CHAMP1* is critical for progression of cytokinesis and maintenance of centrosome number.

3.2 Introduction

3.2.1 Intellectual disability (ID) is caused by mitotic defects

Intellectual disability (ID) is a neurodevelopmental disorder characterized by substantial defects in both intelligence and adaptive behavior in the 5th edition of the Diagnostic and Statistical Manual [DSM-5; American Psychiatric Association (APA) 2013]. Aberration in mitotic process of neural progenitor cells has been considered as one of causes for ID, because mutations in several genes associated with mitotic process have been found in ID.

In most animal cells, the centrosome consisting of two cylindrical centrioles surrounded by pericentriolar material (PCM) functions as the microtubule-organizing centers (MTOC). Tight control of the centrosome number in a cell is essential for robust formation of bipolar spindles and proper chromosome segregation during mitosis (Gönczy, 2015). Indeed, centrosome amplification can lead to severe problems, such as multipolar spindle formation, chromosome missegregation and genomic instability, which are generally known as the hallmarks of cancer. Abnormal centrosome and spindle morphology are also found in a patient with autosomal recessive primary microcephaly (MCPH), which typically causes intellectual disability (Nigg and Raff, 2009). The mutations of centrosome-related genes identified in MCPH are likely to be loss-of-function. However, it has been suggested that centrosome amplification could also cause MCPH phenotypes (Arquint and Nigg 2014), suggesting that the strict regulation on the centrosome copy number is critical for proper brain development.

Formation of multipolar spindles could be induced by various defects in mitotic spindle pole integrity. For example, human cells with centriole over-duplication or

cytokinesis failure undergoes multipolar spindle formation that is associated with centrosome amplification during mitosis. In other cases, precocious centriole disengagement or PCM fragmentation before or during mitosis could result in multipolar spindle formation (Maiato and Logarinho 2014).

3.2.2 Chromosome Alignment Maintaining Phosphoprotein 1 (CHAMP1)

Chromosome Alignment Maintaining Phosphoprotein 1 (CHAMP1) was initially reported to be a protein regulating kinetochore-microtubule attachment (Itoh, G. et al 2011). Interestingly, they suggested that the C-terminal region of CHAMP1 containing the zinc-finger domains was important in regulating CHAMP1 localization to chromosomes and the mitotic spindle. Moreover, a large-scale sequencing study in 1,133 individuals with ID revealed that de novo *CHAMP1* alterations involved in developmental disorders [The Deciphering Developmental Disorders Study 2015]. By trio whole-exome sequencing (WES), another study identified *de novo* deleterious mutations in *CHAMP1* in five unrelated individuals affected by ID (Hempel et al. 2015). Note that all mutations were predicted to lead to the loss of the zinc finger domains regulating CHAMP1 localization to chromosomes and the mitotic spindle. Furthermore, two independent studies reported further 11 patients with *de novo* mutations in *CHAMP1* (Isidor et al., 2016; Tanaka et al., 2016).

In this study, we report a novel patient with *CHAMP1* mutation. In line with the previous reports, we observed chromosome segregation errors during mitosis of the patient lymphocyte cells. Moreover, we found the cytokinesis failure and accompanying centrosome amplification phenotypes in the patient's cells. These data illustrate novel aspects of the phenotypes caused by *CHAMP1* mutations.

3.3 Results

3.3.1 Abnormal spindle assembly in a patient with *CHAMP1* mutation

Although it has recently been reported that CHAMP1 somehow regulates kinetochore-microtubule attachment (Itoh et al., 2011) and also that mutations in *CHAMP1* cause ID [The Deciphering Developmental Disorders Study 2015](Hempel et al., 2015b; Isidor et al., 2016; Tanaka et al., 2016), the biological evidence for linkage between the patient mutations in *CHAMP1* and ID is insufficient.

WES analysis was performed as previously described (Saitsu et al., 2016). Trio-WES identified a *de novo* frameshift mutation of *CHAMP1* (NM_032436.2: c.2068_2069delGA, p.Glu690Serfs*5). Interestingly, this mutation may lead to an early truncating protein lacking the zinc finger domains that were important for CHAMP1 localization to chromosomes and the mitotic spindle. Note that this variant was never observed in ExAC, EVS, 1000 Genome, HGVD, and our in-house exome database (n = 575).

To identify the cytological abnormalities in patient cells with *CHAMP1* mutation, we isolated and analyzed lymphoblast cells from the blood cells of a healthy person and a patient with *CHAMP1* mutation. To investigate overall mitotic features in these cells, I used immunofluorescence analyses with specific antibodies against endogenous centrosomal protein of 192kDa (Cep192) and α-tubulin to mark centrosomes and microtubules, respectively. While control mitotic cells had two Cep192 foci at the opposite sides and formed functional bipolar spindles, I found that patient's cells with the *CHAMP1* mutation showed formation of peudo-bipolar spindles with centrosome clustering or multipolar spindles during mitosis (14% of the *CHAMP1* patient cells with

abnormal spindle formation, compared with 0% of control cells; Figure 58,59). Consistent with the previous studies, I also observed that 3.6% of the patient cells showed misaligned chromosomes during mitosis (Figure 58). Importantly, I found that most multipolar spindles in the *CHAMP1* patient cells harbored 4 foci of Cep192, all of which seemed to have MTOC activity (Figure 59).

3.3.2 The increased number of centrosomes in a patient with *CHAMP1* mutation

Cep192 is known as a component of the centriole as well as pericentriolar material (PCM) which organize a functional centrosome (Sonnen et al. 2013). Therefore, to distinguish whether these excess Cep192 dots reflect centrosome amplification, centriole disengagement, or PCM fragmentation, I next performed immunofluorescence analyses using specific antibodies against centriolar glutamylated microtubules (GT335) and Cep152, a mother centriole marker, in lymphocyte cells (Tsuchiya et al. 2016). I found that, in the *CHAMP1*-mutant patient's cells, all Cep192 foci on the multipolar spindle poles contained GT335 dots (Figure 60). Using triple staining analysis, I further confirmed that these excess foci marked with Cep152 colocalized with a pair of adjacent GT335 dots and served as a MTOC (Figure 61). These data indicate that multipolar spindle formation in our patient's cells is because of the increased number of centrosomes during mitosis.

3.3.3 Depletion of CHAMP1 causes multipolar spindle formation in human cancer cells

Although it has been reported that depletion of *CHAMP1* results in formation of multipolar spindles in human cells (Itoh et al., 2011), its underlying mechanism remains unclear. To address this, we next investigated the phenotype provoked by RNAi-mediated depletion of *CHAMP1* in human cancer cell line. Using siRNAs targeting different sequences of *CHAMP1* ORF (Open Reading Frame), I confirmed that the depletion of *CHAMP1* induced chromosome misalignment in metaphase, which was further confirmed in different human cell lines, HeLa and U2OS cells (Figure 62,63). These results are in line with the previous observation that CHAMP1 is important for proper chromosome alignment during mitosis (Itoh et al., 2011) .

I next aimed to clarify whether the formation of multipolar spindles during mitosis is due to the existence of excess centrosomes. First, we confirmed, in HeLa cells, that depletion of CHAMP1 induced formation of multipolar spindles with excess Cep192 foci as was observed in the *CHAMP1*-mutant patient lymphocyte cells (11% of CHAMP1-depleted cells with multipolar spindle formation, compared with 2% of control cells; Figure 64). I also noticed the clear trend that most *CHAMP1*-depleted cells harbored four Cep192 foci that appeared to act as MTOCs during mitosis. In addition, these Cep192 foci co-localized with GT335 signals, suggesting that all multipolar spindle poles contain a pair of centrioles (Figure 65). As expected from the observation of the *CHAMP-1* patient phenotypes, I next sought to obtain a direct evidence that centrosome amplification upon CHAMP-1 depletion is a secondary effect of cytokinesis failure. Using live cell imaging with HeLa cells expressing GFP-centrin that marks centrioles, I found that depletion of CHAMP1 indeed caused cytokinesis failure (~10% of the cells treated with CHAMP1 siRNA; Figure 66). In *CHAMP1*-depleted cells, I also observed frequent mitotic catastrophe probably due to

defects in kinetochore-microtubule attachment (43.3% of *CHAMP1*-depleted cells, compared with 5.8% of control cells; Figure 66). Taken together, these data strongly suggest that multipolar spindle formation seen in *CHAMP1*-depleted cells is due to centrosome amplification following cytokinesis failure.

3.3.4 Figures

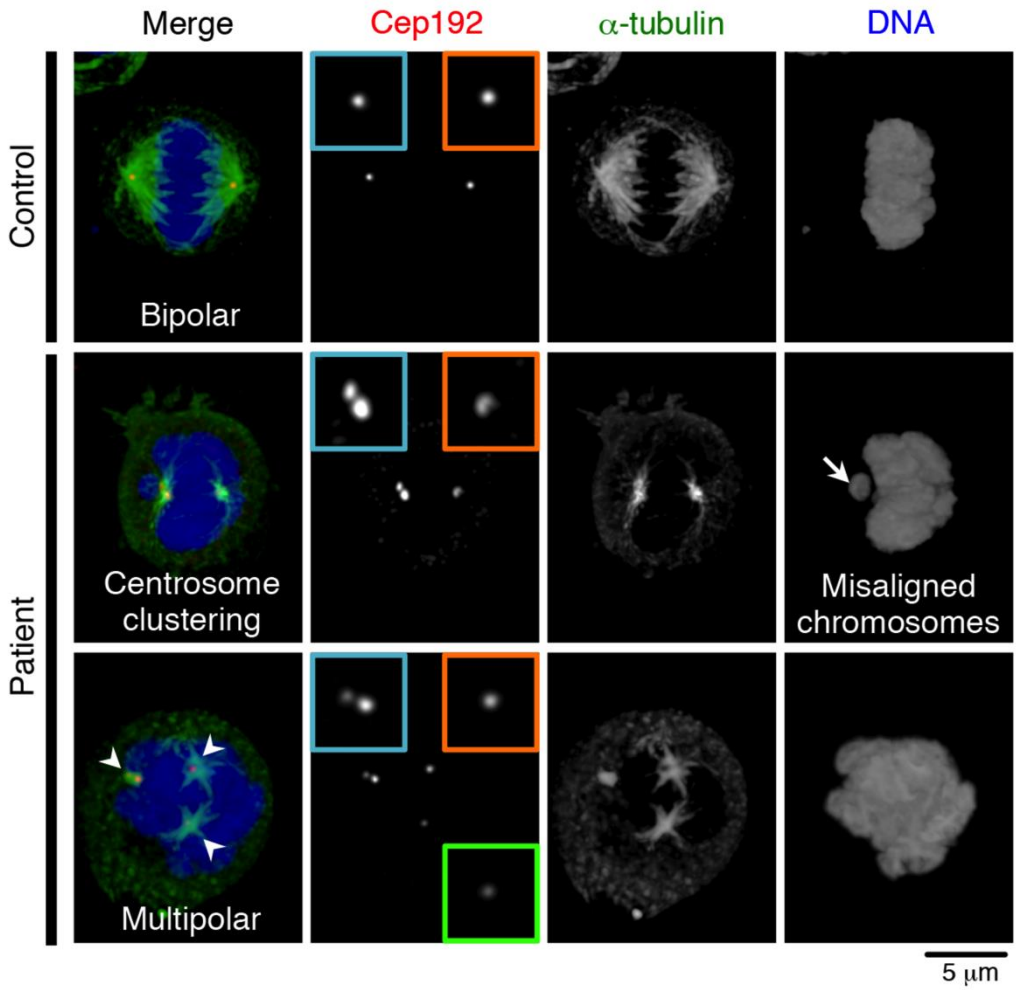

Figure 58: Abnormal spindle formation and chromosome misalignment of patient cells with *CHAMP1* mutation

Lymphoblast cells from a healthy person and a patient with *CHAMP1* mutation were stained with antibodies against Cep192 (red) and α-tubulin (green). Nuclei are shown in blue. Insets show approximately twofold-magnified views of Cep192 signals. White arrow indicates misaligned chromosomes. White arrowheads indicate excess Cep192 foci representing multipolar spindle.

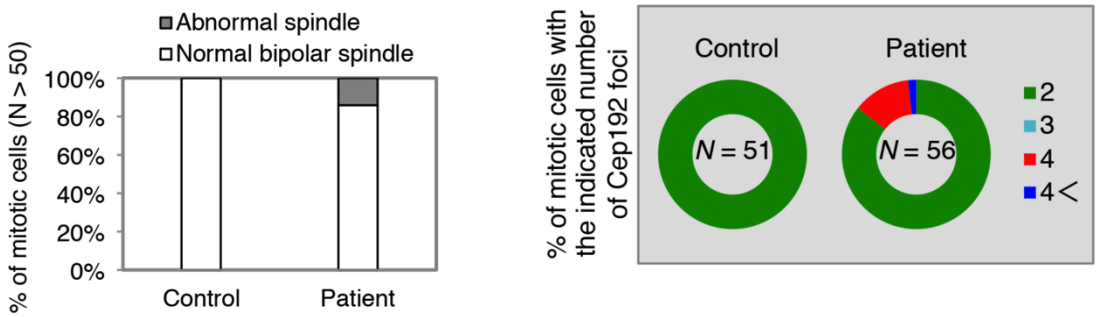

Figure 59: Cytological abnormalities in a patient with CHAMP1 mutation.

Histograms represent frequency of mitotic cells with normal bipolar and abnormal spindles in Lymphoblast cells from a healthy person and a patient with *CHAMP1* mutation.

Pie graphs represent frequency of mitotic cells with the indicated Cep192 foci in each condition.

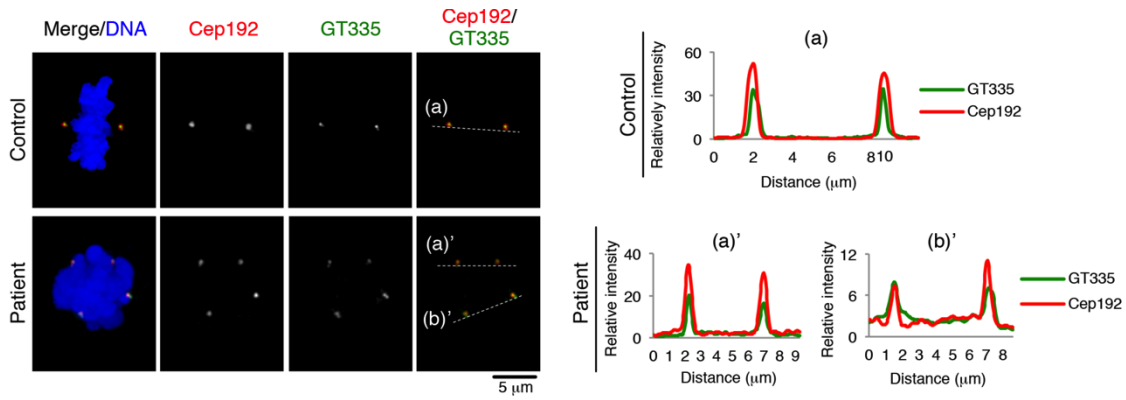

Figure 60: Centrosome amplification of patient cells with *CHAMP1* mutation

Lymphoblast cells from a healthy person and a patient with *CHAMP1* mutation were stained with antibodies against Cep192 (red) and GT335 (green). Nuclei are shown in blue.

The graph shows the signal intensity of GT335 (green) and Cep192 (red) at the centrosomes along the dotted line in representative panels. All Cep192 signals were overlapped with GT335 signals (*N*=10 cells)

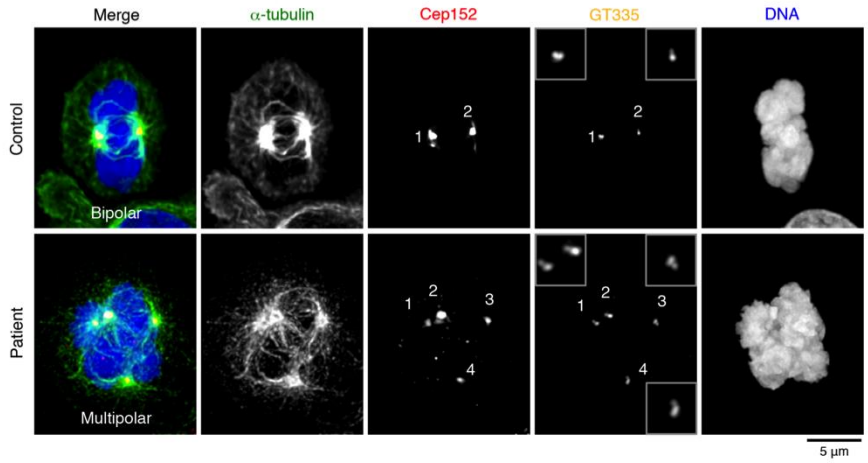

Figure 61: Centrosome amplification in a patient with *CHAMP1* mutation

Three color staining of centrioles in lymphoblast cells from a healthy person and a patient with *CHAMP1* mutation. The cells were stained with the indicated antibodies. The number indicates centrosomes containing mother and daughter centriole and having MTOC activity. Scale bar, 5□µm.

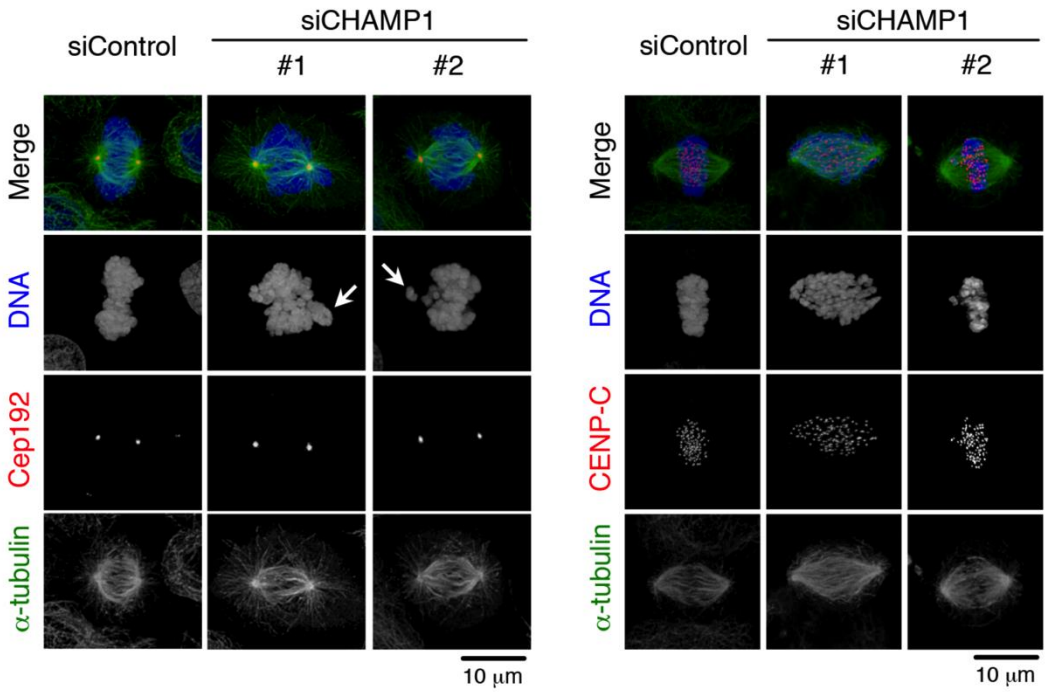

Figure 62: Depletion of CHAMP1 induces chromosome misalignment and instability of kinetochore-microtubules

U2OS cells treated with control siRNA or siRNA targeting endogenous CHAMP1 for 72 hours were stained with the indicated antibodies. Nuclei are shown in blue. White arrow indicates misaligned chromosomes.

HeLa cells treated with control siRNA or siRNA targeting endogenous CHAMP1 for 72 hours were stained with the indicated antibodies. Nuclei are shown in blue.

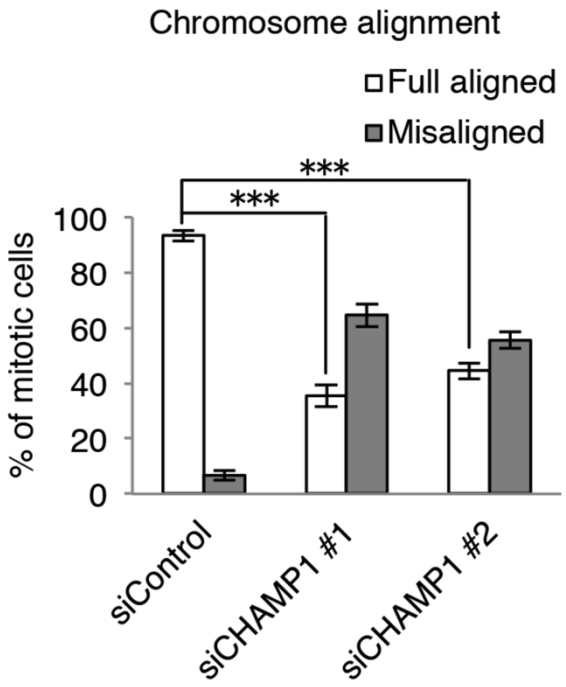

Figure 63: Depletion of CHAMP1 induces chromosome misalignment

Histograms represent frequency of mitotic HeLa cells with the indicated category in each condition. Values are mean percentages ± s.e.m from three independent experiments ($N = 30$ for each condition). ***, $P < 0.001$, (two-tailed *t*-test).

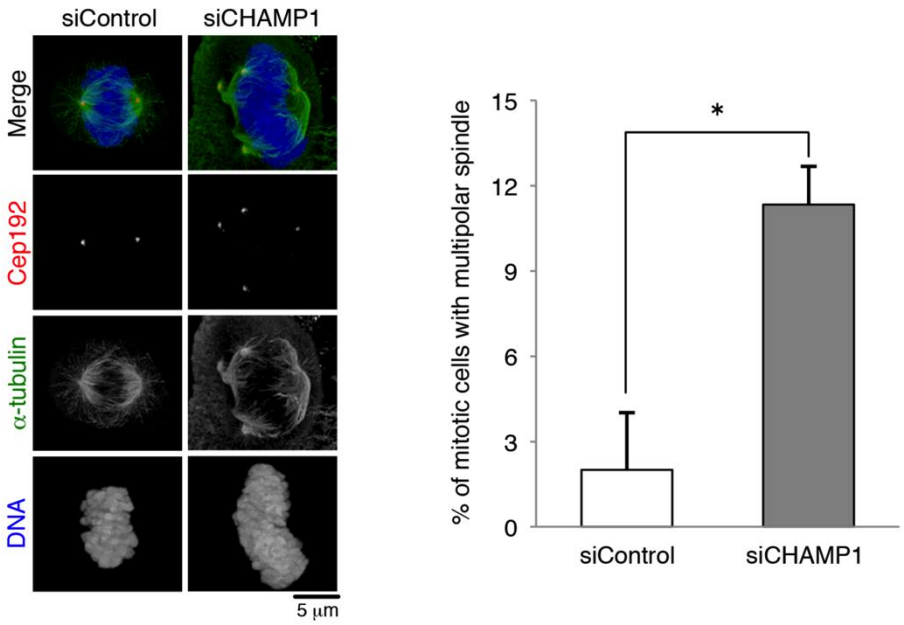

Figure 64: Depletion of CHAMP1 promotes formation of the excess centrosome foci during mitosis

U2OS cells treated with control siRNA or siRNA targeting endogenous CHAMP1 for 48 hours were stained with the indicated antibodies. Nuclei are shown in blue. Cells were treated with MG132 for the last 2 hours.

Histograms represent frequency of mitotic cells with multipolar spindles in each condition. Values are the mean percentages ± s.e.m from three independent experiments ($N = 50$ for each condition). *, $P < 0.05$, (two-tailed *t*-test).

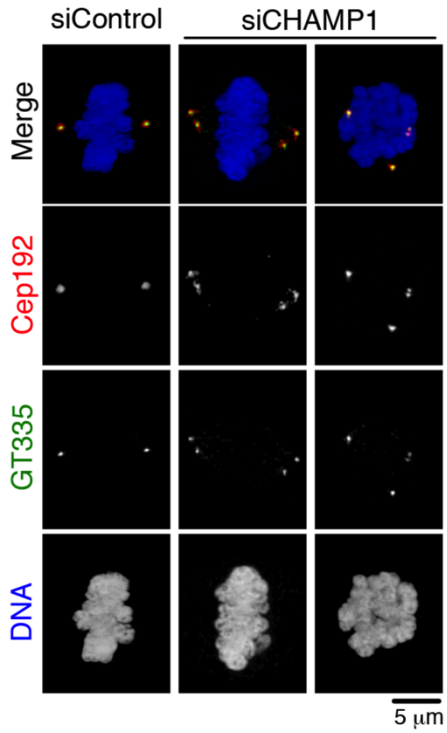

Figure 65: Centrosome amplification in CHAMP1-depleted cells

HeLa cells treated with control siRNA or siRNA targeting endogenous CHAMP1 for 48 hours were stained with the indicated antibodies. Nuclei are shown in blue. Cells were treated with MG132 for the last 2 hours.

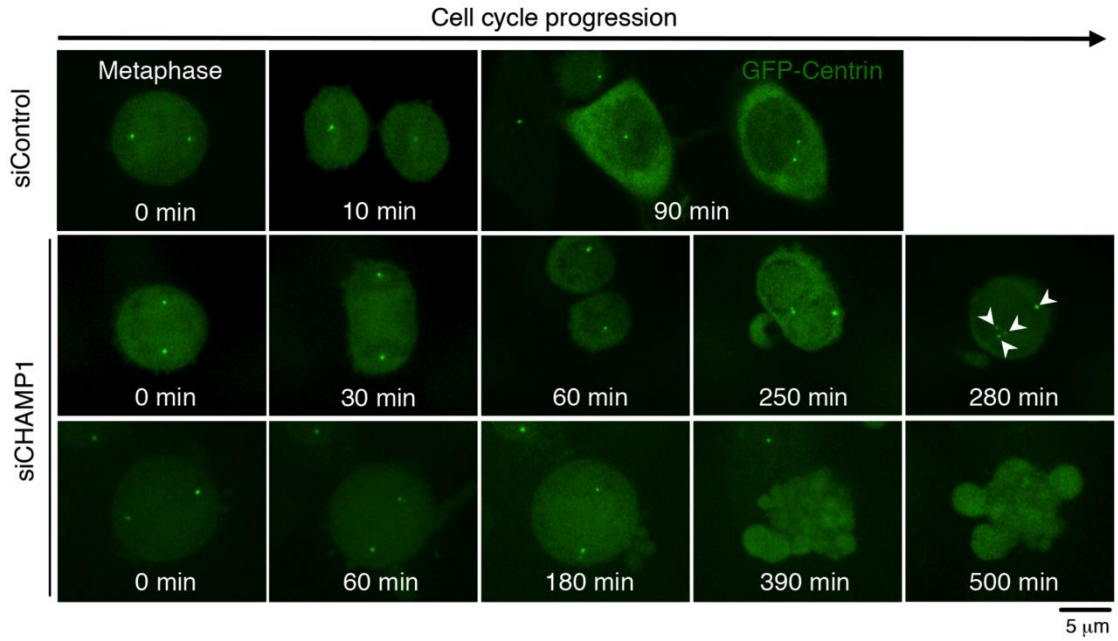

Figure 66: Depletion of CHAMP1 causes cytokinesis failure

Live imaging of cycling HeLa cells expressing GFP-centrin1 (green) and treated with control siRNA or CHAMP1 siRNA. Scale bar, 5 μm. White arrowheads indicate the increased number of centrosomes. 5.8% of control cells showed cell death (N = 17), compared with 43.3% of CHAMP1-depleted cells; 10% of CHAMP1-depleted cells showed cytokinesis defects (N = 30).

3.4 Discussion

3.4.1 Expression level of CHAMP1 contributes to spindle morphology

Our work suggests that depletion of CHAMP1 causes not only misaligned chromosomes but also cytokinesis failure. Symmetrical and asymmetrical divisions of the neural progenitor cells are crucial steps during embryonic neurogenesis. Therefore, it is plausible that such mitotic defects in neural progenitor cells could result in significant reduction of neural progenitor pool and defective neural development. We also note that the cytological analysis used in this study could be useful for diagnosis of an ID patient judging whether a symptom is because of loss-of-function mutations in *CHAMP1*.

Our work indicates that depletion of CHAMP1 results in mitotic delay and eventual cell death, or otherwise in cytokinesis failure (Figure 66). Given that an ID patient also has heterozygous truncating mutations in the *CHAMP1* gene, we speculate that the expression level of CHAMP1 is a critical factor for proceeding mitosis properly. Further detailed studies will be required to understand why a certain protein expression level of CHAMP1 is needed for the proper progression of the cell divisions during brain development.

Ethics: Written informed consent for genetic analysis was obtained from the parents according to the ethical guidance of the institutional review board. The ethics committees of each institution approved this study.

3.5 Material and methods

3.5.1 Cell culture

For preparation of lymphoblast cells, lymphoblast cells from the blood cells of a healthy person and a patient with *CHAMP1* mutation were cultured in Roswell Park Memorial Institute (RPMI) 1640 medium containing 10% fetal bovine serum (FBS) at 37 ºC in a 5% CO_2 atmosphere. These lymphoblast cell lines were immortalized with the virus and treated with Interleukin-2, (IL-2). HeLa cells, U2OS cells and HeLa cells stably expressing GFP-centrin1 were cultured as described chapter 2.

3.5.2 RNA interference

The following siRNAs were used: Silencer Select siRNA (Life Technologies) against ZNF828 (known as CHAMP1) #1 (s49268), ZNF828 #2 (s49269) and negative control #1 (4390843). Transfection of siRNA into HeLa and U2OS cells was conducted using Lipofectamine RNAiMAX (Life Technologies). Unless otherwise noted, silencer Select siRNA (Life Technologies) against ZNF828 (known as CHAMP1) #2 (s49269) was used in this study and the transfected cells were analyzed 48-72 hours after transfection with siRNA.

3.5.3 Antibodies

The following primary antibodies were used in this study: Guinea pig polyclonal antibodies against CENP-C (MBL, PD030, IF 1:1000), Rabbit polyclonal antibodies against Cep192 (Bethyl laboratories, A302-324A, IF 1:1000), Cep152 (Bethyl laboratories, A302-480A, IF 1:1000); mouse monoclonal antibodies against,

Polyglutamylated tubulin (GT335, mAb) (AdipoGen, AG-20B-0020-C100, IF 1:5000), α-tubulin (Sigma-Aldrich, DM1A, IF1:1000); Alexa 647- labeled Cep152 (Bethyl laboratories, A302-480A, IF 1:200) was generated with Alexa Fluor labeling kits (Life Technologies) and used for three color staining in Figure 61. The following secondary antibodies were used: Alexa Fluor 488 goat anti-mouse IgG (H+L) (Molecular probes, A-11001, 1:500), Alexa Fluor 568 goat anti-rabbit IgG (H+L) (Molecular probes, A-11011, 1:500) for IF.

3.5.4 Microscopy

Immunofluorescence analysis was performed as described in chapter 2.

For specimen slide preparation of Lymphoblast cells, cell suspension was mixed with Smear Gell (GenoStaff) and spread on the surface of slide. The same steps as above were repeated to perform immunofluorescence analysis of specimen slide preparation.

Counting the number of immunofluorescence signals was performed as described in chapter 2.

Confocal microscopy images were taken by the Leica TCS SP8 system equipped with a Leica HCX PL APO ×63 / 1.4 oil CS2 objectives and excitation wavelength 405, 488, 561 and 647 nm. Scan speed was set to 200 Hz in combination with 5-fold line average in 1024 x 500 format. The images were collected at 300 nm z steps.

3.5.5 Live cell imaging.

Live cell imaging was performed as described in chapter 2. After 24 hours from si RNA transfection, the cells were visualized every 10 min over 24–36 hours.

Chapter 4:

Final conclusions and discussion

In these experiment, I identified Cep295 as a novel conserved centrosomal protein and analyzed the fundamental roles of Cep295 in human centrosome biology. Moreover, using clinical specimen from the blood cells of a healthy person and a patient with ID, I described the linking between mitotic defects that is caused by CHAMP1 mutation and ID.

In Chapter 2, physical interaction of the two conserved factors, Cep295 and Cep192, was detected in human and yeast cells as well as *in vitro* with the bacterially-purified recombinant proteins. My analysis using deletion mutants revealed that this interaction is considered to be crucial for the recruitment of Cep192 onto the centriole wall and for PCM maturation during mitosis. Given that Cep192 recombinant protein has been recently shown to function as a meshwork to anchor other PCM components and organize functional PCM structure in *C. elegans* (Woodruff et al., 2015), the initial recruitment of Cep192 via Cep295 interaction could be a “seed” for PCM assembly at the centriole. In fact, I showed that Cep295 promotes Cep192 stabilization in a concentration-dependent manner, which presumably serves as a trigger for the meshwork formation.

By using the RNAi based depletion, I also confirmed that Cep295 is needed for proper centriole formation. Cep295 depletion results in defective centriole formation, especially at the proximal end of centrioles. Consistently, using gated STED microscopy, I showed that Cep295 is recruited to the procentriole assembly site in the early stage and

acts as a hub protein for the assembly of proximal centriole components. As for the evolutionarily conserved pathway for centriole formation, Cep192 was known to be the most upstream factor. However, the molecular basis for initial recruitment of Cep192 to the centrioles remains incompletely understood so far. In this study, I suggested that Cep295 functions upstream of Cep192 and other conserved centriole proteins for the first time. Hence, I believe that this analysis leads to a better understanding of the molecular mechanism how a fascinating cylindrical structure “centriole” holds PCM on its surrounding and functions as the MTOC/centrosome.

In Chapter 3, I performed cytological analysis using lymphoblast cells from a healthy person and a patient with ID. First, using multiple staining analyses, I observed mitotic defects such as multipolar spindles or chromosome misalignment in patient’s cells with *CHAMP1* mutation. To back up with the phenotypes observed in actual patient’s cells. I next performed phenotypic analysis in human culture cells. I found that RNAi-mediated depletion of CHAMP1 actually caused identical phenotypes. These data strongly support that *CHAMP1* mutation is considered to be a cause of ID, and suggest that CHAMP1 is required for proper mitotic progression and maintenance of centrosome number in human.

Chapter 5:

References

- Andersen, J., Wilkinson, C., and Mayor, T. (2003). Proteomic characterization of the human centrosome by protein correlation profiling. Nature *426*, 570–574.
- Arquint, C., and Nigg, E.A. (2014). STIL microcephaly mutations interfere with APC/C-mediated degradation and cause centriole amplification. Curr. Biol. *24*, 351–360.
- Arquint, C., Sonnen, K.F., Stierhof, Y.-D., and Nigg, E. a. (2012). Cell-cycle-regulated expression of STIL controls centriole number in human cells. J. Cell Sci. *125*, 1342–1352.
- Avidor-Reiss, T., and Gopalakrishnan, J. (2013). Building a centriole. Curr. Opin. Cell Biol. *25*, 1–6.
- Bettencourt-Dias, M., Rodrigues-Martins, a., Carpenter, L., Riparbelli, M., Lehmann, L., Gatt, M.K., Carmo, N., Balloux, F., Callaini, G., and Glover, D.M. (2005). SAK/PLK4 is required for centriole duplication and flagella development. Curr. Biol. *15*, 2199–2207.
- Bilgüvar, K., Oztürk, A.K., Louvi, A., Kwan, K.Y., Choi, M., Tatli, B., Yalnizoğlu, D., Tüysüz, B., Cağlayan, A.O., Gökben, S., et al. (2010). Whole-exome sequencing identifies recessive WDR62 mutations in severe brain malformations. Nature *467*, 207–210.

- Blachon, S., Cai, X., Roberts, K. a, Yang, K., Polyanovsky, a, Church, a, and Avidor-Reiss, T. (2009). A proximal centriole-like structure is present in Drosophila spermatids and can serve as a model to study centriole duplication. Genetics *182*, 133–144.
- Bloodgood, R.A. (2009). From central to rudimentary to primary: the history of an underappreciated organelle whose time has come. The primary cilium. (Elsevier).
- Bolgioni, A.F., and Ganem, N.J. (2015). The interplay between centrosomes and the Hippo tumor suppressor pathway. Chromosom. Res.
- Bond, J., Roberts, E., Mochida, G.H., Hampshire, D.J., Scott, S., Askham, J.M., Springell, K., Mahadevan, M., Crow, Y.J., Markham, A.F., et al. (2002). ASPM is a major determinant of cerebral cortical size. Nat Genet *32*, 316–320.
- van Breugel, M., Hirono, M., Andreeva, A., Yanagisawa, H., Yamaguchi, S., Nakazawa, Y., Morgner, N., Petrovich, M., Ebong, I.-O., Robinson, C. V, et al. (2011). Structures of SAS-6 suggest its organization in centrioles. Science *331*, 1196–1199.
- Brito, D. a., Gouveia, S.M., and Bettencourt-Dias, M. (2012). Deconstructing the centriole: Structure and number control. Curr. Opin. Cell Biol. *24*, 4–13.
- Cerami, E., Gao, J., Dogrusoz, U., Gross, B.E., Sumer, S.O., Aksoy, B.A., Jacobsen, A., Byrne, C.J., Heuer, M.L., Larsson, E., et al. (2012). The cBio Cancer Genomics Portal: An open platform for exploring multidimensional cancer genomics data. Cancer Discov. *2*, 401–404.
- Chang, C., Hsu, W., Tsai, J., Tang, C.C., and Tang, T.K. (2016). CEP295 interacts with microtubules and is required for centriole elongation. J. Cell Sci. *129*, 2501–

2513.

- Cizmecioglu, O., Arnold, M., Bahtz, R., Settele, F., Ehret, L., Haselmann-Weiss, U., Antony, C., and Hoffmann, I. (2010). Cep152 acts as a scaffold for recruitment of Plk4 and CPAP to the centrosome. J. Cell Biol. *191*, 731–739.
- Clift, D., and Schuh, M. (2015). A three-step MTOC fragmentation mechanism facilitates bipolar spindle assembly in mouse oocytes. Nat. Commun. *6*, doi :10.1038/ncomms8217
- Dammermann, A., Müller-Reichert, T., Pelletier, L., Habermann, B., Desai, A., and Oegema, K. (2004). Centriole assembly requires both centriolar and pericentriolar material proteins. Dev. Cell *7*, 815–829.
- Delattre, M., and Gonczy, P. (2004). The arithmetic of centrosome biogenesis. J Cell Sci *117*, 1619–1630.
- Delattre, M., Leidel, S., Wani, K., Baumer, K., Bamat, J., Schnabel, H., Feichtinger, R., Schnabel, R., and Gonczy, P. (2004). Centriolar SAS-5 is required for centrosome duplication in C. elegans. Nat Cell Biol *6*, 656–664.
- Denu, R.A., Zasadil, L.M., Kanugh, C., Laffin, J., Weaver, B.A., and Burkard, M.E. (2016). Centrosome amplification induces high grade features and is prognostic of worse outcomes in breast cancer. BMC Cancer *16*, 47.
- Dobbelaere, J., Josué, F., Suijkerbuijk, S., Baum, B., Tapon, N., and Raff, J. (2008). A genome-wide RNAi screen to dissect centriole duplication and centrosome maturation in Drosophila. PLoS Biol. *6*, 1975–1990.
- Dzhindzhev, N.S., Yu, Q.D., Weiskopf, K., Tzolovsky, G., Cunha-Ferreira, I., Riparbelli, M., Rodrigues-Martins, A., Bettencourt-Dias, M., Callaini, G., and

Glover, D.M. (2010). Asterless is a scaffold for the onset of centriole assembly. Nature *467*, 714–718.

- Faheem, M., Naseer, M.I., Rasool, M., Chaudhary, A.G., Kumosani, T.A., Ilyas, A.M., Pushparaj, P.N., Ahmed, F., Algahtani, H.A., Al-Qahtani, M.H., et al. (2015). Molecular genetics of human primary microcephaly: an overview. BMC Med. Genomics *8 Suppl 1*, S4.
- Farina, F., Gaillard, J., Guérin, C., Sillibourne, J., Blanchoin, L., and Théry, M. (2015). The centrosome is an actin-organizing center. Under Revis. Nat. Cell Biol. *18*.
- Fu, J., Lipinszki, Z., Rangone, H., Min, M., Mykura, C., Chao-Chu, J., Schneider, S., Dzhindzhev, N.S., Gottardo, M., Riparbelli, M.G., et al. (2016). Conserved molecular interactions in centriole-to-centrosome conversion. Nat. Cell Biol. *18*, 87–99.
- Galletta, B.J., Fagerstrom, C.J., Schoborg, T.A., McLamarrah, T.A., Ryniawec, J.M., Buster, D.W., Slep, K.C., Rogers, G.C., and Rusan, N.M. (2016). A centrosome interactome provides insight into organelle assembly and reveals a non-duplication role for Plk4. Nat. Commun. *7*, doi: 10.1038/ncomms12476.
- Gomez-Ferreria, M.A., Rath, U., Buster, D.W., Chanda, S.K., Caldwell, J.S., Rines, D.R., and Sharp, D.J. (2007). Human Cep192 Is Required for Mitotic Centrosome and Spindle Assembly. Curr. Biol. *17*, 1960–1966.
- Gönczy, P. (2012). Towards a molecular architecture of centriole assembly. Nat. Rev. Mol. Cell Biol. *13*, 425–435.
- Gönczy, P. (2015). Centrosomes and cancer: revisiting a long-standing relationship.

Nat. Rev. Cancer *15*, 639–652.

- Goshima, G., Wollman, R., Goodwin, S.S., Zhang, N., Scholey, J.M., Vale, R.D., and Stuurman, N. (2007). Genes required for mitotic spindle assembly in Drosophila S2 cells. Science *316*, 417–421.
- Graser, S., Stierhof, Y.-D., and Nigg, E. a (2007). Cep68 and Cep215 (Cdk5rap2) are required for centrosome cohesion. J. Cell Sci. *120*, 4321–4331.
- Guernsey, D.L., Jiang, H., Hussin, J., Arnold, M., Bouyakdan, K., Perry, S., Babineau-Sturk, T., Beis, J., Dumas, N., Evans, S.C., et al. (2010). Mutations in centrosomal protein CEP152 in primary microcephaly families linked to MCPH4. Am. J. Hum. Genet. *87*, 40–51.
- Habedanck, R., Stierhof, Y.-D., Wilkinson, C.J., and Nigg, E. a (2005). The Polo kinase Plk4 functions in centriole duplication. Nat. Cell Biol. *7*, 1140–1146.
- Hart, T., Chandrashekhar, M., Aregger, M., Steinhart, Z., Brown, K.R., MacLeod, G., Mis, M., Zimmermann, M., Fradet-Turcotte, A., Sun, S., et al. (2015). High-Resolution CRISPR Screens Reveal Fitness Genes and Genotype-Specific Cancer Liabilities. Cell *163*, 1515–1526.
- Hatch, E.M., Kulukian, A., Holland, A.J., Cleveland, D.W., and Stearns, T. (2010). Cep152 interacts with Plk4 and is required for centriole duplication. J. Cell Biol. *191*, 721–729.
- Hempel, M., Cremer, K., Ockeloen, C.W., Lichtenbelt, K.D., Herkert, J.C., Denecke, J., Haack, T.B., Zink, A.M., Becker, J., Wohlleber, E., et al. (2015a). De Novo Mutations in CHAMP1 Cause Intellectual Disability with Severe Speech Impairment. Am. J. Hum. Genet. *97*, 493–500.

- Hempel, M., Cremer, K., Ockeloen, C.W., Lichtenbelt, K.D., Herkert, J.C., Denecke, J., Haack, T.B., Zink, A.M., Becker, J., Wohlleber, E., et al. (2015b). De Novo Mutations in CHAMP1 Cause Intellectual Disability with Severe Speech Impairment. Am. J. Hum. Genet. *97*, 493–500.
- Hinchcliffe, E.H., Maller F.J., Chem, M., Khodjakov, A., Sluder, G.(2001). Requirement of a Centrosomal Activity for Cell Cycle Progression Through G1 into S Phase. Science. *291*, 1547–1550.
- Hussain, M.S., Baig, S.M., Neumann, S., Nürnberg, G., Farooq, M., Ahmad, I., Alef, T., Hennies, H.C., Technau, M., Altmüller, J., et al. (2012). A truncating mutation of CEP135 causes primary microcephaly and disturbed centrosomal function. Am. J. Hum. Genet. *90*, 871–878.
- Ishikawa, H., Kubo, A., Tsukita, S., and Tsukita, S. (2005). Odf2-deficient mother centrioles lack distal/subdistal appendages and the ability to generate primary cilia. Nat. Cell Biol. *7*, 517–524.
- Isidor, B., Küry, S., Rosenfeld, J.A., Besnard, T., Schmitt, S., Joss, S., Davies, S.J., Roger Lebel, R., Henderson, A., Schaaf, C.P., et al. (2016). De Novo Truncating Mutations in the Kinetochore-Microtubules Attachment Gene CHAMP1 Cause Syndromic Intellectual Disability. Hum. Mutat. *37*, 354–358.
- Issa, L., Kraemer, N., Rickert, C.H., Sifringer, M., Ninnemann, O., Stoltenburg-Didinger, G., and Kaindl, A.M. (2013). CDK5RAP2 expression during murine and human brain development correlates with pathology in primary autosomal recessive microcephaly. Cereb. Cortex *23*, 2245–2260.
- Itoh, G., Kanno, S., Uchida, K.S.K., Chiba, S., Sugino, S., Watanabe, K., Mizuno,

K., Yasui, A., Hirota, T., and Tanaka, K. (2011). CAMP (C13orf8, ZNF828) is a novel regulator of kinetochore-microtubule attachment. EMBO J. *30*, 130–144.

- Izquierdo, D., Wang, W.J., Uryu, K., and Tsou, M.F.B. (2014). Stabilization of Cartwheel-less Centrioles for Duplication Requires CEP295-Mediated Centriole-to-Centrosome Conversion. Cell Rep. *8*, 957–965.
- Jakobsen, L., Vanselow, K., Skogs, M., Toyoda, Y., Lundberg, E., Poser, I., Falkenby, L.G., Bennetzen, M., Westendorf, J., Nigg, E.A., et al. (2011). Novel asymmetrically localizing components of human centrosomes identified by complementary proteomics methods. EMBO J. *30*, 1520–1535.
- Al Jord, A., Lemaître, A.-I., Delgehyr, N., Faucourt, M., Spassky, N., and Meunier, A. (2014). Centriole amplification by mother and daughter centrioles differs in multiciliated cells. Nature *516*, 104–107.
- Khodjakov, A., and Rieder, C.L. (2001). Centrosomes enhance the fidelity of cytokinesis in vertebrates and are required for cell cycle progression. J. Cell Biol. *153*, 237–242.
- Kilburn, C.L., Pearson, C.G., Romijn, E.P., Meehl, J.B., Giddings, T.H., Culver, B.P., Yates, J.R., and Winey, M. (2007). New Tetrahymena basal body protein components identify basal body domain structure. J. Cell Biol. *178*, 905–912.
- Kim, T.-S., Park, J.-E., Shukla, A., Choi, S., Murugan, R.N., Lee, J.H., Ahn, M., Rhee, K., Bang, J.K., Kim, B.Y., et al. (2013). Hierarchical recruitment of Plk4 and regulation of centriole biogenesis by two centrosomal scaffolds, Cep192 and Cep152. Proc. Natl. Acad. Sci. U. S. A. *110*, E4849-57.
- Kirkham, M., Müller-Reichert, T., Oegema, K., Grill, S., and Hyman, A.A. (2003).

SAS-4 is a C. elegans centriolar protein that controls centrosome size. Cell *112*, 575–587.

- Kitagawa, D., Vakonakis, I., Olieric, N., Hilbert, M., Keller, D., Olieric, V., Bortfeld, M., Erat, M.C., Flückiger, I., Gönczy, P., et al. (2011). Structural basis of the 9-fold symmetry of centrioles. Cell *144*, 364–375.
- Kitagawa, D., Kohlmaier, G., Keller, D., Strnad, P., Balestra, F.R., Fluckiger, I., and Gonczy, P. (2011). Spindle positioning in human cells relies on proper centriole formation and on the microcephaly proteins CPAP and STIL. J. Cell Sci. *124*, 3884–3893.
- Kleylein-Sohn, J., Westendorf, J., Le Clech, M., Habedanck, R., Stierhof, Y.D., and Nigg, E. a. (2007). Plk4-Induced Centriole Biogenesis in Human Cells. Dev. Cell *13*, 190–202.
- Knorz, V.J., Spalluto, C., Lessard, M., Purvis, T.L., Adigun, F.F., Collin, G.B., Hanley, N. a, Wilson, D.I., and Hearn, T. (2010). Centriolar association of ALMS1 and likely centrosomal functions of the ALMS motif-containing proteins C10orf90 and KIAA1731. Mol. Biol. Cell *21*, 3617–3629.
- Kohlmaier, G., Lončarek, J., Meng, X., McEwen, B.F., Mogensen, M.M., Spektor, A., Dynlacht, B.D., Khodjakov, A., and Gönczy, P. (2009). Overly Long Centrioles and Defective Cell Division upon Excess of the SAS-4-Related Protein CPAP. Curr. Biol. *19*, 1012–1018.
- Kratz, A.-S., Bärenz, F., Richter, K.T., and Hoffmann, I. (2015). Plk4-dependent phosphorylation of STIL is required for centriole duplication. Biol. Open 1–8.
- Lane, H.A., and Nigg, E.A. (1996). Antibody Microinjection Reveals an Essential

Role for Human Polo-like Kinase 1 (Plkl) in the Functional Maturation of Mitotic Centrosomes. J. Cell Biol. *1*, 1701–1713.

- Leidel, S., and Gönczy, P. (2003). SAS-4 is essential for centrosome duplication in C. elegans and is recruited to daughter centrioles once per cell cycle. Dev. Cell *4*, 431–439.
- Leidel, S., Delattre, M., Cerutti, L., Baumer, K., and Gönczy, P. (2005). SAS-6 defines a protein family required for centrosome duplication in C. elegans and in human cells. Nat. Cell Biol. *7*, 115–125.
- Lin, G.G., and Scott, J.G. (2012). NIH Public Access. *100*, 130–134.
- Lin, Y.-C., Chang, C.-W., Hsu, W.-B., Tang, C.-J.C., Lin, Y.-N., Chou, E.-J., Wu, C.-T., and Tang, T.K. (2013). Human microcephaly protein CEP135 binds to hSAS-6 and CPAP, and is required for centriole assembly. EMBO J. *32*, 1141–1154.
- Lüders, J. (2012). The amorphous pericentriolar cloud takes shape. Nat. Cell Biol. *14*, 1126–1128.
- Maiato, H., and Logarinho, E. (2014). Mitotic spindle multipolarity without centrosome amplification. Nat. Cell Biol. *16*, 386–394.
- Manandhar, G. (2005). Centrosome Reduction During Gametogenesis and Its Significance. Biol. Reprod. *72*, 2–13.
- Marthiens, V., Moers, V., Boeckx, B., Le, M., Lambrechts, D., Basto, R., Recherche, C. De, and Hospital, E. (2016). Transient PLK4 overexpression accelerates tumorigenesis in p53 deficient epidermis. *18*, 1–26.
- Nakazawa, Y., Hiraki, M., Kamiya, R., and Hirono, M. (2007). SAS-6 is a

Cartwheel Protein that Establishes the 9-Fold Symmetry of the Centriole. Curr. Biol. *17*, 2169–2174.

- Nigg, E. a., and Raff, J.W. (2009). Centrioles, Centrosomes, and Cilia in Health and Disease. Cell *139*, 663–678.
- O'Connell, K.F., Caron, C., Kopish, K.R., Hurd, D.D., Kemphues, K.J., Li, Y., and White, J.G. (2001). The C. elegans zyg-1 gene encodes a regulator of centrosome duplication with distinct maternal and paternal roles in the embryo. Cell *105*, 547–558.
- Ohta, M., Ashikawa, T., Nozaki, Y., Kozuka-Hata, H., Goto, H., Inagaki, M., Oyama, M., and Kitagawa, D. (2014). Direct interaction of Plk4 with STIL ensures formation of a single procentriole per parental centriole. Nat. Commun. *5*, DOI: 10.1038/ncomms6267.
- Papari, E., Bastami, M., Farhadi, A., Abedini, S., Hosseini, M., Bahman, I., Mohseni, M., Garshasbi, M., Moheb, L.A., Behjati, F., et al. (2013). Investigation of primary microcephaly in Bushehr province of Iran: Novel STIL and ASPM mutations. Clin. Genet. *83*, 488–490.
- Paweletz, N. (2001). Walther Flemming: pioneer of mitosis research. Nat. Rev. Mol. Cell Biol. *2*, 72–75.
- Godinho, SA., Picone, R., Burute, M., Dagher, R., Su, Y., Leung, CT., Polyak, K., Brugge, JS., Théry, M., Pellman, D. (2014). Oncogene-like induction of cellular invasion from centrosome amplification. Nature *510*, 167–171.
- Petronczki, M., Lénárt, P., and Peters, J.M. (2008). Polo on the Rise-from Mitotic Entry to Cytokinesis with Plk1. Dev. Cell *14*, 646–659.

- Piel, M., Meyer, P., Khodjakov, A., Rieder, C.L., and Bornens, M. (2000). The respective contributions of the mother and daughter centrioles to centrosome activity and behavior in vertebrate cells. J. Cell Biol. *149*, 317–329.
- Post, Y., Wei, J.J., Lander, E.S., and Sabatini, D.M. (2015). Identification and characterization of essential genes in the human genome. Science. *350*, 1096–1101.
- Saitsu, H., Sonoda, M., Higashijima, T., Shirozu, H., Masuda, H., Tohyama, J., Kato, M., Nakashima, M., Tsurusaki, Y., Mizuguchi, T., et al. (2016). Somatic mutations in *GLI3* and *OFD1* involved in sonic hedgehog signaling cause hypothalamic hamartoma. Ann. Clin. Transl. Neurol. *3*, 356–365.
- Saurya, S., Roque, H., Novak, Z.A., Wainman, A., and Mustafa, G. (2016). Drosophila Ana1 is required for centrosome assembly and centriole elongation. J. Cell Sci. *129*, 2514–2525.
- Schmidt, T.I., Kleylein-Sohn, J., Westendorf, J., Le Clech, M., Lavoie, S.B., Stierhof, Y.D., and Nigg, E. a. (2009). Control of Centriole Length by CPAP and CP110. Curr. Biol. *19*, 1005–1011.
- Schuh, M., and Ellenberg, J. (2007). Self-Organization of MTOCs Replaces Centrosome Function during Acentrosomal Spindle Assembly in Live Mouse Oocytes. Cell *130*, 484–498.
- Shiratsuchi, G., Kamiya, R., and Hirono, M. (2011). Scaffolding function of the Chlamydomonas procentriole protein CRC70, a member of the conserved Cep70 family. J. Cell Sci. *124*, 2964–2975.
- Shiratsuchi, G., Takaoka, K., Ashikawa, T., Hamada, H., and Kitagawa, D. (2015). RBM14 prevents assembly of centriolar protein complexes and maintains mitotic

spindle integrity. EMBO J. *34*, 97–114.

- Sonnen, K.F., Schermelleh, L., Leonhardt, H., and Nigg, E. a. (2012). 3D-structured illumination microscopy provides novel insight into architecture of human centrosomes. Biol. Open *1*, 965–976.
- Sonnen, K.F., Gabryjonczyk, A.-M., Anselm, E., Stierhof, Y.-D., and Nigg, E. a (2013). Human Cep192 and Cep152 cooperate in Plk4 recruitment and centriole duplication. J Cell Sci. *126*, 3223–3233.
- Tanaka, A.J., Cho, M.T., Retterer, K., Jones, J.R., Nowak, C., Douglas, J., Jiang, Y.-H., McConkie-Rosell, A., Schaefer, G.B., Kaylor, J., et al. (2016). De novo pathogenic variants in CHAMP1 are associated with global developmental delay, intellectual disability, and dysmorphic facial features. Mol. Case Stud. *2*, a000661.
- Tang, C.-J.C., Fu, R.-H., Wu, K.-S., Hsu, W.-B., and Tang, T.K. (2009). CPAP is a cell-cycle regulated protein that controls centriole length. Nat. Cell Biol. *11*, 825–831.
- Tang, C.-J.C., Lin, S.-Y., Hsu, W.-B., Lin, Y.-N., Wu, C.-T., Lin, Y.-C., Chang, C.-W., Wu, K.-S., and Tang, T.K. (2011). The human microcephaly protein STIL interacts with CPAP and is required for procentriole formation. EMBO J. *30*, 4790–4804.
- Toole, E.T.O., Giddings, T.H., Mcintosh, J.R., and Dutcher, S.K. (2003). Three-dimensional Organization of Basal Bodies from Wild-Type and γ -Tubulin Deletion Strains of. *14*, 2999–3012.
- Tsou, M.-F.B., and Stearns, T. (2006). Mechanism limiting centrosome duplication to once per cell cycle. Nature *442*, 947–951.

- Tsuchiya, Y., Yoshiba, S., Gupta, A., Watanabe, K., and Kitagawa, D. (2016). Cep295 is a conserved scaffold protein required for generation of a bona fide mother centriole. Nat. Commun. *7*, DOI: 10.1038/ncomms12567.
- Vulprecht, J., David, a., Tibelius, a., Castiel, a., Konotop, G., Liu, F., Bestvater, F., Raab, M.S., Zentgraf, H., Izraeli, S., et al. (2012). STIL is required for centriole duplication in human cells. J. Cell Sci. *125*, 1353–1362.
- Wang, G., Jiang, Q., Zhang, C., Abe, Y., Ohsugi, M., Haraguchi, K., Fujimoto, J., Yamamoto, T., Anand, S., Penrhyn-Lowe, S., et al. (2014). The role of mitotic kinases in coupling the centrosome cycle with the assembly of the mitotic spindle. J. Cell Sci. *127*, 4111–4122.
- Wang, W.J., Soni, R.K., Uryu, K., and Tsou, M.F.B. (2011). The conversion of centrioles to centrosomes: Essential coupling of duplication with segregation. J. Cell Biol. *193*, 727–739.
- Wang, X., Yang, Y., Duan, Q., Jiang, N., Huang, Y., Darzynkiewicz, Z., and Dai, W. (2008). sSgo1, a major splice variant of Sgo1, functions in centriole cohesion where it is regulated by Plk1. Dev. Cell *14*, 331–341.
- Wong, Y.L., Anzola, J. V, Davis, R.L., Yoon, M., Motamedi, A., Kroll, A., Seo, C.P., Hsia, J.E., Kim, S.K., Mitchell, J.W., et al. (2015). Cell biology. Reversible centriole depletion with an inhibitor of Polo-like kinase 4. Science. *348*, 1155–1160.
- Woodruff, J.B., Wueseke, O., Viscardi, V., Mahamid, J., Ochoa, S.D., Bunkenborg, J., Widlund, P.O., Pozniakovsky, a., Zanin, E., Bahmanyar, S., et al. (2015). Regulated assembly of a supramolecular centrosome scaffold in vitro. Science. *348*, 808–812.

- Yoshiba, S., and Hamada, H. (2014). Roles of cilia, fluid flow, and Ca2+ signaling in breaking of left-right symmetry. Trends Genet. *30*, 10–17.
- Zhu, F., Lawo, S., Bird, A., Pinchev, D., Ralph, A., Richter, C., Müller-Reichert, T., Kittler, R., Hyman, A. a., and Pelletier, L. (2008). The Mammalian SPD-2 Ortholog Cep192 Regulates Centrosome Biogenesis. Curr. Biol. *18*, 136–141.

Chapter 6:

Acknowledgements

Here, I express my sincere gratitude to all of the members for providing me guidance, technical help, tremendous support and constant encouragement during the preparation of this study.

Most of all, I express my deepest thanks to Prof. Daiju Kitagawa for his valuable suggestions, encouragement, and critical advices for this Ph. D. thesis.

I deeply grateful to Prof. Hiroyuki Araki, Prof. Shin-ya Miyagishima, Assoc. Prof. Yuta Shimamoto, and Dr. Ide Satoru for their helpful advice, specific suggestions and valuable feedback and Prof. Natsuko Chiba for her meaningful discussion.

I am very grateful to Prof. Nobuo Okamoto for insightful comments and feedback of the study of CHAMP1 and Rie Hayashi for technical assistance of the STED microscope. I thank Prof. Erich A Nigg for Flag-Cep192 construct, Prof. Thomas Hearn for pCMV-Myc-Cep295 construct, Prof. Tatsuo Fukagawa for technical advice of the 3D-SIM, Dr. Satoru Mimura for pSM671 and pSM378 vectors, menbers of Kanemaki lab for technical advice, Tomoko Ashikawa and Yuka Nozaki for supporting the experiments, Yoshiki Kanehara for technical help and encouragement.

Finally, I express my thanks to my parents and friends for constant encouragement and enormous help. I also thanks to past and present members of Kitagawa lab for practical advice and constructive comments.